THERMAL INSULATION OF CONCRETE AND MASONRY HOLLOW CONCRETE BRICKS EXPERIMENTALLY AND ANALYTICALLY

BY

AHMED SALEM BARK AL-TAMIMI

A Thesis Presented to the
DEANSHIP OF GRADUATE STUDIES

KING FAHD UNIVERSITY OF PETROLEUM & MINERALS

DHAHRAN, SAUDI ARABIA

In Partial Fulfillment of the
Requirements for the Degree of

MASTER OF SCIENCE

In

CIVIL ENGINEERING

DECEMBER 2017

KING FAHD UNIVERSITY OF PETROLEUM & MINERALS

DHAHRAN- 31261, SAUDI ARABIA

DEANSHIP OF GRADUATE STUDIES

This thesis, written by **AHMED SALEM BARK AL-TAMIMI** under the direction of his thesis advisor and approved by his thesis committee, has been presented and accepted by the Dean of Graduate Studies, in partial fulfillment of the requirements for the degree of **MASTER OF SCIENCE IN CIVIL ENGINEERING.**

Prof. Omar S. Baghabra Al-Amoudi
(Advisor)

Dr. Salah U. Al-Dulaijan
Department Chairman

Dr. Mohammed A. Al-Osta
(Member)

Prof. Salam A. Zummo
Dean, Graduate Studies

Dr. Rached Ben Mansour
(Member)

8/1/13

Date

This Humble Work Is Dedicated to:

My parents, brothers and sisters, lovely wife and blessed baby

For their love, supports, encouragement and prayers

And to Sheikh Eng. Abduallah Ahmed Bugshan

for his continuous support

ACKNOWLEDGMENTS

All praise be to Allah for giving me the chance, knowledge, health and patient to complete this work with success.

I would like to express my gratitude to King Fahd University of Petroleum and Minerals and the Department of Civil and Environmental Engineering for providing me the opportunity to pursue my master degree. Special thanks are directed to my thesis advisor, Prof. Omar S. Baghabra Al-Amoudi for his tremendous effort, help and feedback during my research period. Also, I appreciate the support of my committee members, Dr. Mohammed Al-Osta and Dr. Rached Ben Mansour, for their guidance, motivation and help during my thesis.

I would like to thank the Research Institute (RI) and Prof. Mohammad Maslehuddin for his help and kindness during my experimental work.

Further, I would like to the Saudi Readymix Concrete Company, the Arabian Vermiculite Industries, Alyaf Industrial Company LTD., Saudi Rubber Products CO. and the Advanced Concrete Products, Ltd. for providing all the necessary materials during the experimental work.

Thanks are extended to my KFUPM and Hadhrami colleagues at KFUPM for their motivation, friendship and help. May Allah bless them and reward them Paradise. I grateful for my colleague Waleed Al-Awsh to his continuous help in the laboratory during the experiment work.

I grateful for the patient, support and help of my parents, brothers and sisters to pursue my education away from them, may Allah bless and give them happiness. The support of my blessed wife and baby during my research period is highly appreciated. May Allah reward them Paradise.

I sincerely appreciate the continuous support of Sheikh Abduallah Ahmed Bugshan and Hadhramout Establishment for Human Development for sending me to complete my MS degree at KFUPM. May Allah bless them and support their initiatives.

TABLE OF CONTENTS

LIST OF TABLES

LIST OF FIGURES

LIST OF ABBREVIATIONS

A: Surface Area of the Main Heater, m^2

AR: Aspect Ratio

BC: Boundary Condition

C: Control Brick

CA: Coarse Aggregate

d_1: Thickness of Dummy Sample, m

d_2: Thickness of Test Sample, m

FA: Fine Aggregate

HB: Hollow Brick

HR: Hollow Ratio

I: Main Heater Current, mA

k: Thermal Conductivity Coefficient, W/m.k

k_1: Thermal Conductivity of Dummy Sample, W/m.k

k_2: Thermal Conductivity of Test Sample, W/m.k

M_R: Modulus of Rupture, MPa

N: Correction Factor of the Instrument

NT11: Nodal Temperature Distribution, °K

P: Recorded Load by Data Logger, kN

PE: High-density Polyethylene

PL: Perlite

PS: Polystyrene

Q: Total Heat Flow in Main Heater, W

Q_1: Heat Flow through Dummy Sample, W

Q_2: Heat Flow through Test Sample, W

Ru: Crumb Tires Rubber

SP: Super-plastisizer

Ti: Average Interior Surface Temperature of Hollow brick, °C

V: Main Heater Voltage, mV

V_{cube}: Volume of Cube, m^3

W_d: Oven-dry Weight of Specimen, kg

W_s: Saturated Weight of Specimen, kg

°C: Degrees Centigrade (Celsius)

°K: Degrees Kelvin

ABSTRACT

Full Name: Ahmed Salem Al-Tamimi

Thesis Title: Thermal Insulation of Concrete and Masonry Hollow Concrete Bricks Experimentally and Analytically

Major Field: Civil Engineering - Structures

Date of Degree: December 2017

Saving energy has recently become a critical issue around the world and, hence, many policies have been implemented to reduce and control the consumption of electricity. Therefore, billions of dollars could be saved if these policies are well applied. In Saudi Arabia, the predicted demand for electricity could be reduced by 5 to 10%, which is equivalent approximately to a saving of $1.5 to 3.0 billions over the next 20 years. Further, the returns of reducing the demand for air conditioning only are around $0.25 billion each year.

The aim of this research was to reduce the air conditioning demand in buildings through minimizing the heat flow from outdoor environment to interior building envelopes (walls and roofs). Hence, some insulation materials were used in the concrete mixtures to produce normal concrete and hollow concrete blocks for roofs and walls, respectively, to reduce their thermal conductivity. The normal concrete could be cast as screed concrete on roofs to decrease the thermal flux through roofs in the top floor of buildings. Similarly, the hollow concrete bricks would significantly contribute in reducing the interior surface temperature of the walls as compared with normal hollow bricks. Further, finite element modelling (FEM) was developed to find out the optimum geometry of cavities layout of

bricks in order to reduce the thermal flow of heat and the results would be compared with that of hollow bricks in the market.

Results of the simulation were promising and indicating that the new designed “optimum” geometry of hollow bricks was much better than the market hollow bricks, from thermal point of view with a reduction of about 4.5°C of room temperature (as proved by a study in UAE that reducing 1°C could save up to 6% of electricity consumption). Experimentally, the optimum design of hollow brick improved the thermal insulation by as high as 70% compared with other designs of hollow bricks including the market hollow bricks. Further, the thermal resistance of concrete and masonry bricks with the insulation materials (perlite, rubber and polyethylene) was enticing and significant, which could reach up to 33%. However, the newly developed optimum design of concrete brick with and without the insulation materials satisfied the ASTM C 129 requirements for non-load bearing walls in terms of strength and absorption and was considered as medium weight (without insulation material) and as lightweight (with insulation materials). Therefore, it is recommended that these optimum designed bricks were utilized by the construction industry. Results of this comprehensive investigation indicate that the thermal conductivity reduced by about 40%. Similarly, the strength of normal concrete decreased with increasing the content of the insulation materials (rubber and polyethylene) with a maximum value of 90%, while the flexural strength was reduced with about 40%. Further, the addition of rubber and polyethylene in concrete improved the ductility behavior.

ملخص الرسالة

الاسم الكامل: احمد سالم برك التميمي

عنوان الرسالة: العزل الحراري للخرسانة العادية وطوب البناء المجوف مختبرياً وتحليلياً

التخصص: هندسة مدنية – انشاءات

تاريخ الدرجة العلمية: ديسمبر 2017

اصبح الحفاظ على الطاقه قضية مهمه حالياً في مختلف انحاء العالم، ولذلك فُرضت الكثير من القوانين والأنظمة لتقليل وتنظيم الاستهلاك الكهربائي الذي من خلاله سيتم توفير بلايين الدولارات التي يمكن استخدامها في استثمارات أخرى. ويمكن تقليل الطلب على الكهرباء في المملكة العربية السعودية بمعدل 5 الى 10%، والتي تعادل توفير ما يقارب 1.5 الى 3 بليون دولار خلال العشرين عاماً القادمة بالاضافة الى توفير ربع بليون دولار كل عام من خلال الترشيد في استخدام التكييف فقط. لتلك الأسباب، كان الهدف من هذا البحث هو تقليل استخدام التكييف في المباني عن طريق تقليل انتقال الحرارة من البيئة الخارجية الى السطوح الداخلية للجدران والاسطح.

تم استخدام بعض المواد العازلة في الخلطات الخرسانية لانتاج خرسانة عاية عازلة وطوب (بُلك) بناء مجوف عازل للحرارة، حيث يمكن استخدام الخرسانة العادية كعازل للاسقف لتقليل الانتقال الحراري عن طريق السقف، بينما طوب البناء المجوف يكمن استخدامه في بناء الجدران مما سيقلل درجة الحرارة الداخلية للجدران مقارنة بالطوب العادي. وقد تمّ عمل برنامج محاكاة باستخدام الاباكس لتحديد افضل ابعاد وترتيب للفتحات التي تم تصميمها للطوب المجوف ومن ثم مقارنتها بالطوب المجوف المتوفر في السوق.

كانت نتائج التلحليل واعدة، حيث اثبتت مقاومة عالية للحراره في الطوب المجوف الذي تم تصميمه مقارنة بالطوب المتوفر في السوق وذلك بمقدار 4.5ْم مع العلم بأن كل درجة مئوية تعادل توفير 6% من الاستهلاك الكهربائي حسبما اثبتت بعض الأبحاث. كما اثبتت التجارب في هذا البحث ان الطوب المجوف الذي تم انتاجه في المختبر (التصميم الجديد و بدون أي مواد عازله) افضل بـ 70% من الطوب المتوفر في السوق.

كما تم استخدام مواد عازلة في الخلطات الخرسانية لطوب البناء مثل البيرلايت والمطاط والبلاستيك والتي كان لها تاثير كبير في زيادة المقاومة الحرارية التي تصل الى 33%. وكانت جميع أنواع الطوب العازل للحرارة متوافق مع متطلبات المواصفات

الامريكية (ASTM C 129) من حيث القوة التي تزيد عن 3.45 MPa والامتصاص وتم تصنيف الطوب بانه متوسط وخفيف الوزن حسب متطلبات الكثافة في هذه المواصفات. كما تفيد النتائج بان الموصلية الحرارية قد نقصت في الخرسانة العادية بنسبة تصل الى 40% وبالمثل نقصت القوة مع زيادة محتوى المواد العازله (المطاط والبلاستيك) وكذلك عزم الانحناء بمقدار 40% وعلى النقيض تحسنت مرونة الخرسانة باضافه مادتي المطاط واللبلاستيك.

CHAPTER 1

INTRODUCTION

In hot countries, such as Saudi Arabia, air conditioning is indispensable in buildings for supplying thermally comfortable indoor environments. Consequently, the demand for electricity in Saudi Arabia has increased sharply, particularly during the last 40 years with the upsurge of welfare (due to the increase in oil price) [1]. Further, buildings consume about 73% of the total electricity generated in Saudi Arabia, and air-conditioning system constitutes 65% of the building's electrical consumption due to the hot environment in the region [2]. The excessive demand for air conditioning is ascribed to the extremely high temperature at night during summer, when the air temperature could reach around 46°C in Saudi Arabia [3].

The peak loads increased sharply during last five decades. The maximum loads were about 24 GW in 2000, which was 25 times their level in 1975 and is expected to reach 60 GW in 2023. Therefore, the expected investments required to match the growth demand may exceed $90 billions [3]. As a result, there is an urgent need to implement energy conservation policies for sustainable developments. If saving energy strategies are implemented strictly, the predicted demand for electricity could be reduced by 5 to 10%, which was equivalent to 3 to 6 GW of additional capacity, which amounts to about $1.5 to 3.0 billions of saving over the next 20 years [3]. These studies proved that the returns of developing polices for saving energy and decreasing the demand of air conditioning could

reach to about 500MW per annum of generating capacity, that means, the government will save up to $0.25 billion each year [3]. Further, some studies proved that reducing the temperature of air conditioning by one degree centigrade could save about 6% of the electricity consumption [4].

Since energy generation in Saudi Arabia is based on fuel, the fuel demand increases and the rate of air pollution due to the emission of CO_2 will also increase. The energy consumption could be reduced by minimizing the use of air-conditioning systems by decreasing the heat transfer from exterior to interior surfaces of buildings. The masonry walls and roofs are the surfaces that are mostly exposed to the outdoor temperature and solar radiation. Therefore, decreasing the thermal conductivity of these elements will result in reducing the temperature at the inner surfaces. In some local regions, the ambient air temperature could reach up to 50°C during summer days and the exterior surfaces of the building, including roofs and external wall surfaces, could reach up to 80°C or even higher if they are directly exposed to the solar radiation [3,4]. The temperature inside the buildings is often maintained by the air-conditioning system. If the desirable indoor temperature is 25°C and the exterior envelope temperature is 80°C, the temperature difference between the building envelopes could be as high as 55°C, thereby increasing the consumption of energy [1].

The demand for building materials with higher thermal insulation properties has been recognized and numerous researchers have investigated the availability of such materials with the required properties to enhance the thermal insulation of building envelopes [7]. In regard to the walls or roofs, the additional insulation materials would require a change in the conventional thickness (of walls and roofs). Hence, the cost of the building

construction will increase substantially [7]. Therefore, since the concrete is the major component of most buildings in the region, many researches and proposals formulating cement mixes having lightweight, high strength and thermal insulation are urgently needed.

In this research, literature on using materials in concrete and bricks (blocks) to reduce their thermal conductivity was presented in Chapter 2. All previous related works were reported in detail to find out the characteristics of the additive materials, sizes, content, etc. Then, three materials were selected to be used in this research based on their thermal conductivity (low), price (low), availability (widely) in Saudi Arabia. The three selected materials are crushed tire rubber, crushed high density polyethylene and graded size perlite. All the three materials were used in the masonry bricks, while two materials (rubber and polyethylene) were selected for normal concrete, while graded particle of perlite could not be used in normal concrete due to the insufficient structural strength [7].

Since the thermal conductivity of concrete is much higher than that of air, the thermal conductivity can be significantly reduced by making cavities or air gaps in the concrete bricks. Double-skin walls with insulating materials contribute to some extent in decreasing the heat flow to the inside the building envelope, however, the insulation materials are not widely used because of their high cost [8]. Therefore, finite element modelling (FEM) was developed to design an optimum geometry of the cavities [1], to assess the effect of arrangement, number and shape of hollows in bricks on the heat flow. In Chapter 3, new designs of hollow bricks were discussed in detail with the FEM model using ABAQUS software. Further, two of the most widely used hollow bricks in eastern Saudi Arabia were selected from the market to compare their performance with the optimum designed hollow bricks developed in this investigation. FEM was validated in many studies with

experimental programs such as Del Coz Diaz [9] and Zhou [5]. Therefore, the computer simulation will certainly save the time, cost and efforts, which could be spent in conducting the experimental work to assess and select the optimum cavities geometry layout of the hollow bricks. From the FEM in Chapter 3, the optimum hollow brick was selected to be cast with the insulation materials, as would be explained in Chapter 4.

In Chapter 4, all details about selected materials were presented such as their chemical composition, physical and thermal properties. Mix proportions were prepared for both normal concrete and masonry bricks (blocks) for the control mixes and the mixes with replacement materials. Forty trial mixes were tested in order to arrive at the appropriate mixes (satisfying the compressive strength requirements and achieved high thermal resistance) for all substituted martials. Casting, curing and testing specimens were detailed in this chapter based on the following three tests: compression, flexural and thermal conductivity.

Chapter 5 presents the experimental results for normal concrete and masonry hollow bricks. Again, compression, flexural and thermal conductivity tests were conducted for normal concrete and the results were summarized in tables and graphs. For masonry bricks, compression, absorption and thermal conductivity test results were assessed and discussed.

Chapter 6 was the last chapter, which includes the conclusions and recommendations. From the present simulation and experimental work, the solid points of the results were presented including compression, flexural and thermal conductivity for normal concrete and masonry hollow bricks. Further, the recommendations were presented for future studies related to

this work such as using powder perlite as a replacement material to coarse aggregate and changing the ratio of fine to coarse aggregate, etc.

CHAPTER 2

LITERATURE REVIEW

Many studies have been conducted on lightweight and thermal insulation materials in construction to save energy and cost. Since the principal objective of this research was to produce lightweight and high thermal insulation concrete and bricks (blocks), it is well known that the exterior walls and roofs are the most exposed surfaces to outdoor temperature and solar radiation. Hence, reducing their thermal conductivity tends to reduce the heat flow to the interior surfaces and, consequently, the indoor temperature will be decreased significantly thereby reducing the air-conditioning and electricity consumption.

Polymers, rubber and perlite have been used for the insulation in buildings [1, 2]. Thermal conductivity of concrete increases with increasing the moisture content, cement content and thermal conductivity of aggregate and decreasing the porosity [12]. Further, the volume of aggregate in concrete mixture is approximately 75%, hence, the properties of aggregate greatly affect the performance of concrete [13]. Therefore, the replacement of aggregate with insulation materials (such as plastic, rubber and perlite) will significantly contribute in the reduction of the thermal conductivity of concrete. The porosity affects the density and thermal conductivity of the concrete (i.e. increasing the porosity will decrease the density and thermal conductivity) [12]. As a result, the porosity of perlite greatly contributes in the reduction of thermal conductivity of concrete when the aggregate is replaced by perlite.

In this Chapter, a brief review about the replacement materials (perlite, rubber and polyethylene) would be introduced, followed by the literature for each material for normal concrete as well as for masonry blocks. Finally, previous researches on FEM modeling to assess thermal conductivity would be highlighted. The mechanisms of heat transfer through walls would be illustrated with the boundary conditions and heat processes including convection and radiation inside cavities.

2.1 Replacement Materials

In this section, the replacement materials used in the experimental work would be introduced. Then, the literature on the research using these insulation materials in concrete and masonry bricks would be highlighted.

2.1.1 Crushed Tires Rubber (Ru)

Around the world, there are about 450 tire factories with a production of over than 1 billion tires per year [14]. Saudi Arabia is the largest market for vehicle tires in the Middle East to sate the demand, which grows by 12% per year [15]. About 13 million of tires were imported to Saudi market with a cost of $800 million annually and the consumption is expected to keep on rising as the demand increases in the next years [15].

Un-recycled tires are disposed of in the landfills (underground) or stockpiled (above ground). The landfilling of tires takes a wide space of landfill because the tires are relatively incompressible and 75% of the tire-occupied space is voids. The void spaces provide a convenient environment for gnawers and methane gas, which is sometimes floating upward

shooting and shattering the surface of landfill cover with huge force. Therefore, stored tires underground is more hazardous than disposing them above ground. The stockpiling tires create two significant hazards, which are fires and mosquitoes. The shape and impermeability of tires tend to hold the water for long periods, thereby providing ideal place for mosquitoes. The fire generated from tires causes a huge amount of heat and smokes that is difficult to extinguish [15].

There are two billions of scrap tires in the US disposed of on landfills plus over 250 million tires plus every year [16]. In the European Union, the waste tires were around 180 millions each year [17]. In Saudi Arabia, the amount of waste tires is around twenty millions scrap tires per year. The hazard due to improper storage of the waste tires will affect the public and environment. Therefore, the best solution for these problems would be to recycle the waste tires to have a clean environment and providing economic outcomes through crushing them and using them in the industrial applications [15].

2.1.2 High-density Polyethylene (PE)

Plastic is one of the creative products in 20th century, which is widely used around the world. In the last years, the consumption of plastic was grown incredibly tending to maximize the plastic waste. Therefore, the hazard resulted from the waste plastic is disastrous toward the environment and public life [18]. Plastic is composed of several toxic chemicals, thereby contributing to the pollution of water, air and soil due to its disposal [18]. Plastic consists of polymers, which are not degradable in the natural environment, even after a long period of time. The consumption of plastic has been increased from 50 million tons in 1950s to 100 million tons in 2001 [19]. The plastic consumption is more

than 11 and 23 million tons each year in US and Western Europe, respectively, and 80% of the waste plastic in US is disposed to landfills, 8% burned and just 7% is recycled, which is the same amount of plastic recirculation in UK [6,7]. Plastic has been considered as a constructional material due to its weight, strength and thermal property. Therefore, shredded plastic could be used in concrete mixtures as a replacement of natural aggregate, which accounts to about 65-80% of the concrete volume. As a result, the use of plastic in concrete as aggregate consumes a huge amount of waste materials that could reduce the lack of good quality aggregate (particularly in eastern Saudi Arabia) and pollution problems, as reported in many researches [21].

Plastics could be classified based on the polymers used in their manufacture into two categories: thermoplastic and thermosetting plastics [20]. Thermoplastics, such as polyethylene (PE), polystyrene (PS), polypropylene (PP), polyethylene terephthalate (PET), and high-density polyethylene (HDPE), can be melted and hardened through heating and cooling. On contrary, thermosetting plastic could not be melt or softened through heating [20]. Different types of waste plastics such as PET, HDPE, PS, PVC and mixed waste plastic, were used in cement mortar or concrete as aggregate or fibers in many researches [18], as is highlighted in Section 2.2.

2.1.3 Perlite (PL)

Perlite is a siliceous volcanic glass, which can be expanded tremendously under the effect of heat. The volume of perlite can increase 4 to 20 times compared to its original volume when it is heated above 870°C [13]. Therefore, the porosity and water absorption of perlite

increases significantly. Perlites are used in the construction industries such as plastering, concrete, underfloor insulation, agriculture and oil gas wells [22].

Perlite mineral deposits exist in many countries of the world [10] and Turkey has one of the largest deposits in the world with approximately 4.5 billion tons reserved around the country [13], which is about 70% of the perlite world reserves [23]. However, the production of perlite is around 150,000 tons each year around Turkey, which is mostly utilized for plastering and as filling materials [13].

2.2 Normal Concrete with Tires Rubber and Polyethylene

Many researches have been conducted on the use of tires rubber in concrete in order to enhance its thermal resistance, but all experiments proved that the addition of rubber reduces the compressive and flexural strengths as well as the thermal conductivity. Therefore, the rubberized concrete could not be directly used in structural fields. On the other hand, with its lower density and thermal conductivity, tire rubber seems to be used as insulators and partitions.

High density polyethylene (HDPE) is a polyethylene terephthalate (PET) made from the petroleum refineries and it is often used in the production of plastic bottles. Very few researches reported the application of HDPE as a replacement material in concrete, while PET has been widely utilized in concrete mixtures in many researches, as summarized in the literature [11, 39, 19].

The use of plastic bottles in concrete mixtures is not as common as the use of crumb rubber because plastic shredding and retreating processes are relatively more complex and costly [11]. Waste plastic bottles have been used in concrete as a replacement to natural aggregate to produce lightweight concrete, which granted environmental and economic benefits [11]. The recycled PET became an important material for producing thermal insulating partitions for buildings [11].

Toutanji [25] investigated the effect of rubber graded particles with a maximum size of 12.7 mm on concrete strength whereby rubber aggregate replaced coarse aggregate by 25, 50, 75 and 100% by volume. The author found out that the compressive strength was sharply decreased to 39% and 76% for rubber substitution of 25 and 100%, while flexural strength was reduced by 8 and 37%.

Fedroff et al. [26] used crumb rubber as an additive material in concrete. The rubber particles had a grading curve between 0.045 and 0.30 mm and the percentages of addition were 10, 20 and 30% by weight of cement. The compressive strength was reduced by 50 and 75% for 10 and 30% rubber additions. Further, the flexural strength dropped by 31, 60 and 67% for the additions of 10, 20 and 30% of rubber.

Khatib et al. [27] used fine and coarse rubber particles in concrete with different percentage and replacements. Fine, coarse and both aggregates were replaced with fine, coarse and both rubber particles, which were used with percentages varying from 5 to 100% by volume. The results showed that the compressive strength was reduced by 90% for a replacement of 100%. Therefore, rubber content should not be more than 20% by volume from practical point of view [27].

Ghaly et al. [28] replaced fine aggregate with fine rubber in concrete with different water cement ratios (0.47, 0.54 and 0.61). Fine rubber was substituted with dosages of 5, 10 and 15% of sand by volume. They developed a correlation to predict the compressive strength of rubber concrete at any age with the same w/c ratio (R^2= 0.39). The compressive strength for rubberized concrete was reduced due to the lower stiffness of rubber particles and surface bonding with cement paste.

Benazzouk et al. [29] investigated experimentally the effect of waste rubber in cement composites. Rubber pieces replaced cement with 10, 20, 30, 40, and 50% of cement by volume. The size of waste rubber particles was less than 1 mm and containing 20% steel fibers. The outcomes of the experimental program demonstrated that the thermal conductivity of the composite was reduced by about 60% with rubber replacement of 50%. Contrary, the compressive strength was sharply reduced by 40 and 87% for 10 and 50% rubber replacements.

Khaloo et al. [30] utilized two types of scraped rubber in the mix of concrete. They used crumb rubber with closer grading curve to sand, and coarse rubber chips with a max size of 15 mm. The coarse and fine rubbers replaced fine and coarse mineral aggregates with different volume percentages (12.5, 25, 37.5 and 50%). Further, both mineral aggregates were replaced with fine and coarse rubber sizes with replacements of 25 and 50%. The outcomes illustrated that the substitution of rubber aggregate reduced the strengths sharply. Therefore, rubber content exceeding 25% is not recommended and surface treatment is required to increase the bond between the cement past and rubber particles [30].

Piti Sukontasukkul [31] conducted an experimental work with rubberized concrete (W/C = 0.47). Rubber pieces with two sizes (No. 6 and No. 26) and three dosages (10, 20 and 30% by weight) were used to replace fine aggregate in precast concrete panels. The results showed that the 10% of rubber replacement reduced the compressive and flexural strengths by 35% and 28%, respectively. Further, the 20% replacement decreased both strengths by only 22 to 28%. Therefore, the crumb rubber concrete does not seem to find a use in structural applications. On the other hand, the thermal conductivity was reduced significantly by about 20 to 50%.

Yesilata et al. [11] investigated the effect of using tires rubber and polyethylene (PET) on the thermal performance of concrete. The authors used square rubber pieces with 2 mm thickness and three shapes of PET (square, strips, irregular) with a thickness of 1 mm. In each sample, the total volumes of rubber and PET were 80 cm^3 and 40 cm^3, and the total volume of the specimens was 40x40x3 cm^3. The highest thermal resistance was noticed with the square rubber specimen with improvement of 18.52%, while specimens with square pieces of PET achieved the least improvement in the thermal resistance with about 10%. Strips and irregular PET specimens had almost the same thermal enhancement of about 17%.

Issa and Salem [17] used crumb rubber from tires to replace the sand in concrete. The crumb rubber had a similar grading curve as the fine aggregate (sand). The substitution of graded rubber was 15, 25, 50 and 100% by volume. The compressive strength was reduced by 18 and 84% for the rubber replacements of 15 and 100%, respectively.

Naik et al. [32] added shredded small particles of high density polyethylene (HDPE) in concrete in the range of 0.5 to 5% by the total weight of the mix. The strength was reduced by 45 and 23% for 2 and 1.5% addition of plastic. Further, Ismail et al. 2008 [33] used crushed and sieved waste plastic in concrete as a replacement of sand with three dosages (10, 15, 20%). The authors found out that the strength of plastic concrete was significantly reduced compared to the plain concrete due to the weak bond between cement paste and plastic particles. With 20% plastic replacement, the strength was reduced by 30.5% after 28 days of curing.

Al-Manaseer and Dalal [19] replaced the mineral aggregate with 10, 20 and 30% of plastic aggregates and the reduction in the compressive strength was 34, 51 and 67%, respectively. Further, Yadav et al. 2008 [34] and Swamy et al. 2016 [35] replaced coarse aggregate with three graded sizes of plastic. The results showed that the compressive and splitting tensile strengths were reduced by 70 and 78%, respectively. On the other hand, the thermal conductivity decreased by 50%.

Choi et al. [36] used waste polyethylene (bottles) with particle sizes of 5 to 15 mm in concrete. The polyethylene particles replaced sand by volume with different percentages (25, 50 and 75%). The authors covered the plastic particle surfaces with blast-furnace slag to enhance the bond with cement paste. The results showed that the compressive strength was reduced by 33% with the dosage of 75% of polyethylene particles related to control mix (without polyethylene). In the same trend, the dosages of 25 and 50% dropped the strength by 10 and 15%, respectively. The modulus of elasticity was reduced by 27, 32 and 39% compared to the control mix. The same authors 2009 [37] used polyethylene in mortar

with the same previous percentages (25, 50 and 75%). The reduction in compressive strength was 5, 15 and 30% with the replacement of 25, 50 and 75%, respectively.

Frigione [38] reported a reduction with 2% for PET replacement of 5%. Further, Saikia et al. 2014 [21] used three different sizes of recycled polyethylene (fine flaky, coarse flaky and treated pellet) as replacement of mineral aggregate. The fine flaky and treated-pellet were substituted by fine aggregate, while coarse flaky replaced both fine and coarse aggregate. The substitutions were 5, 10 and 15% of the mineral aggregates volume. The 5% pellets and coarse flaky replacement dropped the strength by 75%, while for the 10 and 15% substitutions, the reductions were 59 and 71%, respectively. The strength of concrete with the fine flaky particles deteriorated by 35, 52 and 73% for the replacements of 5, 10 and 15%, respectively.

Mostafizur Rahman et al [19] used high density polyethylene (HDPE) in concrete. The particle sizes of HDPE were 4 to 12 mm and were used to replace coarse aggregate. The plastic aggregate was used with the replacements of 10, 15, 20 and 25% of the total volume of the sample. The compressive strength was reduced sharply with increasing the content of HDPE. The reductions were 58, 62, 70 and 80% in the compressive strength with the substitutions of 10, 15, 20 and 25%.

Ruiz-Herrero et al. [39] used polyethylene (LDPE) as an additional material in the concrete with four percentages (2.5, 5, 10 and 20%). From the experimental results, the mechanical properties of concrete with polyethylene decreased with increasing the content of the plastic. The reductions in compressive strength were 90, 72, 27 and 14% for plastic content of 20, 10, 5 and 2.5%, respectively, while the reductions in flexural strength were 78, 36,

24 and 13%. The thermal conductivity of the samples was reduced with increasing the content of polyethylene. The reduction in thermal conductivity was negligible for the content of 2.5%, as compared to the control (without LDPE), while it was reduced by 16 and 44% for the plastic content of 5 and 10%, respectively. The samples with plastic content of 20% could not be measured due to their very poor surface (high content of plastic with low volume of paste).

Lei Gu et al. [24] have provided a comprehensive review on the usage of all types of plastics such as HDPE, LDPE, PET, PVC and plastic fibers in concrete. All results proved that the strength of plastic concrete was dropped, while the thermal resistivity was enhanced.

In general, the addition of plastic in the concrete mixtures has beneficial effect on some of the material properties such as thermal insulation, sound insulation, lower-density and higher ductility. On the other hand, other properties (compressive strength and flexural strength) are negatively affected [17-25].

2.3 Concrete Masonry Bricks (Blocks) Made with Rubber, Plastic and Perlite

Although there has been a lot of research on the use of crumb rubber in normal concrete, less studies were focused on its usage in concrete masonry blocks [48]. Therefore, in this research, rubber and plastic were used in masonry bricks to investigate the applicability of their usage in masonry mixes.

Frankowski [49] had a patent on the use of crumb rubber in masonry bricks. The concrete masonry units (CMUs) comprising 100 parts of cement, 100-700 parts of mineral aggregate, 10-50 parts of water and 5-15 parts of rubber (by weight of cement). The average particle size of rubber was in the range of 0.5 to 1.19 mm. The patent claimed that the addition of rubber particles to the blocks decreased thermal conductivity and compressive strength. The strength of masonry bricks satisfied the ASTM C 90 for non-load bearing units (4 to 5.5 MPa).

Cairns et al. [48] used the recycled tires rubber in masonry concrete bricks. The rubber was added to the mixture at three percentages (10, 25 and 50%) with a water to cement ratio of 0.87. Two sizes of coarse aggregate were used (6 and 10 mm), while rubber particles substituted only the largest size of the coarse aggregate. After 28 days of curing, the compressive strength of the rubberized bricks was measured. The strength was reduced by 22, 23 and 41% with a rubber substitution of 10, 25 and 50%, respectively. Further, the same authors coated the rubber particles with cement paste to increase the bond between the rubber and the matrix [48]. Their results displayed a little improvement in the strength.

Piti et al. [50] used crumb rubber as a substitution of fine and coarse aggregates in pedestrian blocks. Two rubber sizes were used (No. 6 and No. 20) with two dosages (10 and 20% by weight). The outcome of the experiments proved that the strength was significantly affected by rubber size and content. For 10 and 20% replacements with No. 6 rubber size, the strength was reduced by almost 45 and 85%, respectively, as compared with the control mix, which was almost similar to the smaller size of rubber particles (No. 20). On the other hand, the combination of the two sizes of rubber particles improved the strength by 15 and 29% compared to the previous two sizes of crumb rubber.

Ling [51] replaced fine aggregate in the mixture of masonry blocks with recycled crumb rubber with 5 to 50% by volume. The size of rubber particles was 1 to 5 mm and the water to cement ratio was 0.45 to 0.55. The results showed that the strength and density were reduced and influenced by the content of rubber and w/c ratio.

Al-Aqeeli et al. [52] has a patent on the usage of crumb tire rubber as replacement to sand in the mixture of masonry blocks satisfying the ASTM C 129 standards for non-load bearing units. The crumb rubber was both coarse (1.5 to 5 mm) and fine (50 to 250 μm) particles. The authors claimed that the block mixture comprising 20-30% cement, 50-60% mineral aggregate and 1-10% water and 10-20% crumb rubber by weight. Three types of blocks were prepared with the addition of fine rubber, coarse rubber and both. The strength of the blocks with fine and both (fine and coarse) rubber was very close to about 3.50 MPa, relatively the coarse rubber particles a higher strength by around 50% was achieved. The highest absorption was noted with fine rubber blocks then the combination and the least with the coarse rubber block. The thermal conductivity of fine and both rubber sizes achieved the least conductivity, while the coarse rubber blocks had a higher conductivity by about 21%.

Sodupe-Ortega et al. [53] have investigated the addition of rubber in masonry bricks. Mortar mixes were prepared with different w/c ratios (0.7 to 0.9) with rubber particle sizes of 1 to 4 mm. The rubber addition was a substitution of sand with percentages of 10 to 40% by weight. The outcomes proved that the strength of the blocks was reduced with increasing the content of rubber and became unrecommended for rubber content higher than 20%. Further, the reduction in the strength was marginal with the increase in the w/c ratios.

Safinia and Alkalbani [54] used plastic bottles inside concrete blocks (8 bottles per block) at equal distances. The results showed that the compressive strength of plastic blocks was 57% higher than the market hollow concrete blocks in Oman market. Similarly, Wonderlich [55], in a master thesis, proved that the strength of blocks with plastic bottles (8 bottles per block) was slightly different compared to the strength of standard cylinders (75 mm dia. and 150 mm thickness). Although the author did not test the block for thermal conductivity, the plastic blocks will give higher thermal resistivity, as his expectations.

Mathew et al. [56] used waste plastic (LDPE) as a replacement of coarse aggregate with different percentages (5 to 30% by volume) in solid concrete blocks. The plastic particle size was similar to the replaced size of natural aggregate. The compressive strength of plastic block was slightly lower than the normal concrete blocks.

Duvier et al. [7] had a patent on perlite blocks. The perlite was mixed with cement, fly ash and air entrainer. For each part of cement, 24 parts of expanded perlite was added to the mixture by volume. This invention was claimed to produce load bearing, lightweight and high thermal insulation blocks. The perlite blocks had a lower density of about 50% of the conventional blocks with the same size. Further, the thermal resistivity was decreased by about 50 to 100%, as compared to the control. The compressive strength was about 7 MPa, thereby satisfying the load bearing blocks (ASTM C 90).

Topcu and Iskdag [10] used perlite in clay bricks to produce high thermal resistant bricks. The binding materials were cement, clay, lime, gypsum and bitumen. Perlite was added by a total volume in the range of 5 to 50%. The results showed that the compressive strength was reduced with increasing the perlite content. For the conventional clay bricks, the

strength was 5.8 MPa, while the least strength was 2.0 MPa depending on the perlite replacement ratio. The thermal conductivity was reduced about by 52% for 30% perlite replacement as compared to the control brick.

Al-Hadhrami et al. [57] have conducted an experimental program to find out the effect of adding insulation materials inside the cavities of concrete and clay bricks such as perlite, polystyrene and mineral wool. The addition of perlite in the hollows of concrete bricks enhanced the thermal conductivity by around 50%, while it was reduced to 10% for clay bricks.

Sengul et al. [13] studied the effect of perlite on the strength and thermal conductivity of lightweight concrete. The particle size of perlite was 0.50 to 2 mm that replaced natural aggregate with percentages of 20 to 100%. Superplasticizer and air entraining admixtures were added to the mix. The results proved that the strength and thermal conductivity were reduced sharply by 84% and 42% for the substitution by 60% perlite.

2.4 Finite Element Modelling (FEM) for Masonry Hollow Bricks

Al-Hazmy [58] studied the heat transfer through masonry hollow bricks to investigate the effect of the cavities. Three types of masonry hollow bricks were prepared with cavities filled by: air, solid polystyrene and hollow polystyrene. The convection inside the cavities was considered using a system of conservation equations. His results proved that the cavities filled with solid polystyrene reduced the heat rate by a maximum of 36%, while the overall daily reduction on the heat rate was 25% for a typical summer day in Jeddah -

Saudi Arabia. On the other hand, the hollow polystyrene decreased slightly the heat rate by only 6% because of the air circulation inside the cavities.

Del Coz Diaz et al. [59] conducted both experimental work and thermal simulation using FEM for hollow concrete brick walls with different thermal conductivity coefficients for the bricks (two k-values) and mortar (three k-values). Their results indicate a good agreement between numerical and experimental results, thereby providing the fact that increasing the thermal conductivity of masonry blocks decreased the insulation of the wall. Therefore, the comparison between the two methods demonstrated the reliability of the finite element method as an accurate method to estimate the thermal conductivity of hollow bricks with reasonable time solution.

Del Coz Diaz et al. [60] conducted a finite element analysis to find the accurate solution of heat transfer equation for five different hollow concrete brick walls (different geometry and arrangements of cavities). The nonlinearity was due to boundary conditions of radiation and convection inside the cavities of the bricks. The other phenomena, such as conduction and convection, were also considered. Finally, from the analysis of the five hollow bricks with different geometries, the optimization of the walls has been carried out from the finite element model with overall thermal efficiency of about 12%, which was double, as compared to the worst model.

Del Coz Diaz et al. [61] also conducted a numerical study to find the optimum brick using finite element model (FEM). Four hollow bricks with different cavities geometry were analyzed and the best candidate was determined, which was simulated with different thermal conductivity coefficients (five values) and three mortar types to investigate the

effect of the difference in thermal conductivity. The simulation was conducted for 15 configurations. The equivalent thermal conductivity depends on conduction through the solid brick, mortar, radiation and convection.

Del Coz Diaz et al. [62] carried out numerical (2-D wall) simulation using FEM to find out the optimum geometry of cavities for six different hollow concrete bricks. The results indicated that the size, width and distribution of holes tend to affect the thermal performance of the walls. Therefore, the best candidate brick has been chosen. Furthermore, an analysis with three-dimensional walls was carried out for the best brick with changing the thermal conductivities of mortar and brick obtained from experimental program. The results showed that the heat transfer through the wall depended on conduction through solid brick and mortar, convection and radiation through the holes of the brick. The higher mass overall thermal efficiency is, the higher will be resistivity and the lower weight of the wall.

Baig and Antar [63] estimated numerically the R-value (thermal resistivity) for five different cavities layout filled with air (normal case). Their results showed that changing the arrangement and number of cavities tend to increase the R-value significantly. Increasing the aspect ratio (width/height of cavity) reduces the convection (air motion) inside the cavities, which tends to reduce the heat flow. Increasing the number of cavities reduced the length (perpendicular to heat flow) of the cavities. Hence, the aspect ratio would be reduced, which means more convection and radiation inside the cavities (i.e. heat transfer through the cavities increased). Further, with increasing the number of cavities, the number of thermal bridges increased, thereby more heat would be transferred through conduction.

Oluwole et al. [8] investigated the effect of holes on heat conduction through conventional and interlocking bricks using MATLAB. Their results showed that the interlocking bricks with four staggered cavities reduced significantly the thermal conductivity. On the other hand, increasing the number of holes more than four did not have a positive impact. For conventional bricks, the staggered arrangement for holes did not achieve significantly the thermal resistance but the bricks with four cavities were considered effective for thermal insulation. Increasing the number of cavities, more than four in conventional bricks, achieved minimal thermal resistivity advantage.

Zhou et al. [5] analyzed numerically (using ABAQUS) and experimentally the thermal insulation performance of a new design of concrete wall panel using gypsum layer inside the concrete. The results of their experiments and simulation have shown that gypsum increases the thermal insulation of building envelopes with 1.1°C.

Del Coz Diaz et al. [9] have recently designed FEM simulation and experimental program for lightweight hollow bricks to measure moisture and temperature distributions with air-filled cavities. Two-dimensional model was satisfying the standards of ISO 6949 for the film coefficient to include the convection and radiation inside the cavities. There was a good agreement between the experiment and the simulation to measure the thermal performance of the wall with various moisture contents. Further, the authors have conducted an experimental setup in the lab using a 1 m^3 hot-box connected to a special climatic chamber. In order to measure the thermal flux, the temperature, thermal transmittance and relative humidity distributions in a one square meter wall, a total of 32 sensors were used (sensors located in the recesses and outer face). These experimental tests have allowed to fit and improve the mathematical models using FEM analysis and design

of experiments (DOE) technique. This procedure has allowed energy and time savings of approximately 70% with respect to the real test procedures.

Roberto et al. [64] have carried out thermal simulation using FEM for hollow clay bricks to investigate the effect of radiation inside the cavities in the heat transfer. Several bricks were analyzed with 12 different geometry and two thermal conductivities of clay. The internal faces of the cavities were painted with many coating materials with different emissivity coefficients. The results showed that coating the interior faces of the cavities reduces the thermal conductivity of the bricks by about 26 to 45% for a surface of emissivity of 0.1.

Al-Tamimi et al. [1] have recently studied the configuration of geometry for hollow concrete bricks in the heat transfer using finite element model. Convection and radiation inside the cavities were included according to EN ISO 6946. The analysis was carried out for 23 models with different arrangements of cavities for hollow concrete bricks. Their results showed that the average inner surface temperature of the hollow brick could be decreased by 7.18°C for concrete brick with a hollow ratio of 51%. Further, it was observed that the shape, number and arrangement of holes had appreciable effect on the heat flow through hollow bricks. The same authors have recently conducted a thermal simulation for a room (with and without plastering) with two types of slab (solid and one way ribbed slab) to investigate the heat flow through the roofs [2]. Their research proved that one-way ribbed slab was thermally more efficient and better than solid slab by 19 and 17% for plastered and non-plastered rooms, respectively. Further, the authors [65] have developed a FEM for a hollow brick masonry wall by filling the cavities with different insulation materials. Three types of mortar were used to join the bricks (ordinary, light and insulation

mortars). The insulation and light mortars reduced the temperature by 1.30 and 0.60°C as compared to ordinary mortar. The effect of mortar was reduced with increasing the thermal conductivity of the cavity insulation material.

CHAPTER 3

FINITE ELEMENT MODELING

3.1 Introduction

In this study, ABAQUS 6.13 software was used to develop a 3D finite element model (FEM) to find the optimum cavities arrangement of hollow bricks from thermal point of view. The hollow brick with the optimum cavities layout could be assessed by using the average interior surface temperature, which was assumed to be T_i °C. The FEM could help to find the temperature distribution and the average temperature of the interior/exterior surfaces of the hollow brick.

In this study, the following three processes of heat transfer were considered: conduction, convection and radiation, as clearly shown in Figure 3.1. The conduction occurs through the solid material of the bricks while the heat transfer by convection and radiation occurs between the ambient air and the outer and inner wall surfaces as well as through air cavities of the hollow bricks. The thermal radiation is attributed to the solar radiation that causes energy emission, the latter being dependent on the material's emissivity coefficient and the temperature variation between the outer and inner wall surfaces [6]. Convection and radiation inside the cavities (air-filled cavity) of the hollow bricks were included in the simulation, whereby the equivalent convection film coefficient was estimated according to EN ISO 6946 [16]. As shown in Figure 3.1, the convection and radiation for the exterior walls released the heat to outside. The same phenomena also occurs for the interior walls.

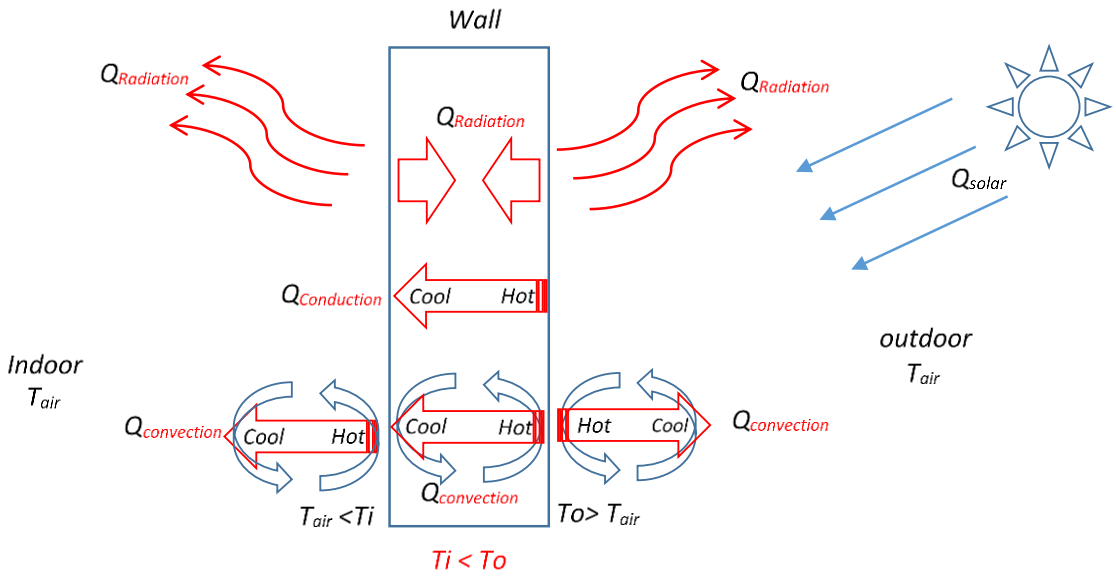

Figure 3.1: Diagram for heat transfer processes (conduction, convection and radiation) through the wall

In this research, three types of media were simulated for the cavities of the hollow bricks (vacuum, polystyrene and air), as clarified in Figure 3.2. First, the cavities were assumed to be vacuum (no air inside the cavities), which means that the heat transfer through the wall would be only by conduction without heat transfer through the cavities. This case does not occur in the field and it was considered only for the sake of relative comparison. Second, the cavities were filled with polystyrene boards, thereby allowing the heat flow through the cavities by conduction, as normally practiced by the construction industry. Third, the cavities were assumed to be filled with air (the normal case), i.e., the heat transfer through the cavities would take place by convection and radiation (air circulation inside the cavities). Therefore, the best hollow bricks from the three simulations would confidently be the optimum. Further, the assumption of the cavities as vacuum was used to obtain the average inner temperature of the cavities walls, which was used as sink

temperature (cavities air temperature) inside the cavities in the next simulations (air-filled cavity).

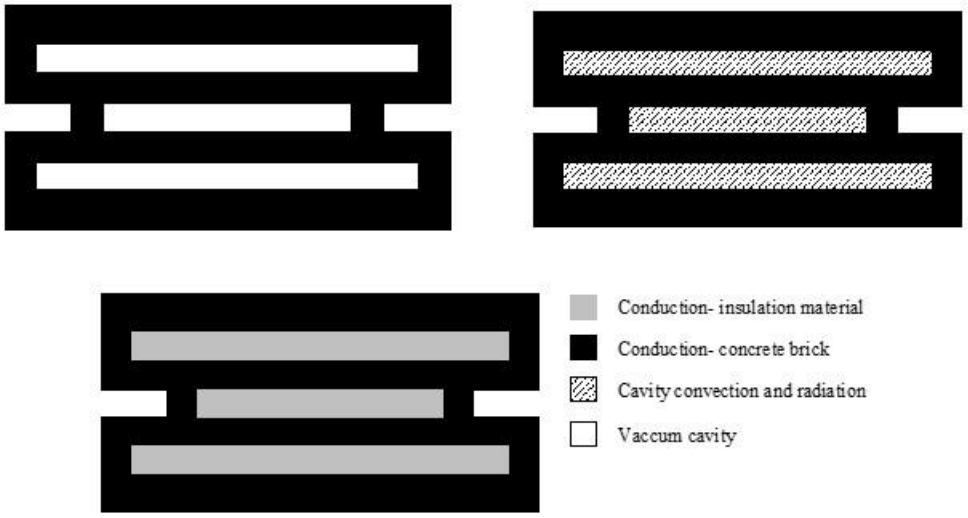

Figure 3.2: Heat transfer through the cavities of hollow brick; (a) Vacuum cavities, (b) Air-filled cavities, (c) Insulation materials filled cavities.

Models of one brick were analyzed to find out the effect of cavity layout on reducing the heat transfer. For this task, eleven hollow bricks with different cavity arrangements (in addition to one solid model for relative comparison) were studied in order to obtain the model with the optimum hollow layout. First, the simulation was run with the assumption of vacuum cavities for the eleven blocks. The second simulation was only majored by conduction because the cavities were filled with boards of polystyrene. In the third simulation, convection and radiation were applied inside the cavities (i.e., cavities were filled with air) with the sink temperature (air temperature inside the cavity) calculated from the first simulation (vacuum cavity).

3.2 Geometry of Masonry Bricks

In this study, eleven hollow bricks with 400 × 200 × 200 mm dimension and different cavity configurations were assessed thermally. Two hollow blocks were chosen based on survey of the commonly used bricks in the construction of buildings in eastern Saudi Arabia. The solid brick (SB) and two-common market hollow bricks (M-HB1 and M-HB2) were with two and three equal cavities are shown in Figure 3.3. The other nine hollow bricks were designed to achieve better thermal performance as compared to the market hollow bricks. The designed hollow bricks (D-HB) were satisfying the minimum dimensions requirements for ASTM C129 standards for non-load bearing masonry units such as the minimum dimensions of web and face shell. In the previous work [1], the factors affecting the heat transfer through the bricks were studied such as the hollow ratio, aspect ratio (width perpendicular to heat flow/height of cavity), thermal bridges, number and arrangement of cavities. These factors were taken into consideration during the design of the hollow bricks, which have high hollow ratio, high aspect ratio, lower number of cavities and thermal bridges. On the other hand, the selected market hollow bricks have higher hollow ratio and lower aspect ratio, as compared to designed hollow bricks. The designed hollow bricks (D-HB) were divided into two groups (G1 and G2) with different hollow and aspect ratios, number and arrangement of cavities, as shown in Figure 3.4 and Figure 3.5. The main difference between the two groups (G1 and G2) was the connection between the bricks, which is the normal case in the field. As shown in Figure 3.6, the polystyrene boards were combined with the brick cavities.

Two joined bricks (D-G1-HB5, D-G1-HB4, D-G2-HB4) were used to investigate the effect of the cavity at the joint. Each group has a different cavity at the joint between the bricks, as illustrated for G1 and G2 in Figure 3.7. The connection area between the bricks does contribute significantly in the heat transfer to the interior brick surface, which works as thermal bridges. Therefore, the designed cavity at the joint between the two bricks will mitigate the heat flow to the inner wall surface.

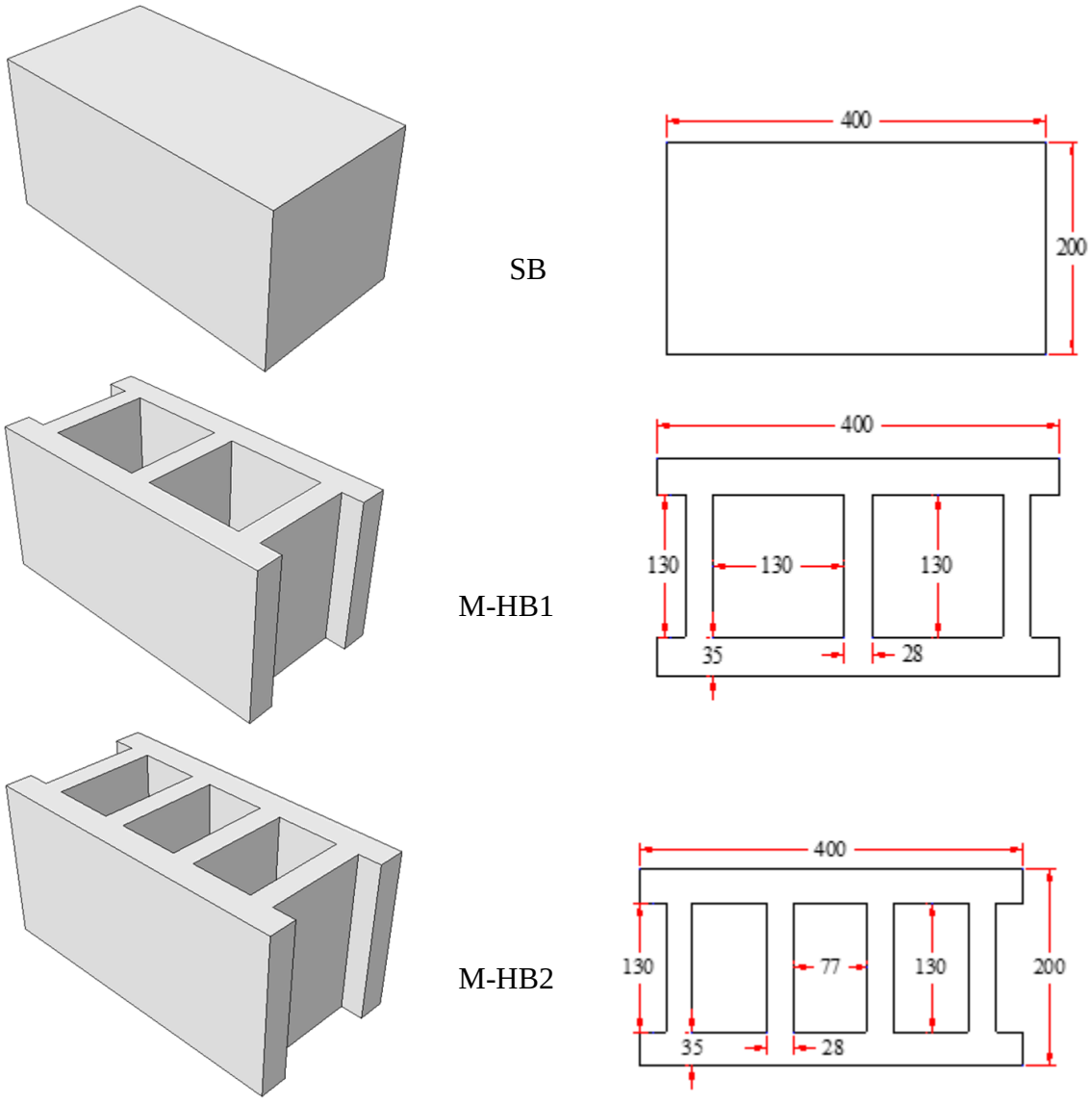

Figure 3.3: Market solid and hollow bricks (M-HB) (SB)

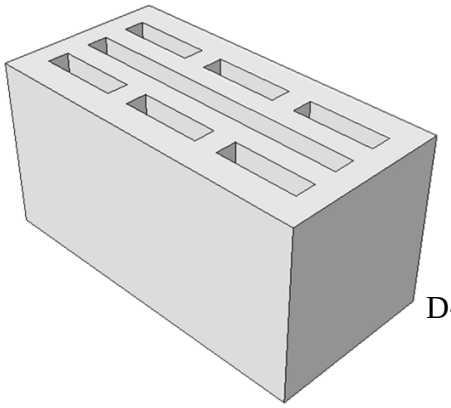

D-G1-HB1

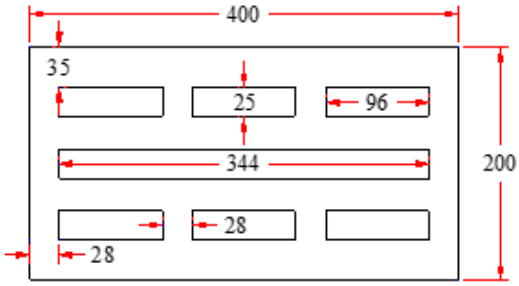

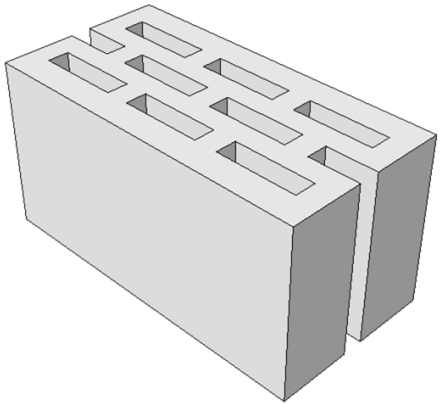

D-G1-HB2

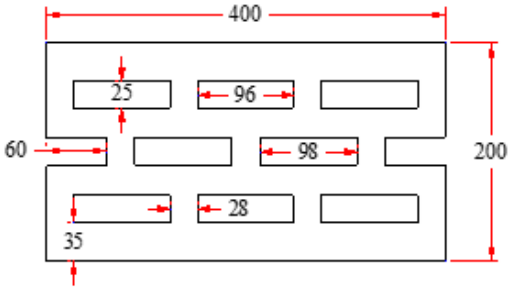

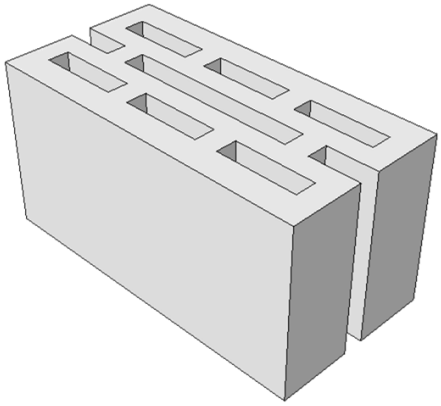

D-G1-HB3

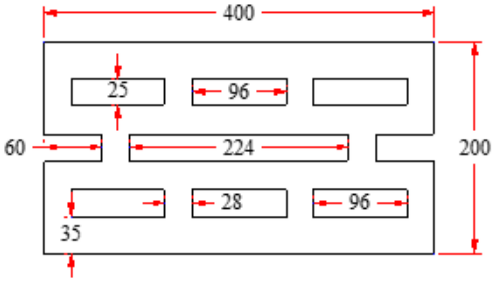

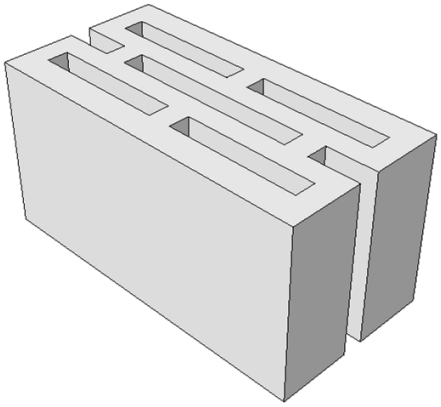

D-G1-HB4

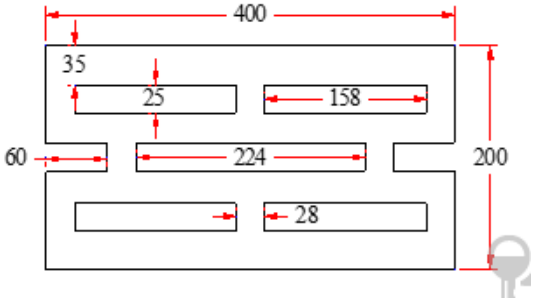

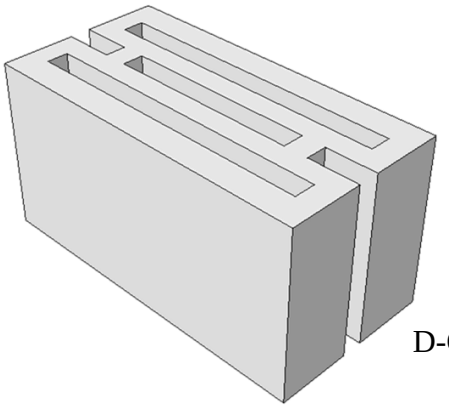

D-G1-HB5

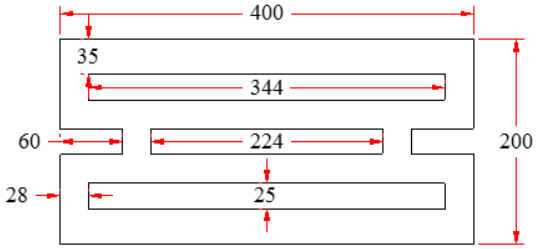

Figure 3.4: Designed hollow bricks - Group 1 (D-G1-HB)

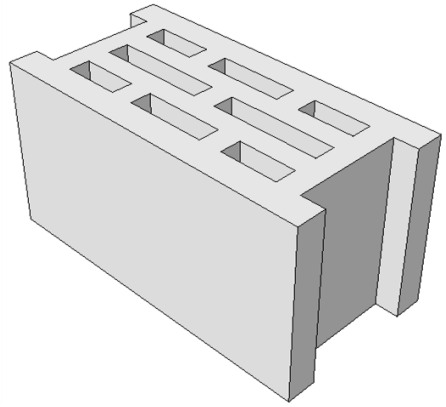

D-G2-HB1

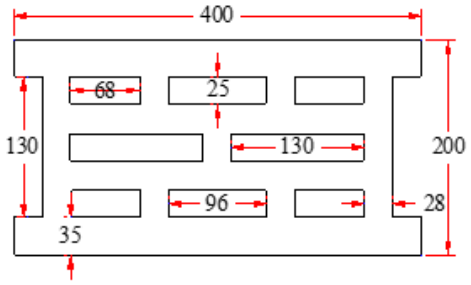

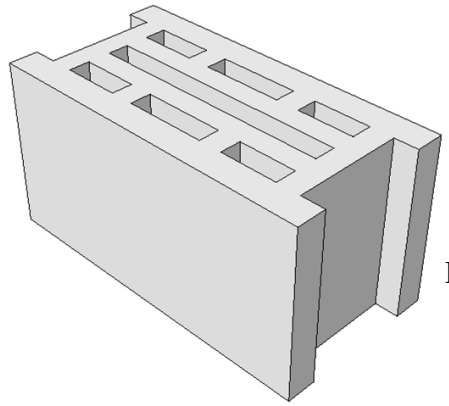

D-G2-HB2

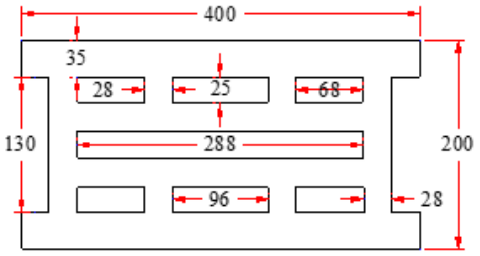

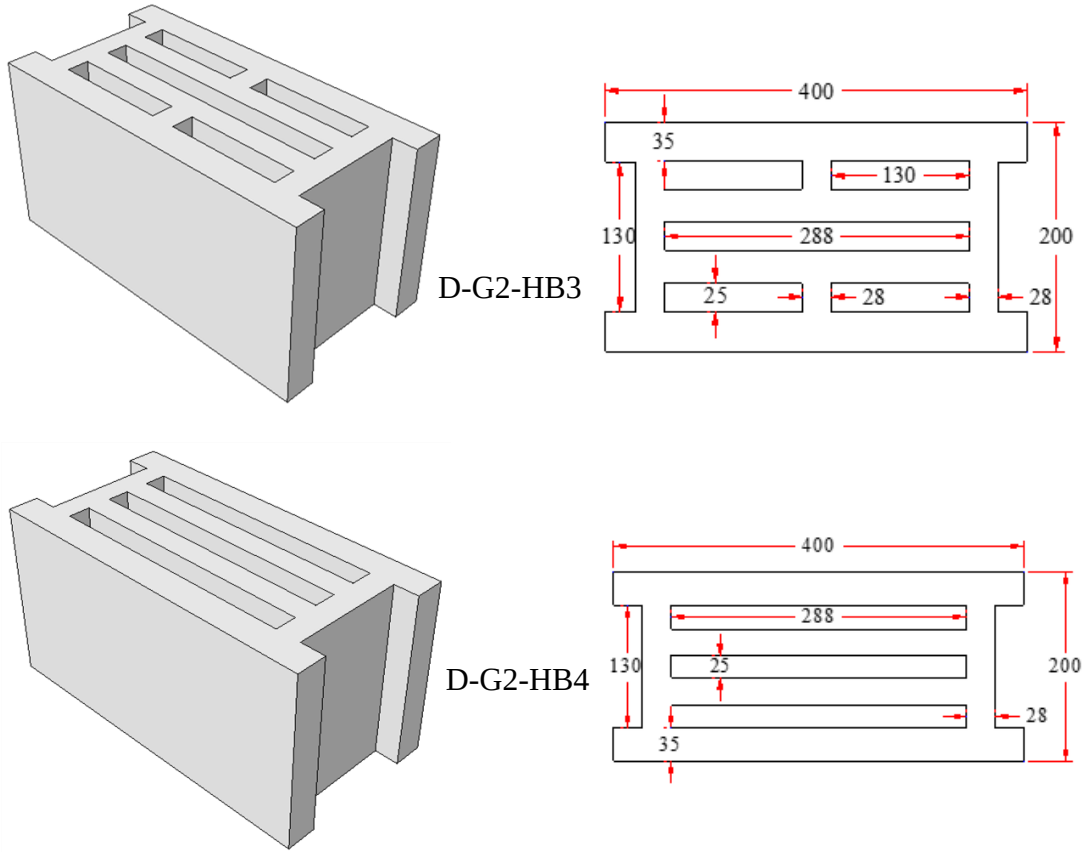

Figure 3.5: Designed hollow bricks - Group 2 (D-G2-HB)

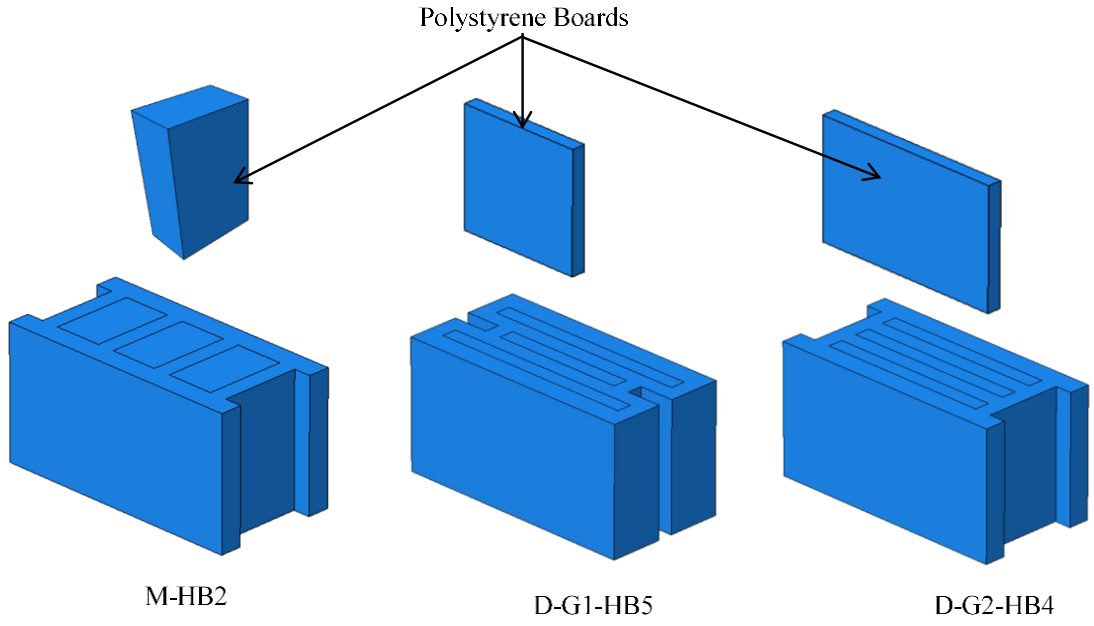

Figure 3.6: Hollow concrete bricks with polystyrene filled cavities

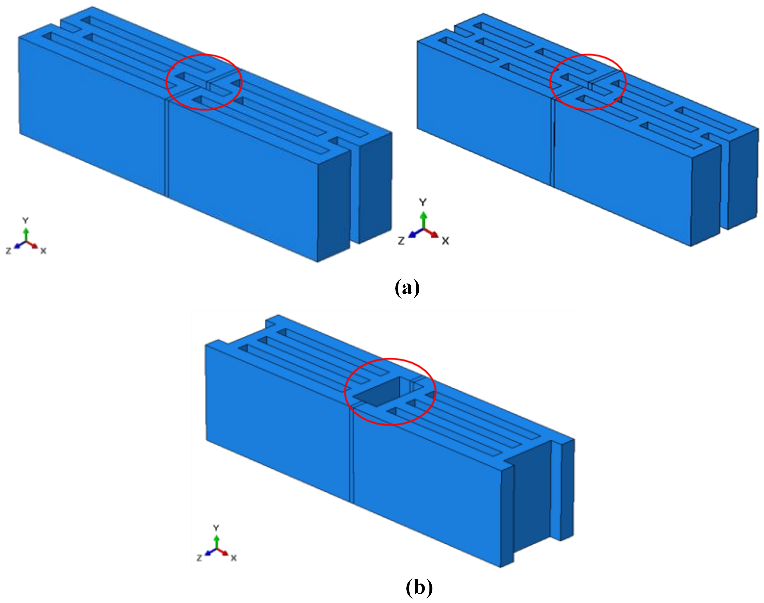

Figure 3.7: Two hollow brick models: (a) Group 1 connection; (b) Group 2 connection

3.3 Mathematical Modeling

The temperature distribution in the brick for a steady state, three-dimensional heat conduction in a homogenous medium with a constant thermal conductivity and no heat source, is governed by the following partial Equation 3.1 (Laplace Equation) [1].

$$\frac{\partial^2 T}{\partial x^2} + \frac{\partial^2 T}{\partial y^2} + \frac{\partial^2 T}{\partial z^2} = 0 \qquad 3.1$$

3.3.1 Boundary Conditions

In order to solve Equation (3.1), the boundary conditions (B.C) at all the surfaces have to be identified. Figure 3.8 shows the boundary conditions at the interior and exterior surfaces of the brick including the convection and radiation.

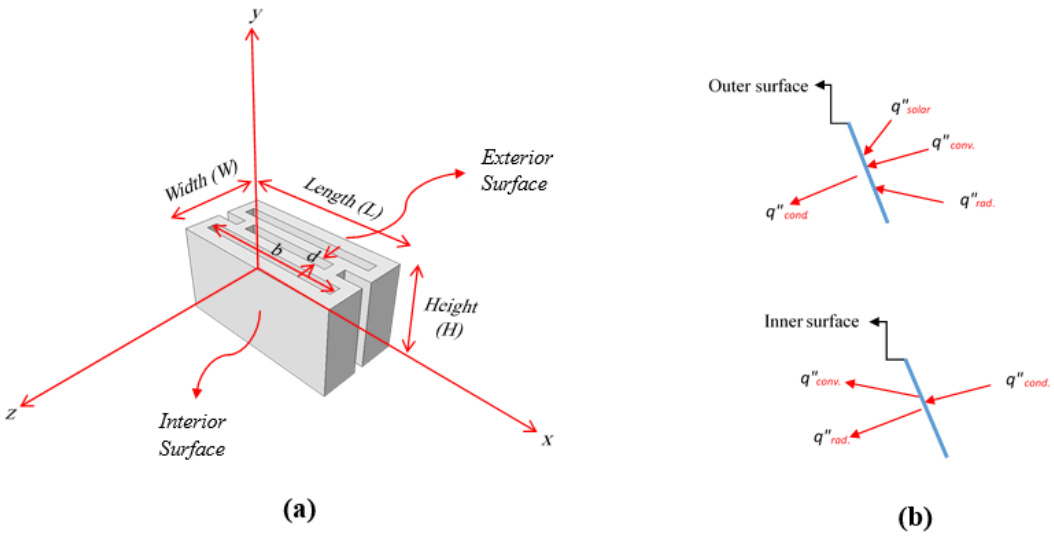

Figure 3.8: Hollow brick: (a) Axis and dimensions; (b) Conduction, convection and radiation on exterior and interior surfaces

For the outer surface of the brick, which is exposed to the solar load (during the day) and natural convection, the B.C can be written as follows:

$$At\ z = 0, -k\frac{\partial T}{\partial z} = q"_{solar} + q"_{conv.} + q"_{rad.} \qquad 3.2$$

$$-k\frac{\partial T}{\partial z} = q"_{solar} + h_{co}[T_{ao} - T(x,y,z=0)] + \varepsilon\sigma[T^4{}_{so} - T^4(x,y,z=0)] \quad 3.3$$

Similarly, the inner surfaces of the bricks have the following conditions:

$$\boldsymbol{At\ z = W,\ -k\frac{\partial T}{\partial z} = q"_{conv.} + q"_{rad}} \quad 3.4$$

$$\boldsymbol{-k\frac{\partial T}{\partial z} = h_{ci}[T(x, y, z = W) - T_{ai}\ ] + \varepsilon\sigma[T^4(x, y, z = 0) - T^4{}_{si}]} \quad 3.5$$

where:

T_{ao} = Air outer temperature = 45°C (318°K), which is the average air temperature during summer in Saudi Arabia.

T_{ai} = Room desired temperature = 25°C (298°K).

For the top, bottom and side surfaces of the brick, symmetrical B.Cs were assumed and, hence, no heat loss occurred. Therefore, the following conditions should be satisfied:

$$\boldsymbol{At\ x = 0,\ x = L} \quad 3.6$$

$$\boldsymbol{-k\frac{\partial T}{\partial x} = 0,\ at\ x = 0, L} \quad 3.7$$

$$\boldsymbol{At\ y = 0,\ y = H} \quad 3.8$$

$$\boldsymbol{-k\frac{\partial T}{\partial y} = 0,\ at\ y = 0, H} \quad 3.9$$

For all the inner surfaces of brick holes, it is assumed that there is no heat transfer, hence, the following condition is satisfied:

$$\boldsymbol{-k\frac{\partial T}{\partial n} = 0, n: normal\ coordinate\ to\ any\ surface} \quad 3.10$$

3.3.2 Convection and Radiation in Air Cavities of Hollow Bricks

For the rectangular and square cavities of hollow bricks, convection and radiation were considered using the EN ISO 6946 standard [16], which an equivalent method to calculate

the convection and radiation inside the cavities. This method was based on the equivalent film coefficient (h_{eq}), which was calculated as following [16]:

$$\boldsymbol{h_{eq} = h_a + h_r} \quad 3.11$$

where: h_a is the convection film coefficient which is the higher value between 1.25 W/m^{2}K and (0.025/d)

Radiative Film Coefficient (h_r):

For unventilated airspaces with cavity length (h) and cavity width (b) both of which are more than 10 times the cavity thickness (d):

$$\boldsymbol{h_r = \frac{h_{r0}}{\frac{1}{\varepsilon 1}+\frac{1}{\varepsilon 2}-1}} \quad 3.12$$

For small airspaces with a cavity width (b) less than 10-times its thickness (d):

$$\boldsymbol{h_r = \frac{h_{r0}}{\frac{1}{\varepsilon 1}+\frac{1}{\varepsilon 2}-2+\frac{2}{\left(1+\sqrt{1+\frac{d^2}{b^2}}-\frac{d}{b}\right)}}} \quad 3.13$$

where: h_{r0} is the radiative film coefficient for a black surface body and can be found from EN ISO 6946 standard [16], which depends on the average temperature of hot and cool surfaces of the air cavity.

Based on the previous calculations, the equivalent film coefficient (h_{eq}) was estimated for each cavity of the hollow bricks, as summarized in Table 3.1. Similar calculations and application for h_{eq} have been implemented in FEM for the study of thermal and moisture transfer by Del Coz Díaz [9]. Further, the sink temperature (air temperature inside the cavity) was estimated form the simulation of vacuum cavities, as shown in Table 3.1.

Table 3.1: Equivalent film coefficient for cavities in all hollow bricks

Brick Models	h_{eq} (W/m^2k)	Cavities Temperature (°C)
M-HB1	5.28	53.31
M-HB2	4.91	53.45 – 53.61
D-G1-HB1	6.18 - 6.73	76.13 – 53.23 – 30.21
D-G1-HB2	6.18 - 6.19	69.1 – 53.32 – 37.56
D-G1-HB3	6.18 - 6.47	70.48 – 53.23 – 36.01
D-G1-HB4	6.38 - 6.47	70.61 – 53.16 – 35.80
D-G1-HB5	6.47 - 6.73	68.43 – 53.19 – 37.78
D-G2-HB1	5.99 - 6.18 - 6.31	69.44 – 53.37 – 36.98
D-G2-HB2	5.99 - 6.18 - 6.73	75.29 – 53.38 – 31.14
D-G2-HB3	6.31 – 6.73	72.14 – 53.23 – 34.30
D-G2-HB4	6.73	69.42 – 53.30 – 36.99

3.4 Thermal Properties of Concrete Bricks

The thermal properties of the materials used in the finite element models were obtained from literature [1, 18], as presented in Table 3.2. These properties were quoted from the literature to represent the indigenous concrete bricks used in the Saudi market.

Table 3.2: Thermal properties of concrete bricks [1, 18]

Property	Value (Units)
Bricks thermal conductivity (K)	0.72 (W/m.k)
Mortar thermal conductivity (K)	0.72 (W/m.k)
Polystyrene thermal conductivity (K)	0.033 (W/m.k)
Inner and outer film coefficient (h_{in}, h_{out})	5 (W/m^2k)
Emissivity coefficient ($\mathcal{E}$)	0.88
Absorption coefficient (α)	0.6

3.5 Finite Element Model

Finite element modelling (FEM) was conducted to investigate the effect of cavities geometry layout of masonry hollow bricks on the heat transfer using ABAQUS software. The heat transfer processes were considered including conduction, convection and radiation. Further, the following three cases were considered for the cavities: vacuum, polystyrene and air cavities. For convection, the inner ambient air temperature was taken as 25°C (298°K) as was often practiced by the Saudi families, while the outer temperature was taken as 45°C (318°K), which is the maximum ambient temperature during summer days in Dhahran, eastern Saudi Arabia [2]. In ABAQUS, convection was applied in both outer and inner surfaces of the brick as well as inside the cavities. Therefore, the film coefficients in Table 3.1 and Table 3.2 were defined in ABAQUS through the interaction phase (Surface Film Condition), which depends mainly on the film coefficient and sink temperature. The sink temperature was calculated as the average interior surface temperature of the cavities (from the simulation of vacuum cavities), as summarized in Table 3.1.

The radiation for both brick surfaces and inside cavities was applied through the surface radiation interaction (in ABAQUS), which depends on the brick emissivity coefficient (Table 3.2). Stefan Boltzmann constant is equal to 5.67×10^{-8} ($W/m^2 k^4$) [17]. The average solar radiation directed to the exterior surface of the brick was 746 W/m^2 (for Dhahran region), and around 60% of the solar radiation was absorbed by the brick, (i.e. the absorbed heat was 448 W/m^2) [20].

3.6 Mesh Optimization

In the preliminary simulation, mesh-independence was conducted for the most complex hollow bricks (D-G1-HB1) because the results in FEM were significantly changed with varying the geometry of the model, as depicted in Figure 3.9 (a). Five mesh sizes were used, which were in the range of 3 to 20 mm to find out the optimum mesh size. As shown in Figure 3.9 (b), reducing the mesh size decreases the difference in the average inner surface temperature (T_i) until the difference was negligible between 5 and 3 mm (less than 0.04%). Therefore, the optimum mesh size of 5 mm was selected for the simulation to save time and reduce error. The total number of nodes varied within the models under consideration where the minimum total number of nodes is for H-1 (with 78,925 nodes) and the maximum number of nodes is for the solid brick (with 136,161 nodes).

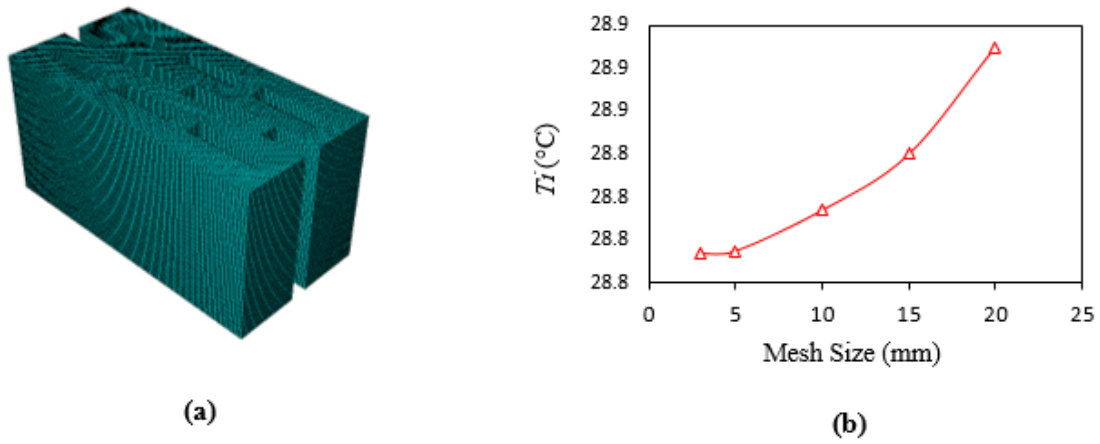

Figure 3.9: Hollow brick: (a) 5-mm mesh size for D-G1-HB1 model; (b) Mesh optimization curve

3.7 Results of Modelling

3.7.1 Nodal Temperature

Figure 3.10 shows the nodal temperature distribution (NT11) (as depicted in the scale in Kelvin degrees) through Models D-G1-HB5 and D-G2-HB4 (as examples) from ABAQUS software. The different colours depict the temperature distribution from higher level (outer surface) to lower level (inner surface) of the block. As shown in Figure 3.10, the maximum NT11 for D-G1-HB4 and D-G2-HB4 Models is 341 and 340.90°K for outer surfaces, respectively, while the minimum NT11 is 301.30°K for both inner surfaces.

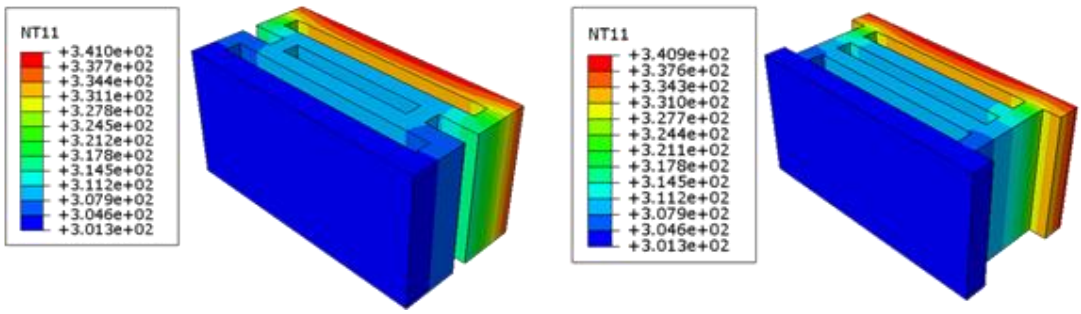

Figure 3.10: Nodal temperature distribution (NT11) (°K) through the hollow bricks

3.7.2 Average Interior Surface Temperature (T_i) of One Brick

In this simulation, the assessment of the hollow bricks was based on the average interior surface temperature (T_i), which was calculated for 3321 nodes, as shown in Figure 3.11.

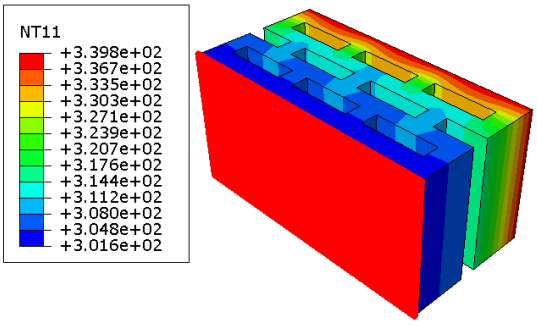

Figure 3.11: 3321-nodes at the inner surface of D-G1-HB2 model

The results of the average interior surface temperature for the twelve bricks were summarized in Table 3.3 with their hollow ratio (HR), aspect ratio (AR) and width of cavities. The hollow ratio (HR) is defined as the total area of the cavities divided by the cross-sectional area of the brick. Figure 3.12 presented he aspect ratio (AR), which is the cavity length (perpendicular to heat flux "a") divided by the height of cavity (h). The cavity width is in the same direction of heat flux (b), as shown in Figure 3.12.

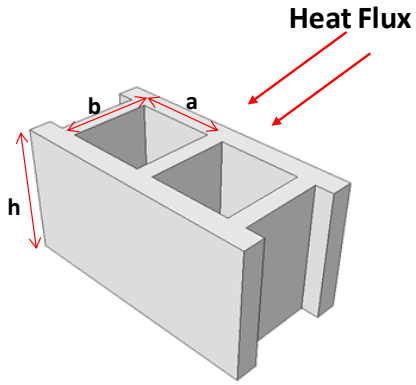

Figure 3.12: Definitions for the cavities of hollow brick

As shown in Table 3.3, the HR and AR for all blocks was in the range of 24 to 42% and 0.30 to 1.72, respectively. Further, the width of cavities (parallel to heat flow) was the same for all the designed and market hollow bricks with values of 25 and 130 mm, respectively, as shown in Figure 3.3, Figure 3.4, Figure 3.5. In this research, the concern was about the average inner surface temperature because the main objective of this FEM investigation was to reduce T_i through changing the geometry and arrangement of the cavities to reduce the heat flow to the inner surface to minimize the energy consumption.

Table 3.3: Simulation results for all bricks and cases

Groups	Brick Models*	Aspect Ratio (AR) %	Cavity Width (mm)	Hollow Ratio (HR) %	T_i (°C)		
					Vacuum cavity	PS cavity	Air cavity
Market	M-HB1	0.65	130	42.25	29.20	29.50	33.95
	M-HB2	0.385	130	37.70	30.39	30.75	34.33
Group 1	D-G1-HB1	0.48-1.72	25	28.75	28.45	30.19	30.50
	D-G1-HB2	0.48-0.30	25	25.06	29.28	30.21	30.98
	D-G1-HB3	1.12-0.48-0.30	25	25.17	28.50	30.16	30.45
	D-G1-HB4	0.79-1.12-0.30	25	27.79	27.8	29.40	29.90
	D-G1-HB5	1.72-1.12	25	29.61	26.97	28.60	29.85
Group 2	D-G2-HB1	0.34-0.65-0.48	25	24.89	29.82	30.73	31.78
	D-G2-HB2	1.44-0.48-0.34	25	25.85	28.77	30.19	30.85
	D-G2-HB3	0.65-1.44	25	27.78	28.46	29.74	30.85
	D-G2-HB4	1.44	25	29.70	27.96	29.19	30.62
Solid	SB	---	---	---	36.75	---	---

* M: Market, HB: Hollow Brick, G1: Group 1, D: Designed, SB: Solid Brick

As shown in Table 3.3, the best block in the market group was M-HB1with the temperature results of 29.20, 29.50 and 33.95 °C for vacuum, polystyrene and air-filled cavities blocks, respectively. Similarly, for designed Group 1 and Group 2, the least temperature was for D-G1-HB5 and D-G2-HB4, respectively, with the values shown in Table 3.3. The main target of the simulation was to determine the best block with the optimum geometry. Hence, in this work, Model D-G1-HB5 seems to be the best hollow concrete brick that has the lowest average inner surface temperature with values of 26.97, 28.60 and 29.85°C for vacuum, polystyrene and air-filled cavity, respectively. Figure 3.13 shows the average temperature for all the bricks that are classified in ascending order based on T_i for three types of cavities: vacuum, polystyrene and air, as shown in Table 3.4.

Table 3.4: Average surface temperature arranged ascending

Vacuum cavity		PS-filled cavity		Air-filled cavity	
Model	T_i (°C)	Model	T_i (°C)	Model	T_i (°C)
D-G1-HB5	26.97	D-G1-HB5	28.6	D-G1-HB5	29.85
D-G1-HB4	27.8	D-G2-HB4	29.19	D-G1-HB4	29.9
D-G2-HB4	27.96	D-G1-HB4	29.4	D-G1-HB3	30.45
D-G1-HB1	28.45	M-HB1	29.5	D-G1-HB1	30.5
D-G2-HB3	28.46	D-G2-HB3	29.74	D-G2-HB4	30.62
D-G1-HB3	28.5	D-G1-HB3	30.16	D-G2-HB2	30.85
D-G2-HB2	28.77	D-G1-HB1	30.19	D-G2-HB3	30.85
M-HB1	29.2	D-G2-HB2	30.19	D-G1-HB2	30.98
D-G1-HB2	29.28	D-G1-HB2	30.21	D-G2-HB1	31.78
D-G2-HB1	29.82	D-G2-HB1	30.73	M-HB1	33.95
M-HB2	30.39	M-HB2	30.75	M-HB2	34.33

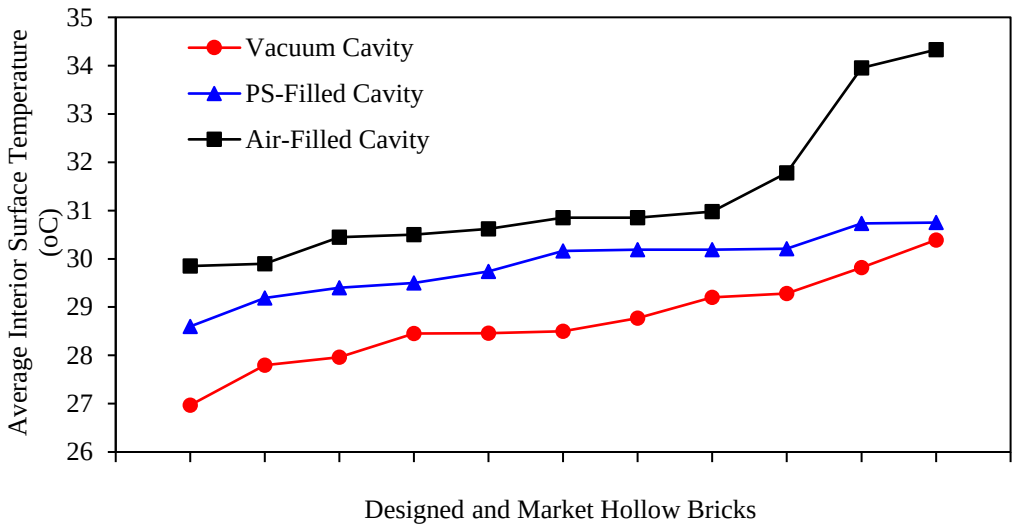

Figure 3.13: T_i for all bricks including vacuum, polystyrene and air cavities

Vacuum Cavity Models:

As shown in Table 3.3 and Figure 3.13, the results of T_i indicated that Model D-G1-HB5 was the best hollow brick with 26.97°C, while Model M-HB2 with 30.39°C was the worst with a difference of 3.42°C, as shown in Figure 3.14. The change in the average temperature for hollow bricks was attributed to the number of thermal bridges (solid channels), which transferred the heat from the exterior to interior surfaces of the hollow brick. Therefore, increasing the number of thermal bridges with decreasing their length would increase the average interior surface temperature. The market hollow bricks (M-HB1 and M-HB2) have 3 and 4 short thermal bridges (length = 200 mm), respectively, with a difference of 1.19°C due to the extra thermal bridge of M-HB2. On the other hand, the D-G1-HB5 brick has two short thermal bridges (length = 345 mm) with a difference of 3.42°C as compared to M-HB2, which was ascribed to the number and length of thermal

bridges. Similarly, the difference in T_i between the D-G1-HB5 and D-G2-HB4 bricks was about 1°C, which was attributed to the short two thermal bridges of the D-G2-HB4 model, as compared to D-G1-HB5 with two long thermal bridges.

Accordingly, it could be concluded that increasing the number of thermal bridges reduced the heat transfer to the interior brick surface because the heat was transferred only by conduction through the solid parts of the brick for the case of vacuum cavities. However, increasing the hollow ratio could not alone reduce the inner temperature unless the number thermal bridges were reduced and elongated.

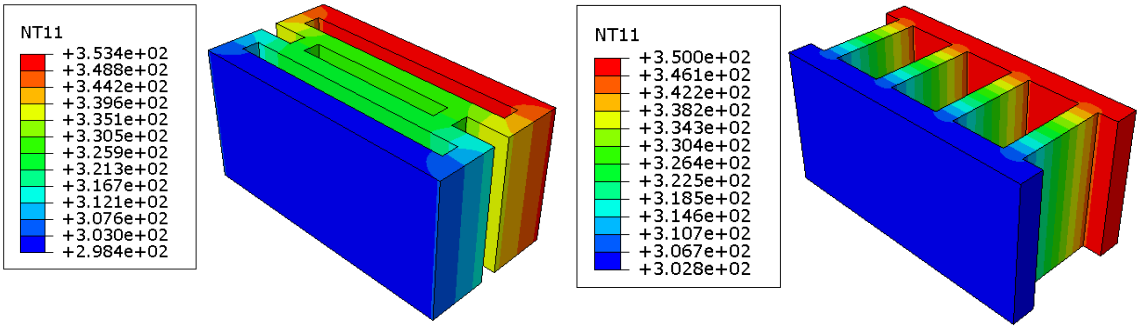

Figure 3.14: Nodal temperature distribution (NT11) (°K) vacuum cavity case

Polystyrene (PS) Cavity Models:

As shown in Table 3.3, the average inner surface temperatures for all bricks with polystyrene cavities indicated that the best and worst models in this phase were the same as was noted in the previous section, which were D-G1-HB5 and M-HB2 (Figure 3.15) with T_i of 28.60 and 30.75°C, respectively with a difference about 2.15°C (7%). The difference was relatively reduced in the case of vacuum cavities because M-HB2 model (HR=37.70) has higher hollow ratio than D-G1-HB5 model (HR=29.61). Hence, the

amount of polystyrene (same as HR in Table 3.3) in the cavities of M-HB2 was larger compared to D-G1-HB5 with a difference of 21%, but the inner temperature was still higher for the market hollow brick. The temperature increment was ascribed to the higher thermal bridges, low aspect ratio and high cavity width for M-HB2, as compared to D-G1-HB5. However, the high aspect ratio and low cavity width provided thermal barriers (resistant walls), which gradually reduced (breaking) the heat flow to the interior surface.

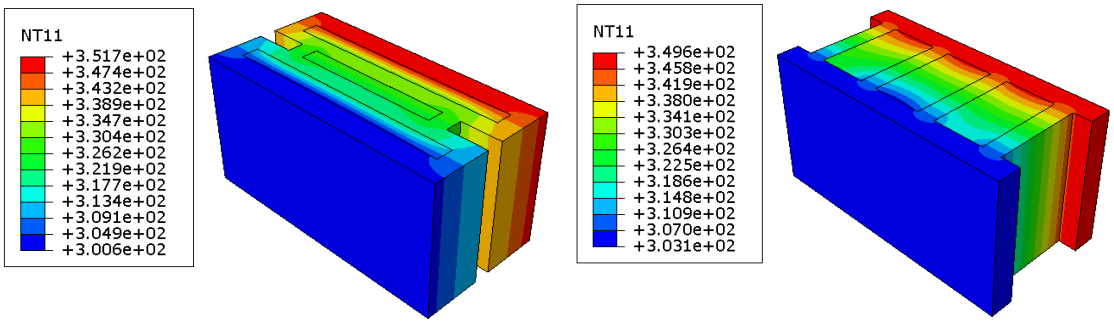

D-G1-HB5 M-HB2

Figure 3.15: Nodal temperature distribution (NT11) (°K) PS-filled cavity case

Air Cavity Models:

In the simulation of these models, the cavities were assumed to be filled with air, which is the normal case in practice. Therefore, the phenomena of convection and radiation inside the cavities were considered. The best and worst models in this phase were the same as was noted in the previous two cases, which were D-G1-HB5 and M-HB2 (Figure 3.16) with T_i of 29.85 and 34.33°C, respectively, with a large difference of 4.48°C, which could be ascribed to the fact that D-G1-HB5 has the highest aspect ratio and lowest cavity width, which reduced the convection and radiation inside the cavities.

Within each group, the difference in the temperature was about 1°C due to the difference in the number of cavities and aspect ratio, as clearly shown in Table 3.5. It is to be noted that increasing the number of cavities tends to reduce the cavity length, hence, the aspect ratio is reduced as well. As a conclusion for this section, the aspect ratio, cavity width and number of cavities were the main factors dominating the heat transfer when convection and radiation inside cavities were considered because these parameters slow the air circulation and reduce the convection and radiation. The higher aspect ratio (low number of cavity and high cavity length) and lower cavity width (parallel to heat flow) are the contributing factors that significantly reduce the inner temperature.

Table 3.5: Average surface temperature for air cavities models

Brick Models*	Aspect Ratio (AR) %	Cavity Width (mm)	Hollow Ratio (HR) %	Number of Cavities	Convection and Radiation Case
					T_i (°C)
M-HB1	0.65	130	42.25	2	33.95
M-HB2	0.385	130	37.70	3	34.33
D-G1-HB1	0.48-1.72	25	28.75	7	30.50
D-G1-HB2	0.48-0.30	25	25.06	10	30.98
D-G1-HB3	1.12-0.48-0.30	25	25.17	9	30.45
D-G1-HB4	0.79-1.12-0.30	25	27.79	7	29.90
D-G1-HB5	1.72-1.12	25	29.61	5	29.85
D-G2-HB1	0.34-0.65-0.48	25	24.89	7	31.78
D-G2-HB2	1.44-0.48-0.34	25	25.85	7	30.85
D-G2-HB3	0.65-1.44	25	27.78	5	30.85
D-G2-HB4	1.44	25	29.70	3	30.62

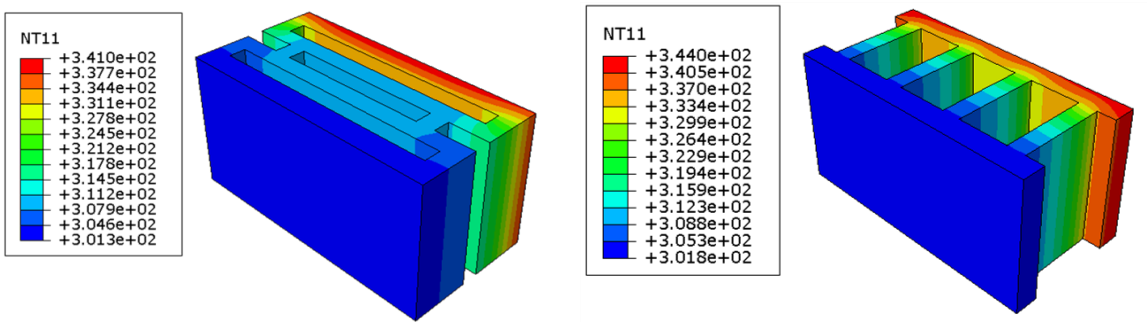

D-G1-HB5 M-HB2

Figure 3.16: Nodal temperature distribution (NT11) (°K) air-filled cavity case

The average inner temperature for the solid brick was 36.75°C, which was higher than the best hollow brick (D-G1-HB5) by around 7 to 8°C (22%) for air and polystyrene cavities, respectively, as shown in Figure 3.17, while the difference was in the range of 2.0 to 6.85°C for the other models for the case of air cavities.

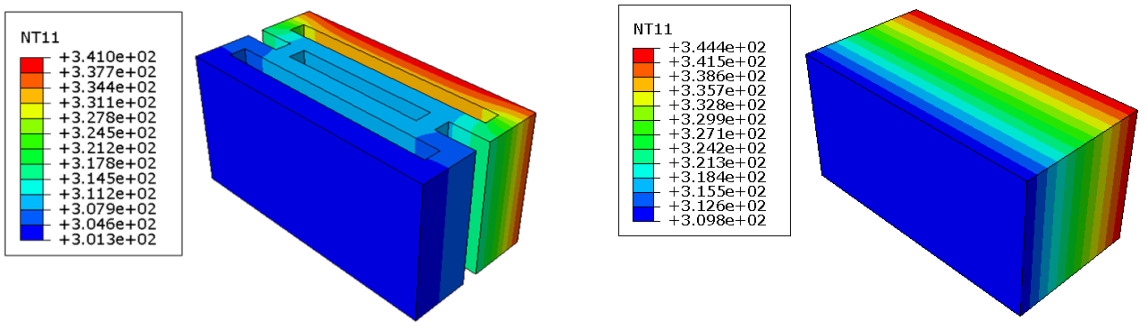

D-G1-HB5 SB

Figure 3.17: Nodal temperature distribution (NT11) (°K) for solid and D-G1-HB5 bricks

3.7.3 Average Surface Temperature of Two Brick Model

The last simulation concerns the combination of two bricks together to study the thermal efficiency of the connection joints between the bricks. Therefore, the best three bricks were selected from the previous simulations (D-G1-HB5, D-G1-HB4 and D-G2-HB4) to find out the best brick geometry and the cavity at the connection area between the two bricks (cavity at brick's joint) that achieves the highest thermal resistivity. As in the previous simulations, the average inner surface temperature was obtained from ABAQUS by selecting the nodes for the internal surfaces. The total number of nodes on each surface of the brick model based on the meshing size (5 mm) was 6765 nodes, as shown in Figure 3.18.

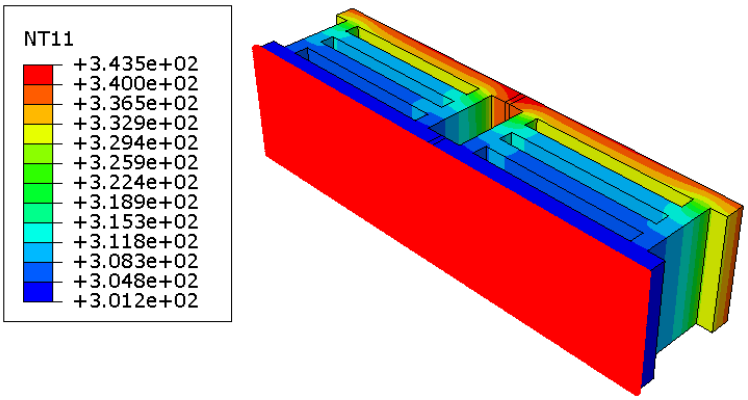

Figure 3.18: (6765 nodes) at the inner surface of D-G2-HB4 model

In this stage, air-filled cavity was considered to assess the performance of brick's edges. As shown in Figure 3.19, the results proved that Model D-G1-HB5 was the best one with T_i of 29.94°C, while D-G1-HB4 and D-G2-HB4 were with 30.12 and 30.88°C, respectively. The difference between the two connections of Groups 1 and 2 was around 1

°C. Because the aspect ratio for the cavity in the connection region of Group 1 (0.65) was higher than that for Group 2 (0.33), convection and radiation inside the cavities would be reduced for Group 1 connection cavity as compared with Group 2.

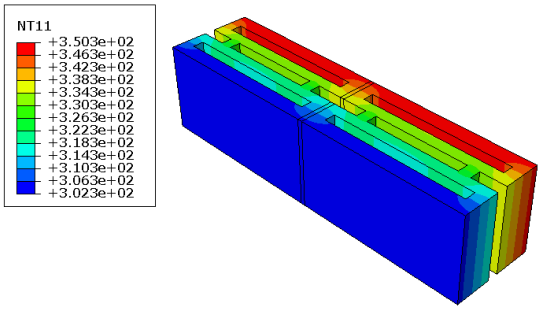

(a) D-G1-HB5

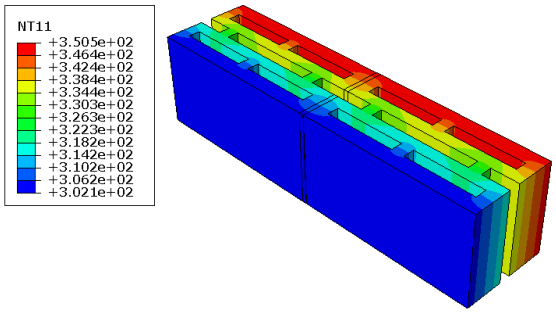

(a) D-G1-HB4

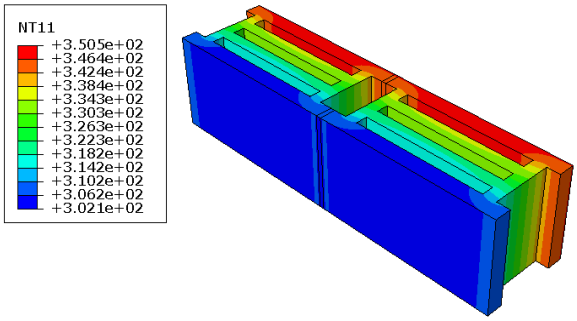

(b) D-G2-HB4

Figure 3.19: Two brick models results (Air Cavity): (a) Group 1 Connection, (b) Group 2 Connection

CHAPTER 4

EXPERIMENTAL PROGRAM

4.1 Introduction

This Chapter covers the details of the selection of materials, mix proportions, trials of concrete and masonry bricks, casting, curing and testing of the specimens. All the materials utilized in the experimental work were declared with their properties and sources. In line with the motives of this investigation, the three additive materials, which are obtainable locally within the Kingdom of Saudi Arabia and extremely cheap, were used to develop thermally efficient concrete and masonry bricks. The experimental program for this research is clarified in three consequent stages. The first stage was the selection of the waste materials and their suppliers, aggregates, chemical admixtures, etc. The second stage included the mix proportions and trials that were conducted till reaching the proper "optimum" mixes. This stage was preceeded by conducting several trials whereby these materials were used to replace fine, coarse and combination aggregates. In this stage, there are two main tasks:

Task 1: Producing insulation normal concrete: Two replacement materials [crushed tire rubber (Ru) and high-density polyethylene (PE)] were used in the concrete mix to replace fine and coarse aggregates.

Task 2: Producing insulation masonry bricks: Fine and coarse aggregates in the mix of the masonry bricks were replaced with three insulation materials [(Ru, PE, and perlite (PL))] with different contents and sizes.

In the third stage, compressive strength, flexural strength and thermal conductivity were measured experimentally to investigate the effect of additive materials on these properties for both the concrete specimens and masonry brick units.

4.2 Materials

4.2.1 Cement

The type of cement used in all the experimental work was ASTM C150 Type I Portland cement, with a typical chemical composition shown in Table 4.1 [66]. This type of cement is currently being widely used in Saudi Arabia for almost all types of construction. Its specific gravity is 3.15 [66].

Table 4.1: Chemical composition of Type I cement

Component	Weight %
CaO	64.35
SiO_2	22.00
Al_2O_3	5.64
Fe_2O_3	3.80
K_2O	0.36
MgO	2.11
Na_2O	0.19
Equivalent alkalis	0.33
SO_3	2.10
Loss on ignition	0.70
C_3S	55.00
C_2S	19.00
C_3A	10.00
C_4AF	7.00

4.2.2 Coarse Aggregate

The coarse aggregate used in the experiments was obtained from masonry bricks company (Advanced Concrete Products, Ltd.) in the Eastern Province in Saudi Arabia. Two sizes of coarse aggregate were used, which were the passing through sieves 3/8 (9.53 mm) and 3/16 in (4.76 mm). The maximum aggregate size was 9.53 mm and its specific gravity was 2.60, while its absorption was 1.10%.

4.2.3 Fine Aggregate

The fine aggregate was widely available in Saudi Arabia in the form of sand dunes. It was procured from Advanced Concrete Products, Ltd. Its specific gravity was 2.56 and absorption was 0.60%.

4.2.4 Chemical Admixtures (Super-plasticizer)

The super-plasticizer (SP) was Fluid PC 314, which utilized in the mixes of concrete and masonry bricks. Its specific gravity was 1.105 and the addition rate was 0.40 to 1.50% by weight of cement.

4.2.5 Mixing Water

The normal sweet (tap) water available in the Concrete Laboratory was used for all the mixes during the experimental work and curing the specimens.

4.2.6 Replacement Materials

In this research, three waste materials were used in the experimental program as replacement materials to fine and coarse aggregates. As shown in Table 4.2, these waste materials replaced the natural aggregates in the mixes of normal concrete and masonry bricks. All of these waste materials are vastly available and cheap in the Kingdom. More details about each waste materials, their availability, contents and suppliers are illustrated below.

Table 4.2: Replacement materials with sizes and contents

Type of Waste Material	Waste Materials	Material ID	Size	Contents (%)
Industrial	Crumb Tires Rubber	Ru	#30, #3/16, #3/8	10, 20, 30, 40, 50
	High Density Polyethylene	PE		
Natural	Perlite	PL	Graded	

Crumb Tire-Rubber (Ru):

Automobile tires are produced using more than 100 raw materials including raw rubber, tire cord, carbon black, bead wire and compound ingredients. Around half of these materials are chemical products [15]. Table 4.3 shows the chemical composition of the tires in details [15]. A detailed literature review about tire rubber was illustrated in Chapter 2 including the production, disposing and environmental hazards.

Table 4.3: Chemical composition of tires [15]

Materials	Rubber	Carbon black	Metal	Textile	Zinc oxide	Sulfur	Additives
Average %	46	22	20.75	5.50	1.50	1	6.25

The sizes and sieve numbers of waste tire-rubber particles are shown in Table 4.4. The crushed tires-rubber supplier was brought from Saudi Rubber Products Co. in the Second Industrial Area in Dammam, which can supply a huge content of crushed rubber with different sizes that are mainly used for asphalt. In this research, the crushed rubber was sieved, and three sizes of rubber were used to replace fine and coarse mineral aggregates, as shown in Figure 4.1. The thermal conductivity coefficient of the rubber pieces was 0.243 W/m.k [67]. The specific gravity and absorption of rubber particles were 1.12 and 0%, respectively [27].

Table 4.4: Waste tire-rubber sizes

Material	Particle type	Size	Passing sieve No.	Retained sieve No.
Rubber	Fine	< 2 mm	#10	#30 (> 0.595 mm)
	Coarse	< 9.53 mm	# 3/8 in	# 3/16 in (> 4.76 mm)
		< 4.76 mm	# 3/16 in	# 3/32 in (> 0.238 mm)

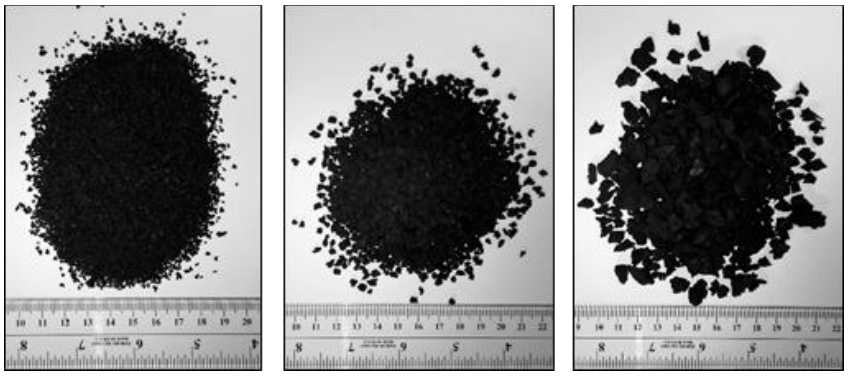

(a) **(b)** **(c)**

Figure 4.1: Sizes of tire rubber: (a) Fine (#10); (b) Coarse (#3/16); (c) Coarse (#3/8)

High-density Polyethylene (PE):

The chemical composition of high-density polyethylene (PE) particles was illustrated in Table 4.5 with the average contents of the composition [39]. The density and water absorption of PE are 0.92 gm/cm^3 and 0%, respectively [19]. The coefficient of thermal conductivity of the high-density polyethylene was 0.502 W/m.k [67]. The high-density polyethylene (PE) was supplied by Alyaf Industrial Company in the Second Industrial Area, eastern Saudi Arabia, which was crushed with different sizes and recycled to produce insulation products. As shown in Figure 4.2 and Table 4.6, three sizes of polyethylene were used as replacement to fine, coarse and both aggregates.

Table 4.5: Chemical composition of high-density polyethylene (PE) [39]

Materials	Water	Inorganic fillers	PE	PP	PA	Alkyd/ acrylic	PVC
Weight %	0.14	3.22	81.30	9.50	1.32	4.03	0.48

Table 4.6: Recycled PE particle sizes

Material	Particle type	Size	Retained sieve No.
PE	Fine	0.6-2 mm	#30
	Coarse	< 9.53 mm	# 3/16 in
		< 4.76 mm	# 3/32 in

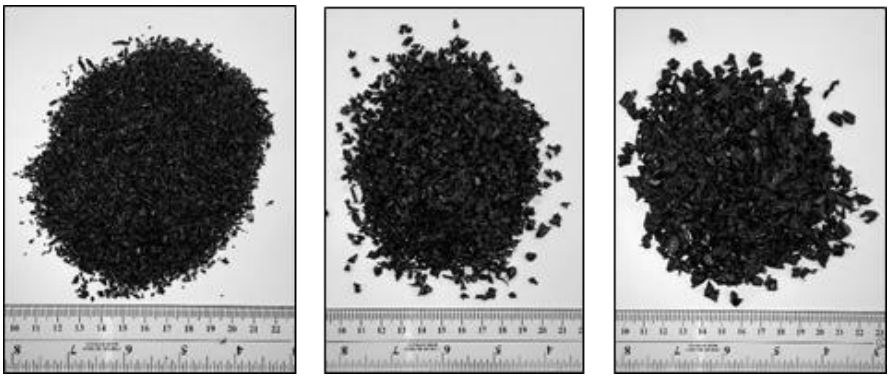

(a) **(b)** **(c)**

Figure 4.2: Sizes of PE: (a) Fine (#10); (b) Coarse (#3/16); (c) Coarse (#3/8)

Perlite (PL):

The perlite aggregate is porous, lightweight, fire-resistant material, which has significant sound and thermal insulation properties [10]. The perlite aggregate was conforming to ASTM C-332 Group 1, used to produce lightweight insulating concrete and bricks. The suppliers for natural perlite was the Arabian Vermiculite Industries Company in Dammam. The chemical composition of perlite is listed in Table 4.7 [68]. The thermal conductivity coefficient of lightweight perlite was 0.04-0.06 W/m.k [22], while the specific gravity and water absorption of perlite were 0.30 [22]. The water absorption of perlite was very high about 100% of perlite weight, which ascribed to the high porous particles of perlite. The size gradation of the lightweight perlite aggregates is given in Table 4.8 and Figure 4.3.

Table 4.7: Chemical composition of perlite [68]

Materials	Si	AL	K	Na	Fe	Ca	Mg	Trace	O	Water
Weight (%)	33.80	7.20	3.50	3.40	0.60	0.60	0.20	0.20	47.50	3.00

Table 4.8: Sieve analysis of perlite

Sieve No.	No. 4	No. 8	No. 16	No. 30	No. 50	No. 100
Weight Passing (%)	100	85-100	40-85	20-60	5-25	0-10

Figure 4.3: Graded sizes of perlite

4.3 Mix Design Proportioning, Casting and Curing

4.3.1 Normal Concrete

The main target of this research is to produce thermally efficient concrete to be used as screed concrete on the roofs, etc. Therefore, the mix proportions for the concrete were obtained from a concrete factory (Advanced Concrete Products, Ltd.), which was used the control mix of normal concrete, as illustrated in Table 4.9 for 1 m^3. The cement content

was 195 kg/m^3 with water to cement ratio of 0.495. The coarse to total aggregate ratio was 0.765 and no superplasticizer was used.

Table 4.9: Control mix proportions for 1 m^3

Materials	Mix Proportion (kg/m^3)
Cement content	195
Water content	103
w/c ratio	0.495
Coarse aggregate (3/8) in	1148
Coarse aggregate (3/16) in	344
Fine aggregate (Sand)	459
CA/TA	0.765
FA/TA	0.235
Super-plasticizer (SP)	---

The mix with the proportions in Table 4.9 was cast in the Concrete Laboratory but it was not working well because it was dry and unworkable. Therefore, many trials were conducted to find out the mix proportions which could be cast in the laboratory and compacted by the vibrating table.

Trial Mixes:

Nine trials were conducted to reach a mix proportion that is workable and compacted by the vibrating table in Concrete Laboratory. Table 4.11 shows the mix proportions of these nine trial mixes in details. The first trial mix (Mix # T1) was the same as the concrete factory. Since this mix was very dry, trial mixes were implemented to improve the workability of the mix by increasing the cement content, water content and super-

plasticizer dosage without changing the water to cement ratio. The techniques used to improve the factory mix proportion was illustrated in

Table 4.10, in which the modifications will be in cement, water content and SP dosage.

Table 4.10: Trials mix proportions

Materials	Mix Proportion (kg/m^3)
Cement content	Variable
Water content	Variable
w/c ratio	0.495
Coarse aggregate (3/8) in	1148
Coarse aggregate (3/16) in	344
Fine aggregate (Sand)	459
CA/TA	0.765
FA/TA	0.235
Super-plasticizer (SP)	Variable

Table 4.11: Mix proportions of trial mixes

Trials	Cement (gm)	Water (gm)	CA (gm) (3/8) in	CA (gm) (3/16) in	Sand (gm)	SP (gm)	Worka-bility	Strength (MPa)
T1	300	160	1773	533	707	---	Very low	3.16
T2	300	160	1773	533	707	3.0		3.20
T3	300	170	1773	533	707	3.0		3.50
T4	300	210	1773	533	707	---		3.30
T5	300	240	1773	533	707	---		3.50
T6	400	213	1773	533	707	---		4.35
T7	680	360	1773	533	707	---	Medium	14.51
T8	680	360	1773	533	707	3.40		12.0
T9	680	360	1773	533	707	6.80	High	44.12

As shown in Table 4.11, the mix proportions of the trial mixes were modified by increasing cement content, water content and superplasticizer dosage in order to increase the workability. The ninth trial mix (Mix # T9) was the best mix that could be easily cast and compacted using the vibrating table in the laboratory and has the necessary strength. Therefore, the control mix was Mix (T9) and designed for 1 cubic meter, as presented in Table 4.12.

Table 4.12: Proportions for control mix (#T9)

Materials	Mix proportion (kg/m^3)
Cement content	378
Water content	205
w/c ratio	0.53
Coarse aggregate (3/8) in	1056
Coarse aggregate (3/16) in	316
Fine aggregate (Sand)	421
CA/TA	0.765
FA/TA	0.235
Super-plasticizer (SP)	5.04 Liter

To achieve the objectives of this investigation, the natural aggregates for the control mix was replaced by Ru and PE with the details in Table 4.13. Three sizes of each of the rubber and polyethylene were used, as shown in Table 4.4 and Table 4.6, respectively. The fine aggregate (sand) was replaced with fine particle (sizes less than 2 mm) and contents of 10 to 50% by weight. The mixes were numbered from 1 to 5 for the replacement of sand, as shown in Table 4.13. The mixes 6 to 10 were used for the replacement of coarse aggregate with two sizes of coarse particles 3/8 ″ (9.53 mm) and 3/16 ″ (4.76 mm). Further, five more mixes (Mix # 11 to 15) were used for the replacements of both fine and coarse aggregates

with fine and coarse particles of the substitution materials (Ru & PE). Therefore, the total number of mixes was thirty mixes for both materials rubber and polyethylene.

Table 4.13: Replacement materials with their mixes classifications

Replaced Natural Aggregates	Aggregate Sizes	Materials Sizes*	Replacing Materials and Mix ID		Replacement by weight (%)
			Rubber (Ru)	Polyethylene (PE)	
Fine Aggregate	< 2 mm	< 2 mm	Ru1 – Ru5	PE1 – PE5	10 – 50
Coarse Aggregate	3/8 in (9.52 mm) 3/16 in (4.76 mm)	3/8 in 3/16 in	Ru6 – Ru10	PE6 – PE10	
Fine and Coarse Aggregates	3/8 in (9.52 mm) 3/16 in (4.76 mm)	3/8 in 3/16 in	Ru11 – Ru15	PE11 – PE15	

* Rubber (Ru) and Polyethylene (PE)

Casting and Curing of Specimens:

From each of the 30 mixes shown in Table 4.13, specimens were cast into various mould sizes to assess the compressive and flexural strengths and thermal conductivity. As shown in Figure 4.4, three cubes (50 mm) and three prisms (40 x 40 x 160 mm) were cast from each mix to test the compressive and flexural strengths. Further, three discs (50 x 25 mm) (Figure 4.4) were cast to measure the thermal conductivity coefficient for each mix. The casting process was done in layers and each layer was vibrated using vibrating table. The specimens were cured in sweet water for a period of 7 days at a fairly constant laboratory temperature of (23 ± 2°C). The specimens were tested after the 7th day.

Figure 4.4: Casting compressive, flexural and thermal specimens

4.3.2 Masonry Hollow Concrete Bricks (Blocks)

The main target of this research was to produce thermally efficient concrete bricks, which could be used to build the walls. Accordingly, the masonry mix was taken from a masonry brick factory (Advanced Concrete Products), as shown in Table 4.14. The mix could not be mixed and compacted properly in the laboratory because it was very dry. Then, extra water and Super-plasticizer were used to improve the workability (Table 4.14). However, trial 2 was mixed and compacted well in the laboratory, hence, this mix was considered as the control mix for the blocks. The control hollow brick was cast with the optimum geometry obtained from FEM and the control mix (T2) in Table 4.14.

The replacement materials (Ru, PE and PL) were mixed with different percentages. Therefore, many trials were conducted to replace fine and coarse aggregates by the insulation materials on the control mix. The target was to design a mix proportion with high percentage of the insulation materials to reduce the thermal conductivity. On the other hand, the strength of the cubic samples was decreased with increasing the content of materials. Therefore, the optimum mix had to balance between the high content of

insulation material and satisfying the ASTM C 129 strength criteria for non-load bearing masonry units.

Casting the compressive cubes was achieved through three layers and tamping using a steel rod because the brick mix was dry and had a large quantity of coarse aggregate, therefore, the aggregate particles were not flying out of the mould. The three materials (Ru, PE and PL) replaced either fine or coarse aggregates. Perlite was used to replace only fine aggregate (sand) because it is a lightweight material (i.e. large surface area that needs more paste) and has finer particles similar to sand. On the other hand, two sizes of coarse plastic and rubber (4.76 and 9.52 mm) replaced the same sizes of coarse aggregates due to the less amount of paste in the masonry mix, in which the coarse aggregates were around 50% of the total mix proportions (Table 4.14). Therefore, the thermal resistivity for concrete sample with coarse aggregate was higher than the other sizes (due to high content of coarse aggregate).

Table 4.14: The reference (control) masonry concrete mix proportions for 1 m^3

Materials	Mix Proportion (kg/m^3)		
	Factory	T1	T2 (control)
Cement content	195	195	195
Water content	103	115	115
w/c ratio	0.432	0.495	0.495
Coarse aggregate (3/8) in	1148	1131	1131
Coarse aggregate (3/16) in	344	338	338
Fine aggregate (Sand)	459	452	452
CA/TA	0.765	0.765	0.765
FA/TA	0.235	0.235	0.235
Super-plasticizer (SP)	--	--	2.6 Liter
Observations	Dry	Dry	Ok

Trial Mixes:

Three replacement materials (perlite, rubber and polyethylene) were used with different contents by replacing fine and coarse aggregate. For each trial mix, the compressive strength was measured. The recommended mix was chosen based on the required (satisfactory) strength (3.45 MPa) with the highest content of the insulation material.

Perlite (PL) Replacement:

Eighteen trials were conducted with 100 mm cubes with different replacement contents of perlite (5, 10, 20, 30, 40 and 50% by weight) and different cement contents (225 to 325 kg/m^3). As shown in Table 4.15, the strength was very low when high content of perlite was used if the cement content was not increased because perlite is a lightweight material (because of its high surface area, it needs high cement content) and weak, but with high thermal insulation property. Therefore, the cement content was increased from 225 to 325 kg/m^3. Therefore, the trials mix proportions and the corresponding compressive strength were shown in Table 4.15.

The final mix could be selected for the hollow brick based on the higher perlite content and strength. According to ASTM C 129 standards, the minimum strength required for non-load bearing hollow blocks was 3.45 MPa for individual units [69]. Therefore, Mix T-17 was selected to be the final mix for perlite with the content of 30% because the cubic strength was 4.92 MPa, as shown in Table 4.15.

Table 4.15: Trial mix proportions for perlite (PL) replacements (in grams)

Trial No.	T1	T2	T3	T4	T5	T6	T7	T8	T9	T10	T11	T12	T13	T14	T15	T16	T17	T18
PL- Replacement (%)	50	40	30	50	50	50	50	40	30	20	10	5	40	30	20	40	30	20
Cement (kg/m^3)	225	225	225	225	225	250	275	275	275	275	225	225	300	300	300	325	325	325
Cement	205	205	205	235	236	263	289	289	289	289	236	236	315	315	315	341	341	341
Water	240	215	203	250	316	292	303	302	266	244	191	167	291	275	254	300	385	264
Coarse Aggregate 3/8 in	627	692	773	627	364	360	356	383	443	527	704	796	371	430	511	360	417	496
Coarse Aggregate 3/16 in	187	207	231	187	109	108	106	114	132	158	210	238	111	128	153	107	125	148
Sand	125	166	216	125	158	156	154	199	269	365	548	655	193	261	354	187	253	343
Perlite (PL)	125	110	92	125	158	156	154	132	115	91	61	34	129	112	89	125	108	86
SP (ml)	3	3	3	3	3	3.5	3.85	4	4	4	3	3	4	4	4	4.5	4.5	4.5
Observation	Very weak - Need paste	Very weak - Need paste	Very weak - Need paste	Very weak - Need paste	Very weak - Need paste	Good	Good	Good	Good	Good	Good	Good	Good	Good	Good	Good	Good	Good
Compressive Strength (MPa)	<1	<1	<1	<1	<1	1.15	1.82	2.24	2.59	4.09	5.87	8.17	1.82	3	4.96	2.46	4.92	5.31

Rubber (Ru) Replacement:

Seven trials were conducted in the laboratory with different contents of rubber (50, 20, 15 and 10%) and different cement contents. The mix proportions of the trials are presented in Table 4.16 with the corresponding compressive strength. Similarly, the brick mix selected with respect to the higher rubber content that satisfied the strength requirements. Therefore, T-4 mix was selected to be the final mix for rubber with a rubber content of 20% by weight of coarse aggregate and a cubic strength of 4.27 MPa. This rubber content of 20% does agree with many studies that recommend the rubber content not to be more than 20% [9,10].

Polyethylene (PE) Replacement:

In the same way, seven trials were cast in the laboratory with different content of plastic (50, 30, 20 and 15%) and cement (225 and 250 kg/m^3). As shown in Table 4.17, all trials with their mix proportions and strengths were presented. Similarly, the brick mix was selected with respect to the higher plastic content and strength. T-6 mix was selected to be the proper mix for casting the blocks, which has a plastic content of 20%, cement content of 250 kg/m^3 and strength of 7.86 MPa. Similar recommendations of a plastic content in the range of 15 to 20% were reported in the literature [56].

Table 4.16: Trial mix proportions for rubber (Ru) replacements (in grams)

Trial No.	T1	T2	T3	T4	T5	T6	T7
Ru-Replacement (%)	50	50	50	20	20	15	10
Cement (kg/m^3)	225	225	225	225	250	225	225
Cement	205	215	214	236	263	236	236
Water	108	108	113	130	143	132	133
Coarse Aggregate 3/8 in	356	356	340	731	710	826	913
Coarse Aggregate 3/16in	106	106	102	218	212	247	273
Coarse Rubber 3/8 in	356	356	340	183	178	146	101
Coarse Rubber 3/16in	106	1.06	102	55	53	44	30
Sand	284	284	335	450	437	479	500
SP (ml)	2	2	2	1.5	2	2	2
Observation	Very weak Need paste			Good	Thin cement layer at bottom	Good	Good
Compressive Strength (MPa)	<1	<1	<1	4.27	4.85	5.27	8.72

Table 4.17: Trial mix proportions for polyethylene (PE) replacements (in grams)

Trial No.	T1	T2	T3	T4	T5	T6	T7
PE-Replacement (%)	40	30	30	30	20	20	15
Cement (kg/m^3)	225	225	225	225	225	250	225
Cement	205	185	215	214	236	263	236
Water	110	101	111	115	130	142	131
Coarse Aggregate 3/8 in	458	528	528	504	703	670	788
Coarse Aggregate 3/16in	137	158	158	151	210	200	235
Coarse PE 3/8 in	305	226	226	216	176	167	139
Coarse PE 3/16in	91	68	68	65	53	50	42
Sand	304	301	301	355	433	412	457
SP (ml)	3	2	2	2	2	1.5	2
Observation	Very weak Need paste	Need paste			Good		
Compressive Strength (MPa)	---	1.81	1.03	1.53	3.35	7.86	6.25

Finally, the recommended mixes for all replacement materials were summarized in Table 4.18 and Table 4.19 for the replacement by weight and volume, respectively, for 1 m^3. The main criteria for selecting the proper mix was the lowest cement content, highest replacement material and highest compressive strength.

Table 4.18: Recommended mix proportions by weight

Materials	Mix proportions by weight (kg/m^3)			
	Control	PL	Ru	PE
Cement content	195	325	225	250
Water content	115	271	124	135
w/c ratio	0.495	0.495	0.495	0.495
Coarse aggregate (3/8) in	1131	397	696	638
Coarse aggregate (3/16) in	338	119	208	190
Replacement (3/8) in	---	103	174	159
Replacement (3/16) in	---		52	48
Fine aggregate (Sand)	452	241	429	393
CA/TA	0.765	0.60	0.725	0.725
FA/TA	0.235	0.40	0.275	0.275
Super-plasticizer(SP) Liter	2.60	4.30	1.4	1.5
Compressive strength (MPa)- 100 mm cube	14.96	3.85	4.27	7.86

Table 4.19: Recommended mix proportions by volume

Materials	Mix proportions by volume (%)			
	Control	PL	Ru	PE
Cement content	6.19	10.32	7.14	7.94
Water content	11.54	27.11	123.9	13.52
w/c ratio	0.495	0.495	0.495	0.495
Coarse aggregate (3/8) in	43.52	15.27	26.78	24.52
Coarse aggregate (3/16) in	13.00	4.56	8.00	7.33
Replacement (3/8) in	---	34.37	15.54	17.33
Replacement (3/16) in	---		4.64	5.18
Fine aggregate (Sand)	17.63	9.40	16.75	15.34
CA/TA	0.765	0.60	0.725	0.725
FA/TA	0.235	0.40	0.275	0.275
Super-plasticizer(SP) Liter	0.169	0.361	0.117	0.122

Casting and Curing Specimens:

All the mixes in Table 4.18 and Table 4.19 were cast in the designed "optimum" mould of hollow brick, as shown in Figure 4.5. The compressive strength, thermal conductivity, density and absorption were examined for each hollow brick. Special wooden molds were fabricated in the Research Institute at KFUPM with the optimum geometry of cavities, as shown in Figure 4.5. The mould consisted of a wooden base to hold the polystyrene boards and a wooden box, which was fabricated with the most widely used dimensions of the brick (200 x 200 x 400 mm) and fixed at the base. The polystyrene boards were designed with the same dimensions of cavities and fixed in the wooden base. The mix was poured inside the mould in three layers and tamping by a steel rod (Figure 4.6). After 24 hours of casting, the bricks were demolded carefully by removing the wooden box, as shown in Figure 4.7. Then, the specimens were cured in sweet water for a period of 6 days at a fairly constant laboratory temperature of 23 ± 2°C. After the 7th day, the polystyrene boards were removed from the cavities and the brick samples prepared for testing, as illustrated in Figure 4.7.

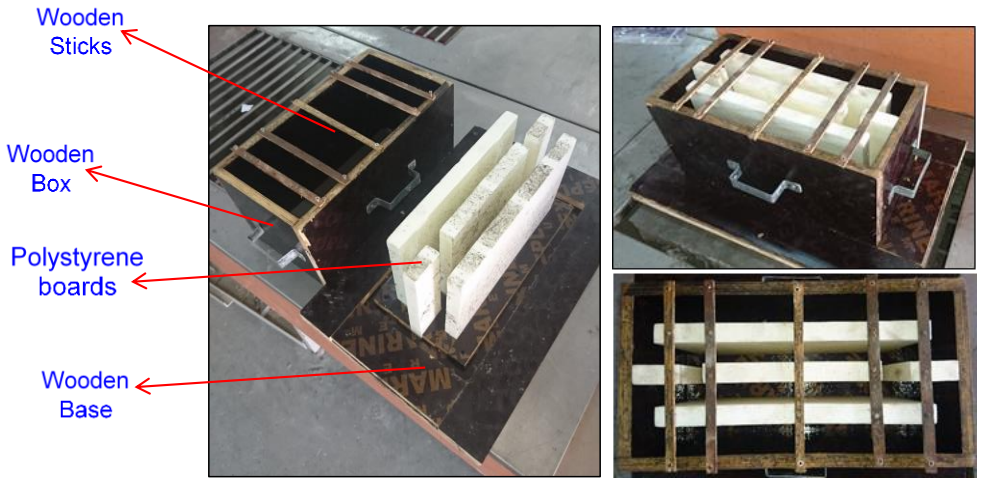

Figure 4.5: Hollow masonry brick wooden mould "optimum geometry"

Figure 4.6: Casting hollow masonry brick

Figure 4.7: Demolding and removing polystyrene boards

4.4 Testing Specimens

The specimens were prepared for evaluating the mechanical properties (compressive and flexural strengths) as well as the thermal conductivity, absorption and density.

4.4.1 Testing Mechanical Properties

Compressive Strength:

100 and 50 mm concrete cubes were used to assess the compressive strength according to ASTM C 39 after 6 days of water curing. The specimens were tested using an automatic

compressive testing machine (MATEST) of hydraulic type with a capacity up to 3000 kN, as shown in Fig. 3.8. Compressive loading was applied at a constant rate of 0.50 kN/s until the failure of the specimen. The maximum load (kN) and the compressive strength (MPa) were noted on the screen of the machine (Figure 4.8).

Figure 4.8 Compressive Strength Testing Machine

For normal concrete, 50 mm cubes were tested for all the thirty mixes (rubber and plastic). However, three cubes were tested for each mix, with a total number of tested cubes of 90. For masonry block mixes, three 100-mm cubes were tested for each material (i.e. the total number of tested cubes was 108).

The hollow concrete bricks (HCB) were prepared to be tested in the compression machine according to ASTM C140 [70]. Cement mortar capping was implemented on both top and bottom surfaces of the hollow bricks to keep these surfaces in one level according to ASTM C 1552 [71], as shown in Figure 4.9. Therefore, the load could be distributed uniformly upon all the area of the brick. In this research, high strength cement mortar, called Master

Emaco S 488 (1 cement: 0.25 water), was used as the capping material with a thickness of less than 13 mm. Loading plates with 25-mm thickness were adjusted at the bottom and top surfaces of the brick to distribute the load uniformly over the cross-sectional area of the hollow brick, as shown in Figure 4.10. A similar procedure was reported for compressive test of hollow concrete bricks [55].

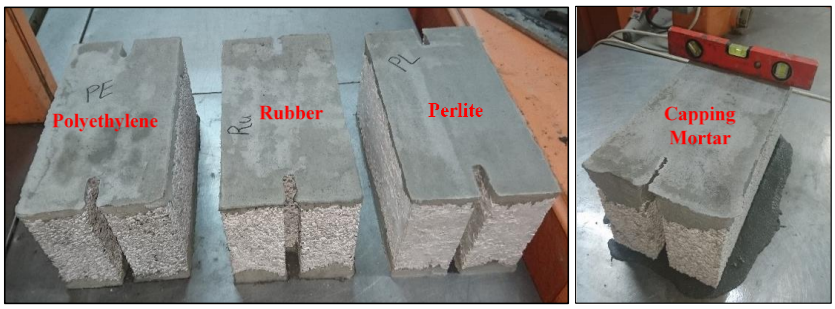

Figure 4.9: Prepared HCB for compression test

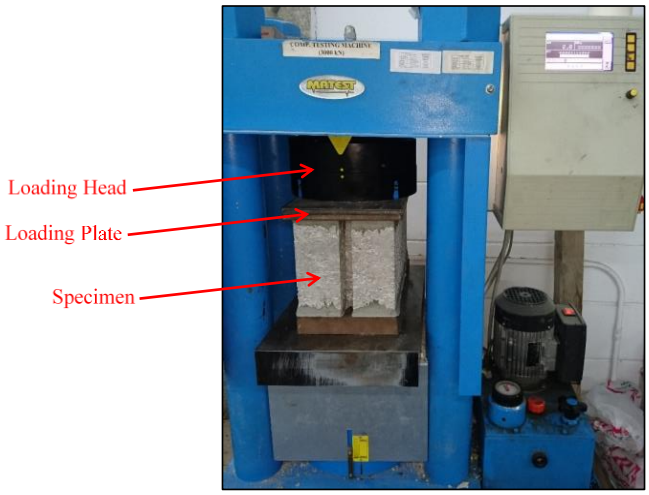

Figure 4.10: Compression test for hollow concrete bricks

Flexural Strength:

The test to assess the flexural behavior of all the mixes was conducted according to ASTM C 1018 [35]. Two-point loading setup was used to test 40 × 40 × 160 mm prisms, in which the load was applied by INSTRON Machine. One LVDT was placed below the prism at mid-span to measure deflection of the beam at the middle point. During the test, loads and deflections of the prisms were monitored using a data logger. The test setup is as shown in Figure 4.11.

Figure 4.11: Flexural test setup

As shown in Figure 4.12, a two-point load was applied equally in three equal spaced spans. The stress was calculated according to the following equations [25]:

$$\sigma = \frac{M\,y}{I} \qquad 4.1$$

$$M = \frac{P\,L}{6} \qquad 4.2$$

$$I = \frac{b\,d^2}{12} \qquad 4.3$$

$$y = \frac{d}{2} \quad (4.4)$$

$$\sigma = \frac{P\,L}{b\,d^2} \quad (4.5)$$

Hence,

The flexural strength (σ) was calculated accordingly to Equation 5, while P was recorded load by the data logger.

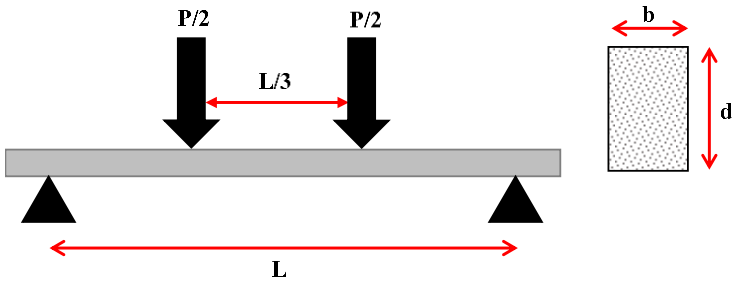

Figure 4.12: Two point loaded beam

4.4.2 Testing the Physical Properties

Density and Absorption:

For the four mixes of the bricks shown in Table 4.18, wet and oven dry densities were measured to ensure that the optimum hollow bricks satisfy the absorption limitation specified in ASTM C-140 [70] for masonry bricks. Equation (8) below was used to calculate the amount of absorption for each brick. Therefore, 100 mm cubes were cast from each mix and cured for 6 days then weighed (saturated weight). After that, the cubes were inserted inside the oven at 105°C for 24 hours and weighed (dry weight). The wet and dry densities were calculated according to the following equations:

$$\boldsymbol{Wet\ Density} = \frac{\boldsymbol{W_s}}{\boldsymbol{V_{cube}}} \quad 4.6$$

$$\boldsymbol{Dry\ Density} = \frac{\boldsymbol{W_d}}{\boldsymbol{V_{cube}}} \quad 4.7$$

$$\boldsymbol{Absorption}, \% = \frac{\boldsymbol{W_s - W_d}}{\boldsymbol{W_d}} * \mathbf{100} \quad 4.8$$

where,

W_s = Saturated weight of specimen, kg

W_d = Oven-dry weight of specimen, kg

V_{cube} = volume of cube, m^3

4.4.3 Testing the Thermal Conductivity

Disc Specimens:

For each mix, three discs (50 dia. x 25 mm thickness) were prepared to assess the thermal conductivity coefficient. FOX50 heat flow meter instrument was used to measure the thermal conductivity according to ASTM C518-04 and E1530-06. As depicted in Figure 4.13, the FOX50 instrument works in connection with air pump, water flow and an IBM-compatible personal computer through a serial RS-232 interface using Laser Comp's "WinTherm50" software package. The instrument is easy to operate using "WithTherm50" software whereby the user must enter only the name of the result file, and the temperatures (for upper and lower plates) at which the measurements should be tested. Normally, the

temperature of the lower plate should always be 10 °C (18 F) lower than that of the upper plate [72]. Each plate has sensitive heat flow transducers and thermocouples. Signals of the heat flow transducers (typically, several thousand microvolts) are proportional to the heat flow through the sample [72].

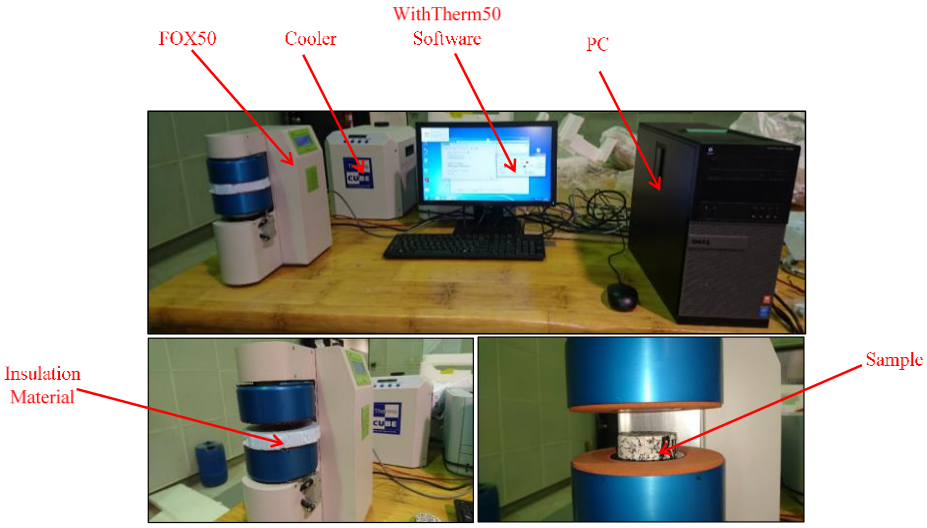

Figure 4.13: FOX50 heat flow meter instrument setup

As shown in Figure 4.14, the specimens must be polished at the top and bottom surfaces because the plates of the thermal machine are very sensitive and smoothening both surfaces of the samples reduce the thermal resistivity due to air gaps [72].

Figure 4.14: Polished specimen from both surfaces

After polishing, all the specimens must be inserted inside the oven under 60°C for 48 hr (Figure 4.15) to ensure that the samples are totally dried because the moisture inside the concrete will affect the readings for thermal conductivity.

Figure 4.15: All samples inside the oven under 60 °C

Hollow Concrete Bricks:

The guarded hot plate instrument (Dynatech, model TCFG-R4-6) was used to measure the equivalent thermal conductivity for the hollow concrete bricks. The measurements were under a steady state with a constant heat flow, according to ASTM standards C 177 [73]. The Dynatech instrument consists of guarded plates, cooling unit, control unit, data logger and computer with necessary software, as shown in Figure 4.16. The guarded plates consist of the main heater, two auxiliary heaters, two cooling boxes, tested sample and dummy sample (expanded polystyrene) (Figure 4.16). The main heater emits the heat vertically from both sides (upper and lower) towards the dummy and tested samples, respectively. The auxiliary heaters maintain the outer surfaces of the tested and dummy samples at a

specific temperature. The cooling boxes were connected to the cooling unit to control the temperature of the test. The other unit of Dynatech instrument is the control unit, which is controlling the auxiliary hot surface temperatures, voltage and current to adjust the heat generating from the main heater. Further, the data logger is connected with the thermocouples (fixed on both surfaces of the test sample) and the computer to record and show the resulting surface temperatures of both sample faces each hour until a steady state condition is attained. The external thermometer is used to measure the temperatures of the main heater surfaces and hot side of auxiliary heaters.

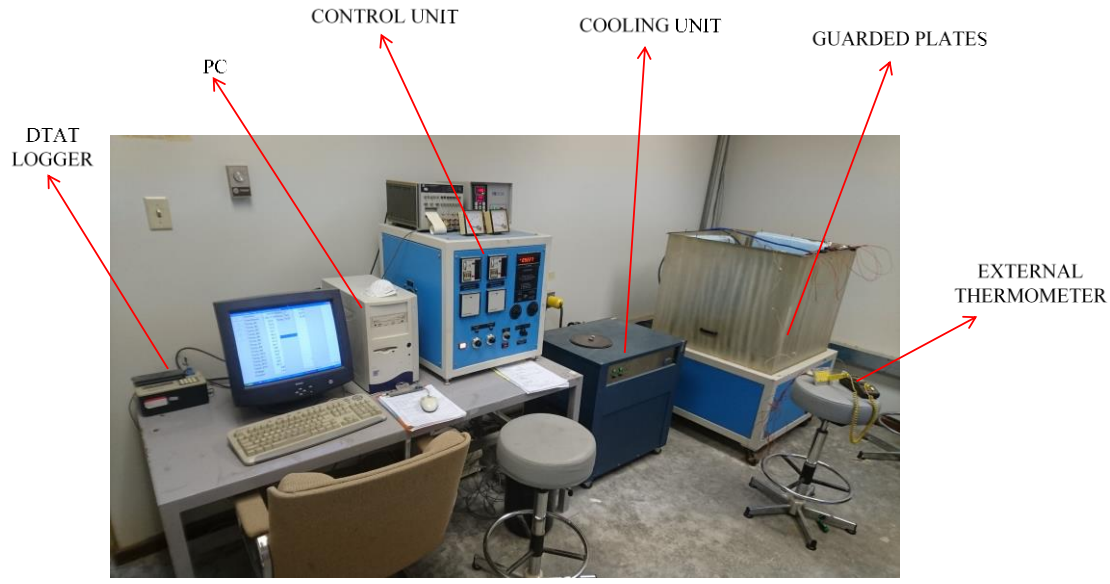

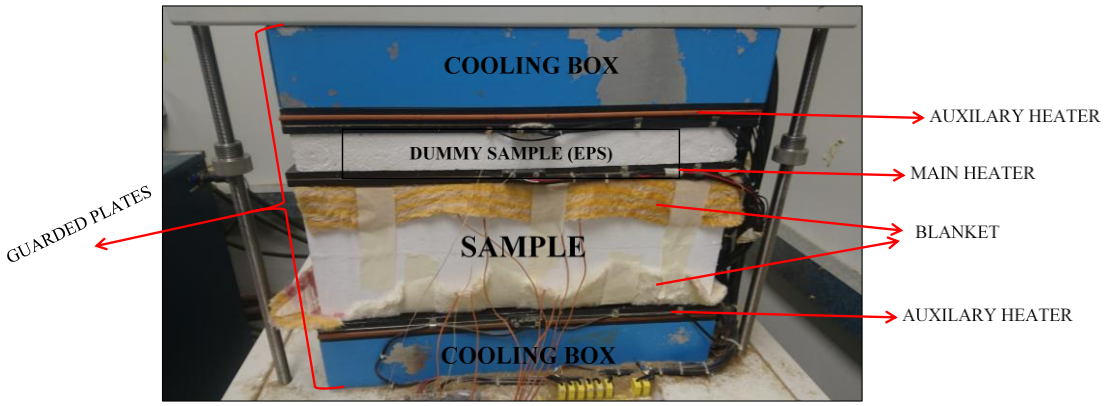

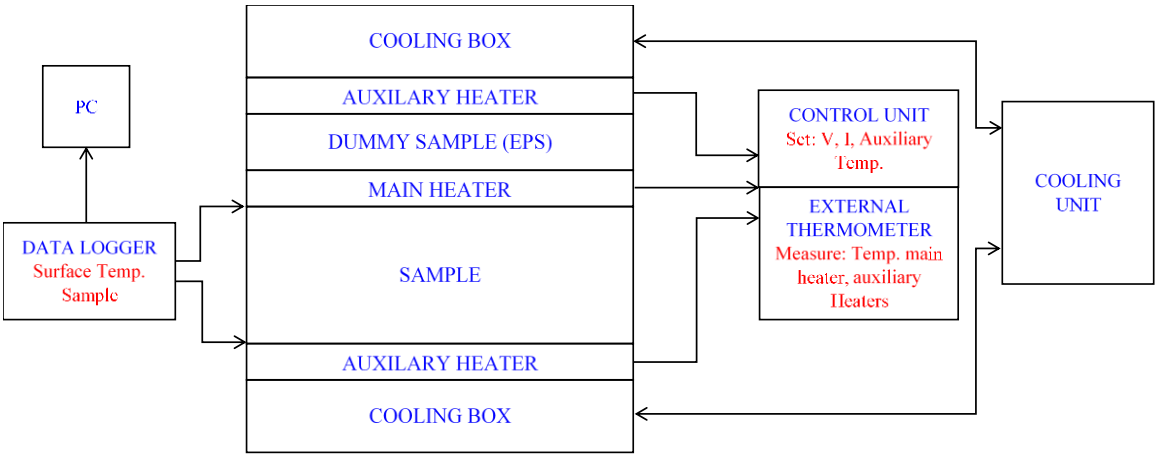

Figure 4.16: Guarded hot plate instrument (Dynatech, model TCFG-R4-6)

The guarded hot plate equipment is used to measure the thermal conductivity of solid brick, hollow bricks (concrete and clay) and insulation materials (perlite, rubber, etc.) [74]. However, the accuracy of the instrument is reported around ± 4% of the resulted thermal conductivity [74].

The machine was designed to carry two samples with different or same dimensions with a maximum thickness of 150 mm. Therefore, two-inch (50-mm) thickness of calibrated dummy sample (expanded polystyrene) with a known thermal conductivity on the upper surface of the main heater, as shown in Figure 4.16. Hence, the test sample with more than 150 mm thicknesses could be installed on the lower side of the main heater [75]. The maximum dimensions of the samples are 610 x 610 mm (2 ft x 2 ft), thereby covering the whole heater plate (consisting of main heater and guard heater), as shown in Figure 4.17. On the other hand, the minimum dimensions of the bricks specimens are 350 x 350 mm (1ft x 1ft) to cover at least the main heater. The temperature difference between the main and guard heaters has to be adjusted to zero to prevent any heat loss in the lateral directions.

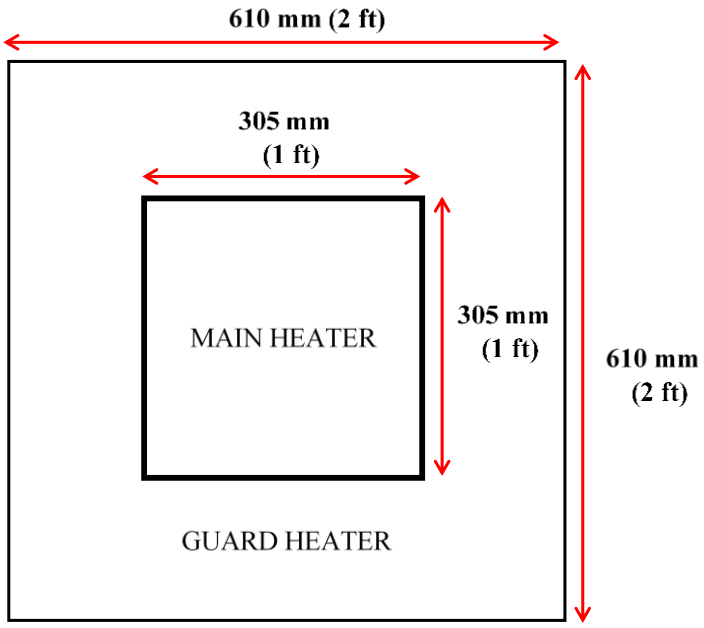

Figure 4.17: Heater plate (main and guard heater)

In this work, each sample consisted of two hollow bricks joined together with mortar in the laboratory. The dimensions of the samples were (420 x 400 x 200 mm), which is a little larger than the main heater, as shown in Figure 4.18. Four samples were prepared in the same manner and dimensions in order to determine their equivalent thermal conductivity.

The samples had to be prepared before the test and, therefore, the following tasks ought to be done: First, the cavities had to be taped to close them perfectly (Figure 4.19), so as the air inside the cavities could be trapped out and heat loss does not occur. Since the sample's dimension was just less than the guard heater (610 x 610 mm), as shown in Figure 4.17, the hollow polystyrene board was used with the same thickness of the sample to cover the remaining area of the guard heater, hence, the heat would not be scattering in the transverse directions, as shown in Figure 4.19. Both surfaces of the samples (upper and lower) have

to be flat and smooth to minimize the friction and heat loss between both the sample surfaces and the corresponding hot and cold surfaces of the heater plates. Therefore, as shown in Figure 4.19, four thermocouples were fixed on each side of the sample within the area of the main heater (350 x 350 mm). The temperature was monitored using automatic data acquisition system (Campbell Scientific 21X). Further, both surfaces of the sample were covered with blankets to reduce the friction and heat loss between the rough surface of the sample and the plates.

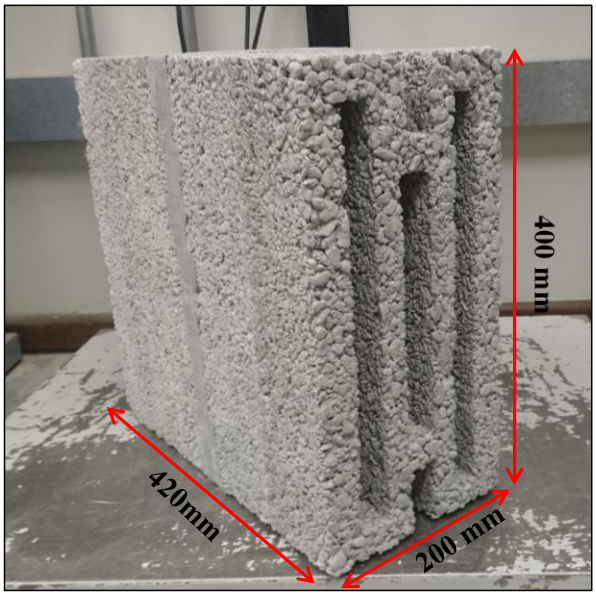

Figure 4.18: Wall samples of masonry hollow bricks

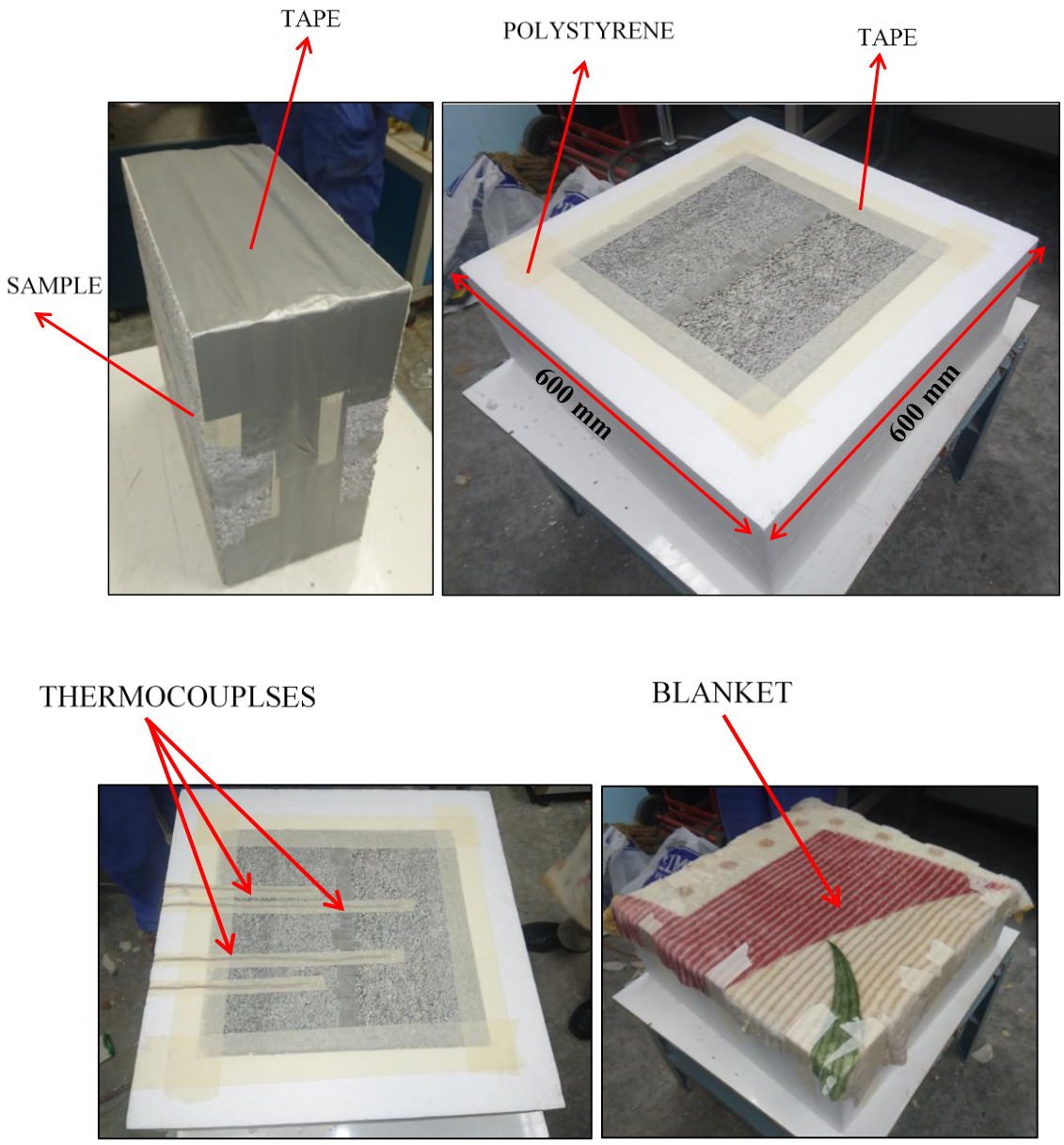

Figure 4.19: Preparing samples before testing

The temperature of hot and cold surfaces of the test sample were maintained at 55 and 25°C for the upper and lower faces, respectively, with an average temperature of about 40°C. During the experiment, a multi-channel data logger (attached to the computer) was recording the temperatures of the hot and cold surfaces of the sample hourly. The

temperatures of hot and cold surfaces were monitored until a steady state was achieved and the temperature difference between the last three or four hours was equal to zero.

When a steady state takes place, the hot and cold temperatures of the sample were determined with the voltage (V) and current (I). Then:

$$\boldsymbol{Q = N * V * I} \quad 4.9$$

$$\boldsymbol{Q_1 = k_1 * A * \frac{T_{hot} - T_{cold}}{d_1}}\ \boldsymbol{, for\ the\ dummy\ sample} \quad 4.10$$

$$\boldsymbol{Q_2 = Q - Q_1} \quad 4.11$$

Therefore,

$$\boldsymbol{k_2 = \frac{Q_2 * d_2}{A * (T_{hot} - T_{cold})}}\ \boldsymbol{, for\ the\ tested\ sample} \quad 4.12$$

where,

N: The correction factor of the instrument = 0.986

V: Main heater voltage, millivolts (mV)

I: Main heater current, milliampere (mA)

Q_1: Heat flow through dummy sample (W)

k_1: Thermal conductivity of dummy sample (W/m.k)

A: Surface area of the main heater (m^2)

T_{hot}: Hot surface of dummy or tested sample (°C)

T_{cold}: Cold surface of dummy or tested sample (°C)

d_1: Thickness of dummy sample (m)

Q_2: Heat flow through test sample (W)

Q: Total heat flow in main heater (W)

k_2: Thermal conductivity of test sample (W/m.k)

D_2: Thickness of test sample (m)

CHAPTER 5

EXPERIMENTAL RESULTS AND DISCUSSION

5.1 Introduction

This Chapter presents the results and discussions of the experimental work. In the experimental work, the mechanical and thermal properties were measured in the laboratory for the concrete specimens as well as for the hollow concrete bricks. Compressive strength was measured for all the concrete samples with two types of cubes (50 and 100 mm) and the flexural strength was determined on prisms using two-point loading (40x40x160 mm) until cracking. Further, thermal conductivity coefficient was gauged using FOX50 heat flow meter instrument for concrete discs (50 mm diameter and 25 mm thickness). All the previous measurements were for normal concrete with aggregate replacements by rubber (Ru) and polyethylene (PE). Four hollow concrete bricks were cast and cured with a new designed (optimum) geometry using the three insulation materials (rubber, polyethylene, perlite) with different contents. The compressive strength, density and absorption were measured for the hollow bricks and compared to the requirements in ASTM C-129 standards. The thermal conductivity of the hollow concrete bricks was measured using guarded hot plate, as per ASTM Standard C 177-85.

5.2 Experimental Results for Concrete

5.2.1 Compressive Strength

Table 5.1 presents a summary of the compressive strength for the 30 mixes after 7 days of curing. The reported values of compressive strengths are the average of three specimens (50 mm cubes) prepared from each mix with a total number of 90 cubes. Fine and coarse aggregates were replaced with fine and coarse rubber and polyethylene, separately, with contents of 10 – 50%. The first five mixes were for the replacement of fine aggregate (Mixes No. Ru1 – Ru5 and PE1 – PE5 for rubber and polyethylene, respectively), as shown in Table 4.1. Similarly, replacing the coarse aggregate was in Mixes Ru6 – Ru10 and PE6 – PE10. Further, both aggregates (fine and coarse) were replaced by fine and coarse rubber in Mixes Ru11 – Ru15, and with polyethylene in Mixes PE11 – PE15. The compressive strength for the control mix was 44.12 MPa, which was the average for three cubes.

Table 5.1 Summary of compressive strength of all concrete mixes (MPa)

Replaced by	Rubber (Ru)					Polyethylene (PE)				
Content %	10	20	30	40	50	10	20	30	40	50
Fine Agg.*	Ru1	Ru2	Ru3	Ru4	Ru5	PE1	PE2	PE3	PE4	PE5
	31.93	20.49	15.61	9.56	6.55	39.44	30.29	23.72	17.27	12.41
Coarse Agg.	Ru6	Ru7	Ru8	Ru9	M10	PE6	PE7	PE8	PE9	PE10
	30.35	18.89	12.35	8.25	4.5	34.25	24.05	19.08	12.14	8.12
Fine+ Coarse Agg.	Ru11	Ru12	Ru13	Ru14	Ru15	PE11	PE12	PE13	PE14	PE15
	34.44	23.93	19.22	12.63	7.89	36.24	27.04	22.16	15.8	10.36

*Aggregate

As shown in Table 5.1, the compressive strength decreased significantly due to the addition of both materials (Rubber and Polyethylene), as compared to the control mix. Such reduction could be ascribed to the loss of strong adhesion between cement paste and the surface of Ru and PE particles (due to the smooth surfaces of these materials) [33]. Further, the impermeability of PE and Ru restricted the water for cement hydration during curing period [33]. Khatib [27] observed that the particles of rubber and polyethylene were more elastically deformable than the surrounding matrix (cement paste). Therefore, the cracks were initiated quickly around plastic and rubber particles and failure took place earlier. The reduction in compressive strength depends on material structure, particle size and replacement content. Rubber replacements reduced the strength more than polyethylene because polyethylene particles were more rigid than rubber particles. Further, the small particle size of rubber and polyethylene minimized the drop in the strength as compared with coarse particles and the combination between fine and coarse sizes (Table 5.1), in a way similar to the results reported elsewhere [76, 27]. The compressive strengths were reduced with increasing the dosage of both replacement materials (Ru and PE) for all particle sizes (fine and coarse) [27].

Figure 5.1 indicates that the compressive strength decreases with increasing the content of rubber from 10 to 50% with a reduction of 22 to 90% as similarly reported by others [4,3,5]. The results therein indicate that the coarse rubber achieved the least strengths, as compared to fine and both sizes of rubber replacements. For the specimens with fine rubber, the strength was reduced with increasing the rubber content from 10 to 50% with a reduction in the range of 28 to 85%, which is similar to the results reported elsewhere [4,3,5]. The difference in compressive strength between coarse and both rubber (fine and coarse)

replacements was in the range of 11 to 43%, as clearly shown in Table 5.1. On the other hand, the difference in compressive strength was decreased between fine and both replacements by 7 to 17%.

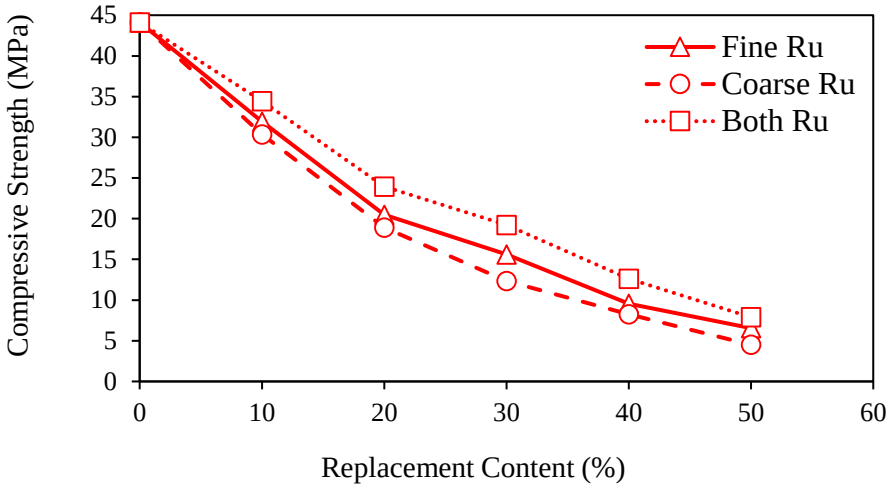

Figure 5.1: Compressive strengths for all the rubber replacement samples

Similarly, for polyethylene (PE) replacement, the strength decreased with increasing the PE content, as depicted in Figure 5.2. The fine aggregate replacement acquired the highest strength, while the coarse aggregate substitutions resulted in the least strength. However, the strength curve of both aggregate replacements (fine and coarse) was between fine and coarse replacement (Figure 5.2), as observed by Saikia et al. [21]. The worst scenario was for the coarse aggregate replacements of PE, which reduced the strength significantly with 22 to 82% for the substitutions of 10 to 50%, respectively, as compared to the control. On the other hand, the reduction decreased to 11 to 72% for fine particle replacement, as compared with the control concrete (i.e. without any replacement).

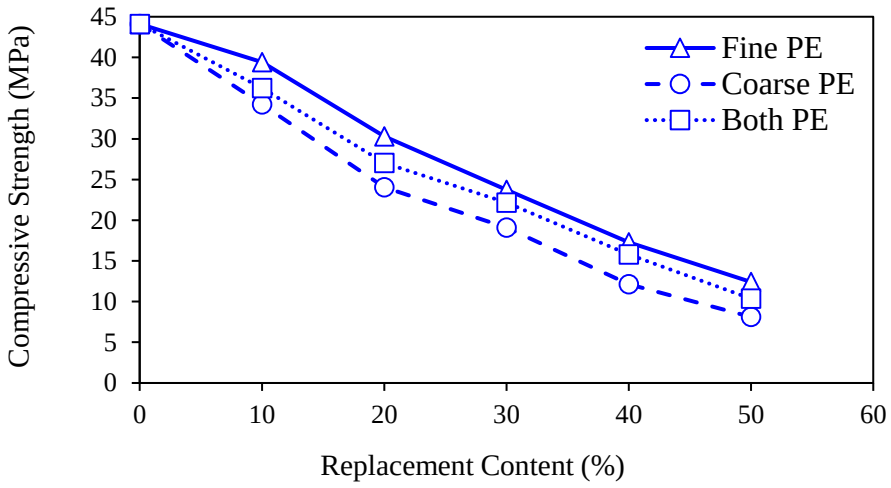

Figure 5.2: Compressive strengths for all the polyethylene replacement samples

As shown in Figure 5.3, the fine aggregate replacement (by rubber and polyethylene) reduced the strength crucially. The 10% fine aggregate replacement reduced the strength by about 27.63 and 10.61% for rubber and polyethylene, respectively, as compared to the control mix (0% replacement). The maximum reduction of the compressive strength of fine rubber was about 32%, as compared with fine polyethylene (Figure 5.3). Similarly, the reduction was decreased to 21% for the coarse rubber and plastic replacements, as shown in Figure 5.4. Continuously, Figure 5.5 presented the compressive strength for both particle size replacements (fine and coarse) of rubber and polyethylene, in which the reduction in the strength was about 13%.

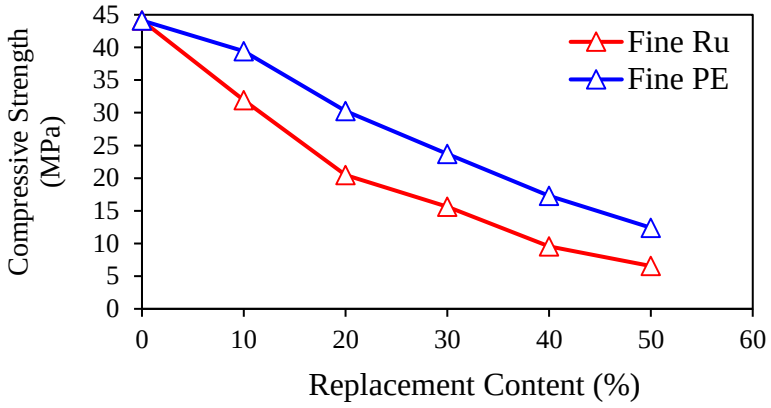

Figure 5.3: Compressive strength for fine rubber and polyethylene replacements

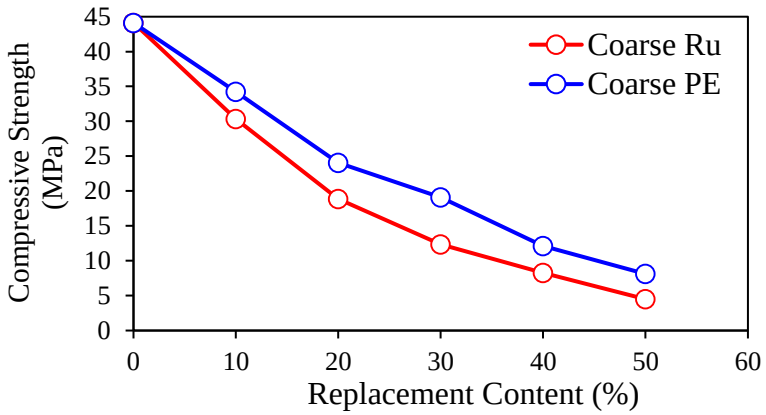

Figure 5.4: Compressive strengths for coarse rubber and plastic replacements

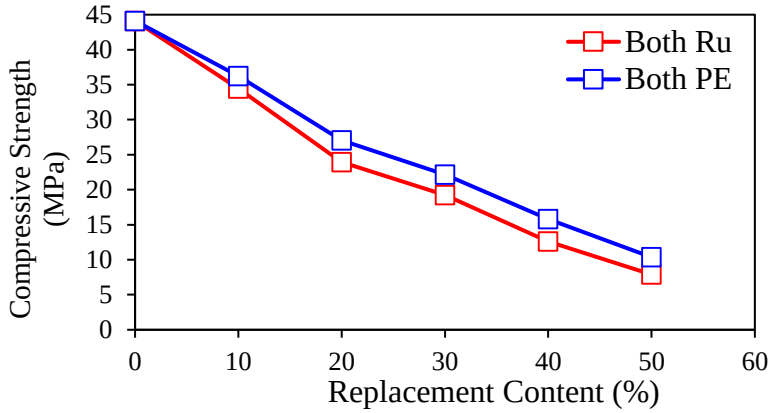

Figure 5.5: Compressive strengths for both fine and coarse Ru and PE replacements

5.2.2 Flexural Strength

The flexural strength is known as the modulus of rupture, which is the stress in the material just before yielding in the flexural test. A total number of ninety prisms (measuring 40x40x160 mm) were tested in the laboratory to find the average modulus of rupture (M_R), as shown in Table 5.2. Fifteen mixes for rubber replacements (Ru1-15) and another fifteen mixes for polyethylene replacements (PE1-15) were used to assess the effect of the replacement on M_R. For the control mix (without replacement), the average modulus of rupture for the three prisms was 4.80 MPa, which is in the range reported in the literature [21, 26].

Table 5.2: Average modulus of rupture (M_R) (MPa) for all mixes

Replaced	By Rubber (Ru)					By Polyethylene (PE)				
Fine Aggregate	Ru1	Ru 2	Ru 3	Ru 4	Ru 5	PE 1	PE 2	PE 3	PE 4	PE 5
	3.91	3.76	3.52	3.10	2.82	4.00	3.82	3.65	3.39	2.94
Coarse Aggregate	Ru 6	Ru 7	Ru 8	Ru 9	Ru 10	PE 6	PE 7	PE 8	PE 9	PE 10
	3.88	3.64	3.41	2.98	2.43	3.89	3.71	3.53	3.25	2.54
Fine + Coarse Aggregate	Ru 11	Ru 12	Ru 13	Ru 14	Ru 15	PE 11	PE 12	PE 13	PE 14	PE 15
	3.80	3.55	3.36	2.89	2.39	3.85	3.66	3.45	3.16	2.51

The data in Table 5.2 indicate that M_R decreased with increasing the dosage of replacements (Ru and PE), which could be attributed to the reduction in the adhesion between the cement paste and particle surfaces of Ru and PE [33]. The presence of plastic and rubber in concrete works as reinforcement, which absorb energy during fracture and reduces the brittle behavior of unreinforced concrete [33]. The ductility of concrete with

rubber particles was higher as compared to the same concrete with plastic, which was ascribed to the higher flexibility rubber particles.

As shown in Table 5.2, M_R was the highest for fine replacements (Ru and PE), while it was the least for coarse particles due to the loss of the bond between the cement paste and the replacement particles [6, 3]. In Figure 5.6, M_R is depicted for all the specimens with different rubber contents. For fine rubber specimens, M_R for 10% replacement decreased by around 19%, as compared to the control mix, while the reduction amounts to 22 and 27% for 20 and 30% replacements, respectively. The values were dropped gradually to 35 and 41% for the substitutions of 40 and 50%. On the other hand, the specimens with coarse and both mixed-size particles (fine and coarse) of rubber had a considerable reduction in M_R, as compared to fine rubber, which was almost less than 15%, which is somewhat similar to the reduction reported in the literature [27].

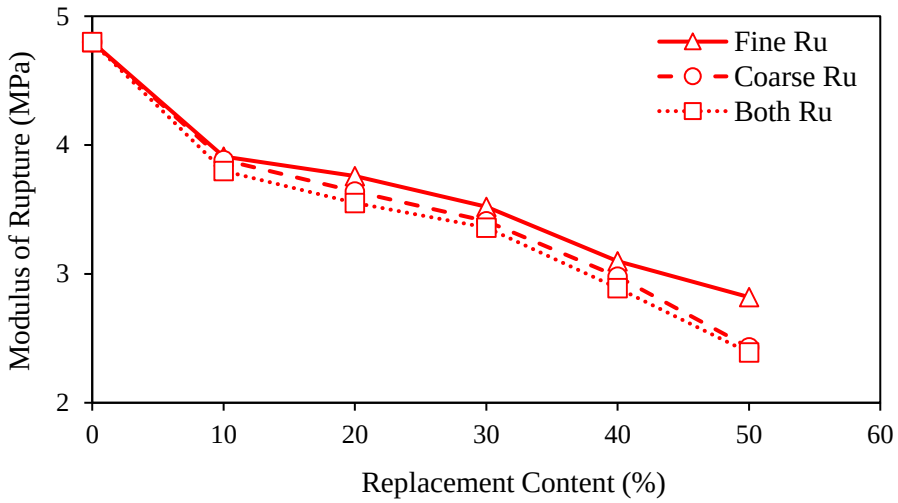

Figure 5.6: Modulus of rupture for all rubber replacements

Similarly, Figure 5.7 presents M_R for concrete with PE aggregates. The data therein indicate that the first five mixes with fine plastic particles have the highest values. On the other hand, the coarse particles gave lower values of M_R as compared to fine PE particles, while the combination of particles (fine and coarse) resulted in the lowest M_R. Fine plastic particles alterations with 10 and 20% reduced M_R less than 20% relative to the referenced mix (without any PE), which is somewhat similar to the reduction reported in the literature [21], and as the PE particle's content increased to 50%, the reduction increased to 39%. The worst scenario was with the combination particles of plastic that sharply decreased M_R to 2.51 MPa (48%). It is obvious that fine particles surpassed positively all the other types of particles, which was less than 15% as related to the other substitutions, which is similar to values reported in the literature [21].

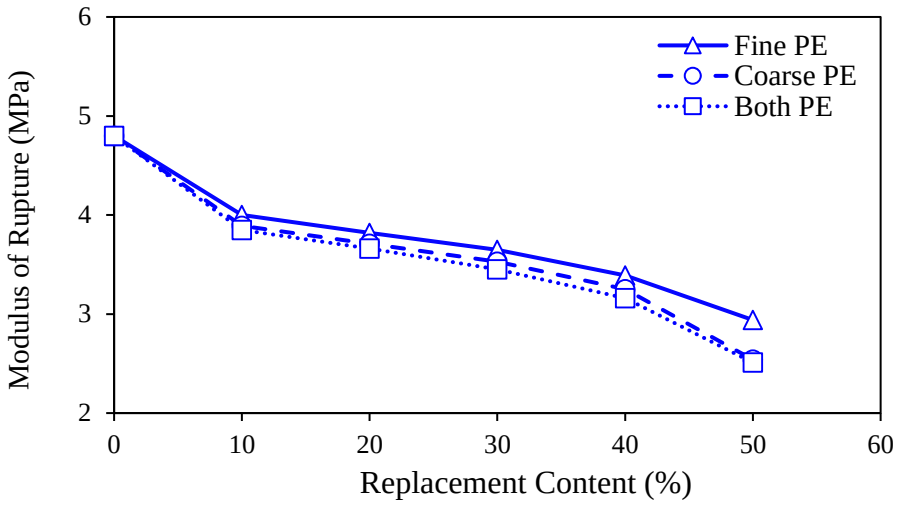

Figure 5.7: Modulus of rupture for all polyethylene replacements

Figure 5.8 (a,b,c) presents a comparison between the addition of rubber and polyethylene on M_R. The data therein indicate that there is a slight difference in M_R values between PE

and Ru, which was ascribed to the smooth surface of rubber and polyethylene particles. Therefore, the bond between cement paste and theses particles was reduced and cracks were initiated. As shown in Figure 5.8 and Table 5.2, the difference in M_R between the specimens of rubber and polyethylene with fine particles, coarse particles and both sizes was generally less than 9%.

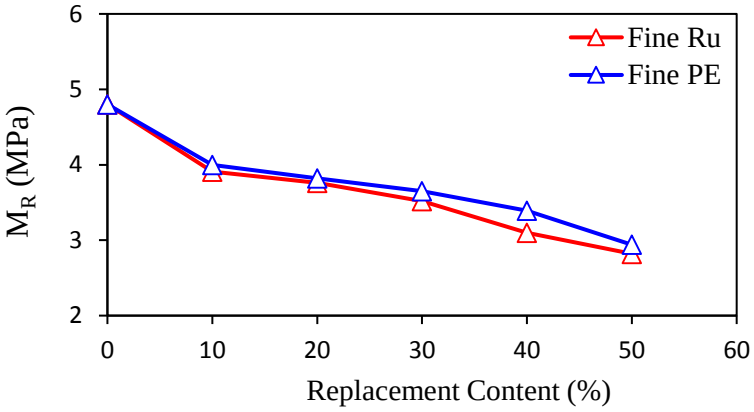

(a)

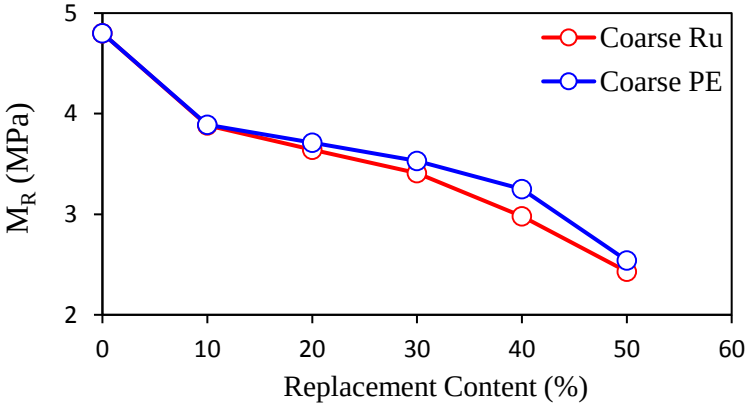

(b)

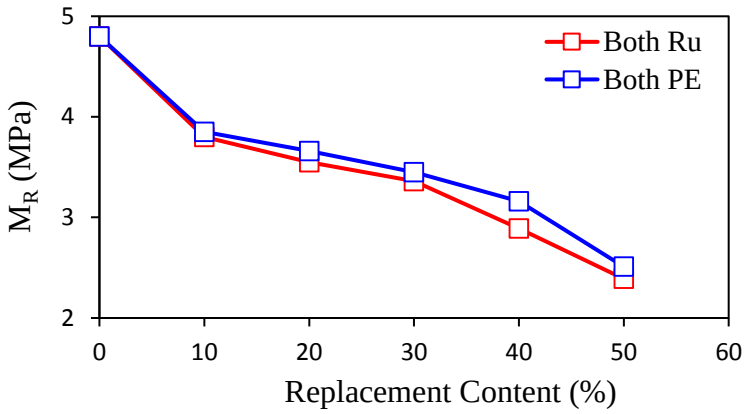

(c)

Figure 5.8: Modulus of rupture for all Ru and PE replacements

5.2.3 Thermal Conductivity

From each of the thirty mixes, three discs (50 mm dia. with 25 mm thickness) were prepared to assess the thermal conductivity coefficient (k value) for both replacement materials (rubber and polyethylene). Therefore, ninety samples were examined and the average of three specimens for each mix was considered as the thermal conductivity coefficient, as shown in Table 5.3. Further, three samples for the control mix were tested and the average k value was 1.331 W/m.k, which is somewhat to that reported elsewhere [77].

As the data in Table 5.3 clearly indicate, thermal conductivity coefficient varies with the replacement material, content and size of particles. It is shown that the concrete with rubber aggregate was thermally better relative to that with PE aggregate due to the lower thermal conductivity coefficient of rubber. For the rubber replacement samples, the coarse rubber resulted in higher thermal resistance compared to the fine and combination substitutions, as numerically presented in Table 5.3 and schematically shown in Figure 5.9. The data therein indicate that the reduction in thermal conductivity depends on the content and size

of rubber, as the rubber proportion increases in the mix, the k value decreases [31]. Further, the usage of larger particle size reduced the k value more than the smaller particles, as also reported elsewhere [31].

Table 5.3: Average thermal conductivity coefficient for ninety samples (W/m.k)

Replaced by	Rubber (Ru)					Polyethylene (PE)				
Fine Aggregate	Ru1	Ru 2	Ru 3	Ru 4	Ru 5	PE 1	PE 2	PE 3	PE 4	PE 5
	1.150	1.129	1.018	0.931	0.875	1.196	1.160	1.076	1.014	0.981
Coarse Aggregate	Ru 6	Ru 7	Ru 8	Ru 9	Ru 10	PE 6	PE 7	PE 8	PE 9	PE 10
	1.161	1.068	0.956	0.895	0.835	1.201	1.110	0.998	0.938	0.898
Fine + Coarse Aggregate	Ru 11	Ru 12	Ru 13	Ru 14	Ru 15	PE 11	PE 12	PE 13	PE 14	PE 15
	1.190	1.174	1.052	0.964	0.929	1.228	1.201	1.110	1.071	1.051

For the rubber samples, the k value decreased with increasing the content of rubber by 6 to 37% for the content of 10 to 50%, respectively, as could be seen in Figure 5.9. Furthermore, it can be clearly observed that when the rubber content in the range of 10 to 20% the reduction in k values decreased by about 15%. The same behavior was reported in the literature [77]. However, the coarse size of rubber reduced the heat transfer more than the fine and combination sizes with a difference of 10%, as depicted in Figure 5.9 [31] because the coarse aggregates were around 50% of the total mix proportions (Table 4.14). Therefore, the thermal resistivity for concrete sample with coarse aggregate was higher than the other sizes (due to high content of coarse aggregate).

Similarly, the replacement of polyethylene followed the same trend as that by rubber, as shown in Figure 5.10. The coarse content showed the highest thermal resistivity as compared to fine and both aggregates (fine and coarse). Further, the thermal conductivity

for all the samples was reduced with increasing the content of plastic. For 10% PE content, the reduction was in the range of 14 to 6% for fine and coarse substitutions, respectively, while the reduction was increased to 25, 29 and 32% for the replacements of 30, 40 and 50% for coarse PE, which is somewhat similar to that reported elsewhere [41]. Further, the depreciation in thermal conductivity for coarse PE was not exceeding 5 to 10% as compared to fine and both plastic sizes.

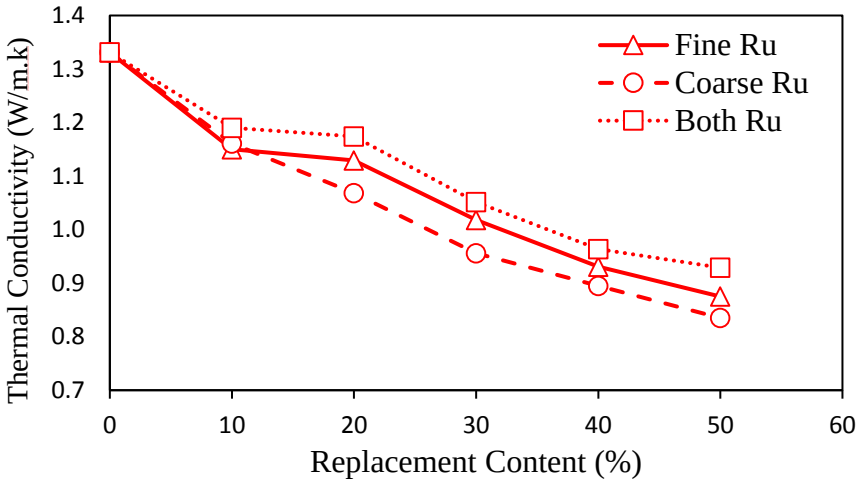

Figure 5.9: Thermal conductivity coefficients of all Ru replacements

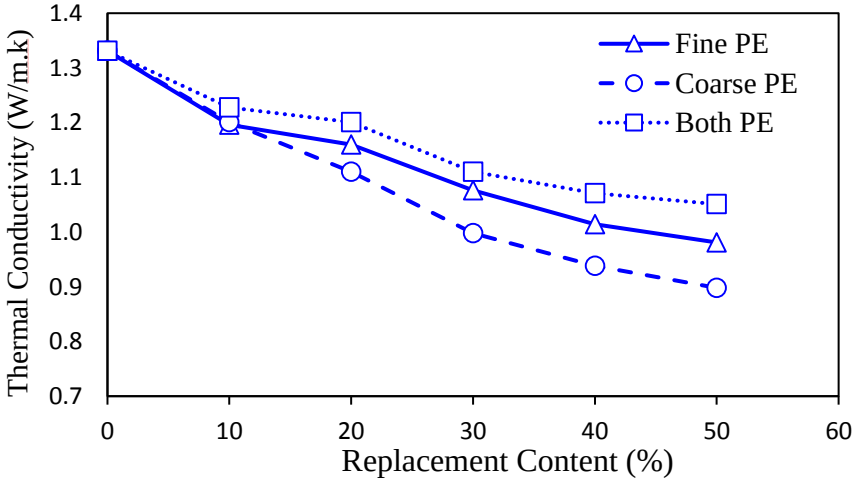

Figure 5.10: Thermal conductivity coefficients of all PE replacements

As shown in Figure 5.11, the replacement of normal aggregate by rubber and polyethylene into concrete at different dosages for fine, coarse and combination size of particles indicates that rubber specimens achieved higher thermal resistance (i.e. less thermal conductivity) compared to polyethylene for all particle sizes (fine, coarse and both) due to the lower thermal conductivity of rubber. The difference between Ru and PE replacements for fine and combination sizes were in the range of 3 to12%, while it was less than 7% for the coarse replacements.

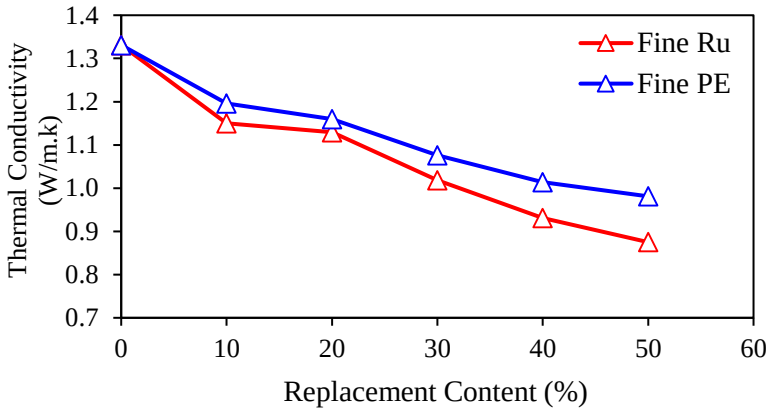

(a)

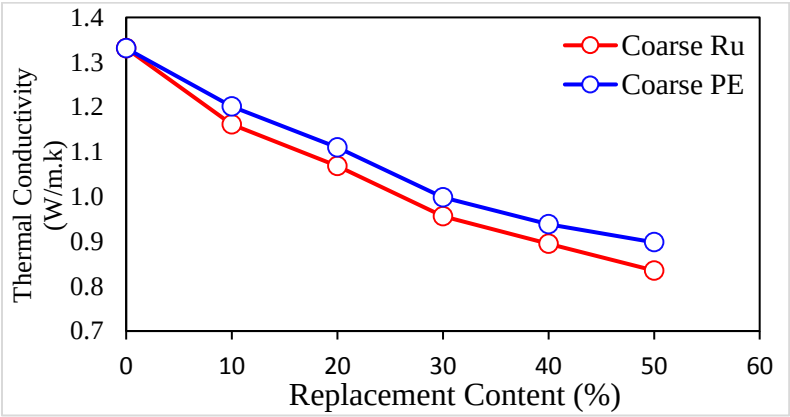

(b)

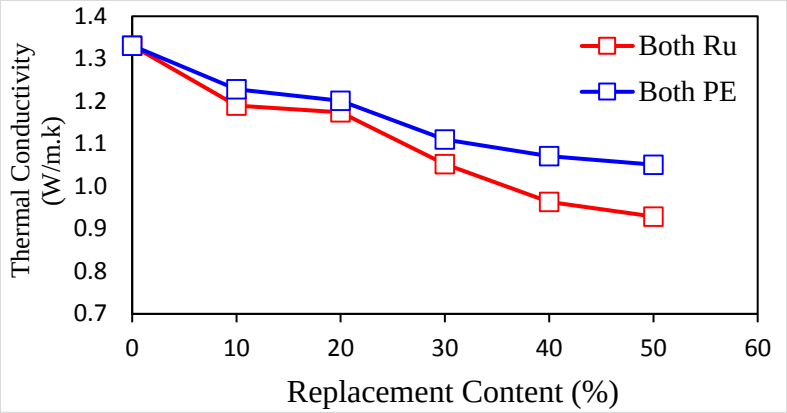

(c)

Figure 5.11: Thermal conductivity coefficients for all Ru and PE replacements

5.3 Experimental Results for Hollow Bricks

5.3.1 Compressive Strength

Four hollow bricks (control, perlite, rubber and polyethylene bricks) were used to perform the compressive strength test. As shown in Table 5.4 and Figure 5.12, all the compressive strength results of hollow bricks were presented.

Table 5.4: Compressive strength of cubes and hollow bricks

Mix	Strength of Hollow Brick (MPa) (Individual units)	Observations at Failure of Bricks
Control	6.90	Longitudinal cracks
PL-HB*	3.50	Longitudinal cracks
Ru-HB**	3.61	High flexibility, Absorb load
PE-HB***	3.84	Medium flexibility, small cracks

*PL-HB: Perlite Hollow Brick

**Ru-HB: Rubber Hollow Brick

***PE-HB: Polyethylene Hollow Brick

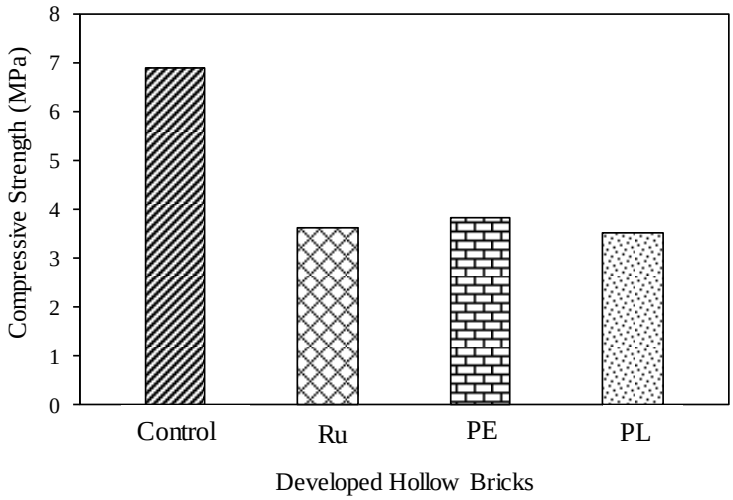

Figure 5.12: Compressive strengths for hollow bricks

The compressive strength for the control hollow bricks (with the optimum designed geometry) in Table 5.4 (6.90 MPa) satisfied the requirement of ASTM C-129 standards for non-load bearing hollow concrete masonry bricks [69]. Further, according to the same standard, non-load bearing units could be used as exterior walls, which is not sustaining loads and protected from the weather [69]. The compressive strength for the control brick achieved the highest value with 6.90 MPa, while perlite brick gave the least value of 3.50 MPa with a difference of 51%. The strength of polyethylene and rubber bricks was 3.84 and 3.61 MPa satisfied the ASTM C-129 requirement of 3.45 MPa. However, the reduction in strength for rubber and polyethylene bricks were 44 and 48%, respectively, as compared to the control brick. As shown in Figure 5.13, longitudinal cracks were initiated on the short side of the hollow bricks due to stress concentration.

C-HB

PL-HB

Ru-HB

PE-HB

Figure 5.13: Cracks of tested hollow bricks

5.3.2 Density and Absorption

According to ASTM C 129 [69], all the hollow bricks with replacement materials (PL, Ru, PE) were considered as lightweight masonry bricks because their dry density is less than 1680 kg/m^3, as shown in Table 5.5 and Figure 5.14 (a). Further, results of density and absorption for the various types of blocks indicate that the control brick was medium weight masonry brick (less than 2000 kg/m^3). The water absorption for the control bricks was 109.85 kg/m^3 (5.54%), while it was slightly higher for the developed bricks with rubber and plastic (Ru and PE) with percentages of 6.71% (117.73 kg/m^3) and 6.19% (99.53 kg/m^3), respectively, as depicted in Figure 5.14 (b). However, the absorption was

doubled for perlite bricks with a high value of 12.21%. This could be ascribed to the high absorption ability for perlite. According to ASTM C 90, the maximum water absorption for light-weight masonry bricks is 320 and 272 kg/m^3 for light and medium weight masonry bricks, respectively. Therefore, the control and developed bricks satisfied the absorption limitations for masonry bricks.

For rubberized bricks, the dry density was lower than 1776 kg/m^3 obtained by Sodupe-Ortega [53]. As shown in Table 5.5 and Figure 5.14 (c), the weight of the control block was 19.46 kg, which was the highest, as compared to other developed hollow bricks with the three replacements. Further, perlite hollow brick was the lightest (11.34 kg) with the differences of 8.12 kg (42%), 5.5 kg (33%) and 4.46 kg (24%), as compared to the control, rubber and polyethylene bricks, respectively. The polyethylene brick was the second lightest with a weight of 15.80 kg, which is lower than the control and rubber bricks by 3.66 kg (19%) and 1.04 kg (6%), respectively. However, the weight of rubber brick was lower than the control brick with a weight of 2.62 kg (13.50%). It is to be reported that the weight of the control and rubber bricks were lower than the same bricks developed by Al-Aqeeli [52] by 0.69 kg and 1.75 kg, respectively.

Table 5.5: Weight, absorption, wet and dry densities for developed hollow bricks

Mix	Weight/ Brick (kg)	Wet Density (kg/m^3)	Dry Density (kg/m^3)	Water Absorption	
				(kg/m^3)	(%)
Control (C)	19.46	1980.15	1870.30	109.85	5.54
PL-HB	11.34	1536.6	1349	187.60	12.21
Ru-HB	16.84	1753.33	1635.60	117.73	6.71
PE-HB	15.80	1608.43	1508.90	99.53	6.19

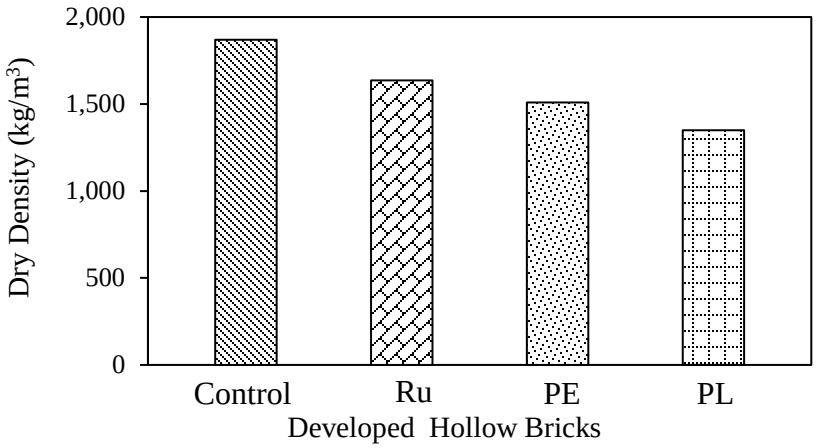
2,000
1,500
1,000
500
0
Dry Density (kg/m3)
Control
Ru
PE
PL
Developed Hollow Bricks

(a)

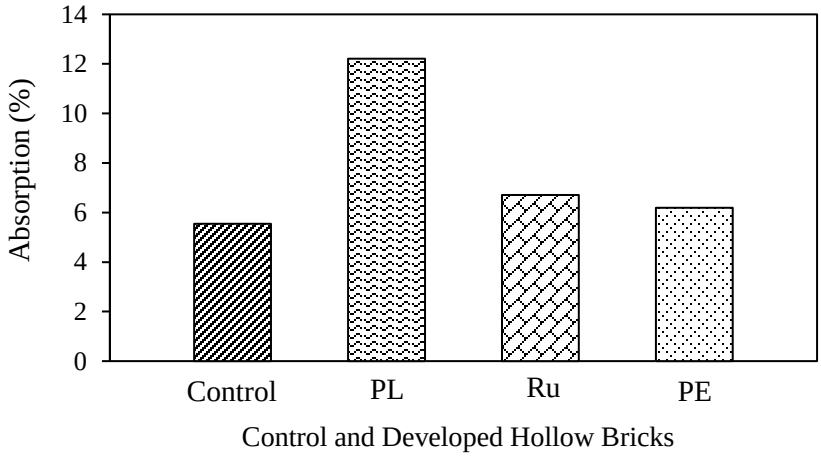
14
12
10
8
6
4
2
0
Absorption (%)
Control
PL
Ru
PE
Control and Developed Hollow Bricks

(b)

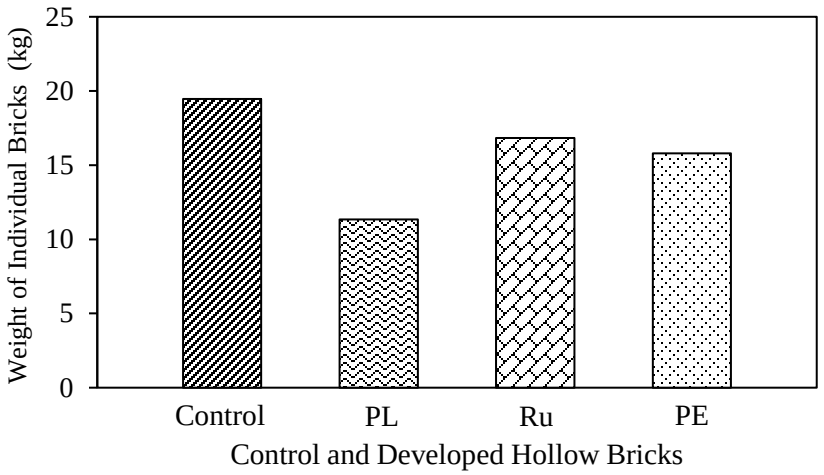

(c)

Figure 5.14: Absorption, density and weight of developed hollow bricks

5.3.3 Equivalent Thermal Conductivity

As shown in Table 5.6, the thermal conductivity of the developed hollow bricks was measured by the guarded hot plate (ASTM C 177). This test takes almost four days for sample preparation, setting the equipment, recording measurements and obtaining the results. The results of the equivalent thermal conductivity for all hollow bricks was depicted numerically in Table 5.6 and schematically in Figure 5.15. The data therein report the reduction of the equivalent thermal conductivity for the developed hollow bricks (30% PL, 20% Ru and 20% PE) as compared with the control hollow brick. The equivalent thermal conductivity for the control hollow brick (with no additive material) was 0.460 W/m.k, which was, as expected, the highest value as compared to the other hollow bricks produced with three replacements (Figure 5.15). The equivalent thermal conductivity of the perlite, rubber and polyethylene hollow bricks was lower than the control by 33, 12 and 16%, respectively, as compared to the control (optimum) hollow brick. Since, the geometry

layout of the cavities was the same for all the hollow bricks, the reduction was ascribed to the thermal conductivity of the replacement materials.

Table 5.6: Equivalent thermal conductivity of developed hollow bricks

Mix	K value (W/m.k)	Improvement (%)
Control	0.460	---
PL-HB	0.309	33
Ru-HB	0.404	12
PE-HB	0.387	16

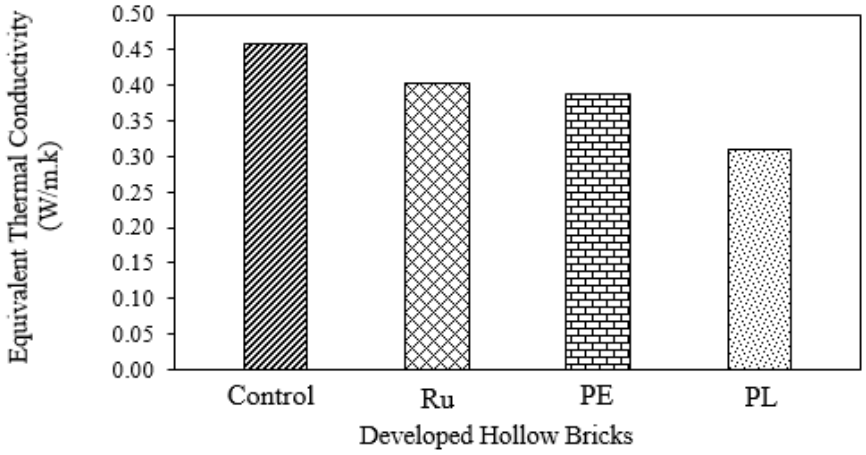

Figure 5.15: Equivalent thermal conductivity of control and developed hollow bricks

The equivalent thermal conductivity of the control hollow brick was 0.460 W/m.k, which was lower than the normal concrete bricks produced and tested by many researches, as shown in Table 5.7 and Figure 5.16. Since all these bricks were cast from concrete only (with no replacement materials), the enhancement was solely attributed to the optimum geometry of the cavities layout, which significantly increased the thermal resistance. As shown in Table 5.7, the improvement in the thermal conductivity was in the range of 21%

to 71%, as compared to the other control hollow bricks (without insulation materials). The data in Table 5.7 and Figure 5.16 proved the high thermal efficiency of the newly designed hollow brick, which could be highly efficient in minimizing the electrical consumption.

Table 5.7: Equivalent thermal conductivity of control hollow bricks

ID	Author	Description	No. of cavity	k_{equ} * (W/m.k)	Improvement (%)**
1	This work	Hollow brick	5 longitudinal	0.460	0
2	Al-Aqeeli et al. [52]	Hollow brick	2 square	0.585	21
3	Al-[57]et al.	Hollow brick	2 square	0.976	53
4	KFUPM (RI) [78]	Hordi hollow brick	---	1.092	58
5	KFUPM (RI) [78]	Hollow brick	3 rectangular	1.389	67
6	Al-Jabri et al.[79]	Hollow brick	2 square	1.60	71

* k_{equ} : Equivalent Thermal Conductivity

** Improvement = $100\times(k_{equ} -0.460)/ k_{equ}$

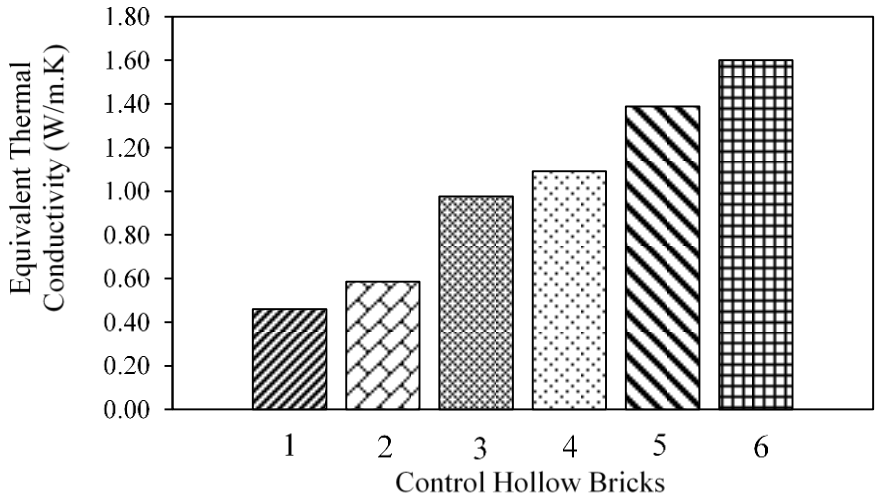

Figure 5.16: Equivalent thermal conductivity of normal hollow bricks*

* Numbers in x-axis are referred to Table 5.7

The data in Table 5.8 depicts the equivalent thermal conductivity of the developed hollow bricks and the normal hollow bricks (without insulation materials). For perlite hollow brick (with 30% perlite) achieved the least k value with a reduction of 20 to 80%, which was ascribed to the optimum design of cavities and the usage of perlite. Polyethylene hollow brick has a higher k value as compared to perlite with about 20% due to the higher density and k value of polyethylene particles. Further, the reduction for PE hollow brick was in the range of 4 to 76%, as shown in Table 5.8, while it was 12 to 75% for Ru hollow brick. Perlite and polyethylene hollow bricks had lower k value as compared with rubber hollow brick with about 24 and 4%, respectively.

Table 5.8: Equivalent thermal conductivity of the developed and normal hollow bricks

Author	k_{equ} (W/m.k)	Description	Improvement %		
			PL	PE	Ru
This work	0.309	PL: 30% replacement with sand by weight	0	-20	-24
	0.387	PE: 20% replacement with coarse aggregate by weight	20	0	- 4
	0.404	Ru: 20% replacement with coarse aggregate by weight	24	4	0
	0.46	Control (Optimum) hollow concrete brick "without any insulation material"	33	16	12
Al-Aqeeli et al., [52]	0.585	Hollow concrete brick with coarse rubber	47	34	31
Aftab et al., [74]	0.976	Normal hollow concrete brick	68	60	59
KFUPM (RI), [78]	1.389	Normal hollow concrete brick	78	72	71
	1.092	Hordi normal hollow concrete brick	72	65	63
Al-Jabri et al., [79]	1.6	Normal hollow concrete brick	81	76	75

Table 5.9 presents the equivalent thermal conductivity of perlite hollow brick (with 30% perlite). As clearly shown in Figure 5.17, the results proved that the PL hollow brick for this work achieved the lowest thermal conductivity in the range of 11 to 37%, as compared to elsewhere in the literature [13, 57].

Table 5.9: Equivalent thermal conductivity of perlite hollow bricks

Author	Brick ID	k_{equ} (W/m.k)	Description	Improvement %
This work,	1	0.309	30% replacement with sand by weight	0
Sengul et al. [13]	2	0.45	Lightweight concrete with perlite	31
Al-Hadhrami and Aftab [57]	3	0.389	Hollow clay brick with cavities filled with perlite and cement mix	21
	4	0.348	Hollow clay brick with body added perlite	11
	5	0.489	Hollow concrete brick with body added perlite	37

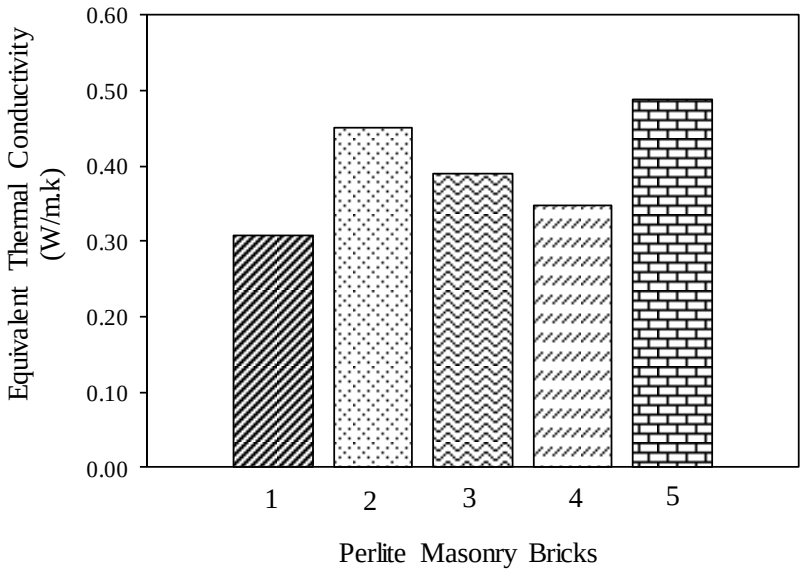

Figure 5.17: Equivalent thermal conductivity of perlite hollow bricks*

* Numbers in x-axis are referred to Table 5.9

For relative comparison, Table 5.10 includes the thermal conductivity of the developed perlite hollow brick, polystyrene bricks, clay bricks and vermiculite hollow bricks. The data indicated that the reduction of perlite hollow brick was in the range of 19 to 59% including hollow clay bricks with polystyrene (in the mix and cavity) and mineral wool, sandwich polystyrene brick and vermiculite hollow brick, as schematically shown in Figure 5.18 [74, 79].

Table 5.10: Equivalent thermal conductivity of perlite and insulation hollow bricks

Brick ID	Author	k_{equ} (W/m.k)	Description	Improvement %
1	This work	0.309	Perlite: 30% replacement with sand by weight	0
2	Aftab et al. [74]	0.473	Hollow clay brick with body added polystyrene	35
3		0.419	Hollow clay brick with cavities filled with polystyrene	26
4		0.382	Hollow clay brick with cavities filled with mineral wool	19
5	Al-Jabri et al. [79]	0.626	Hollow concrete brick with body added polystyrene	51
6		0.616	Polystyrene sandwich concrete brick	50
7		0.76	Hollow concrete brick with body added vermiculite	59

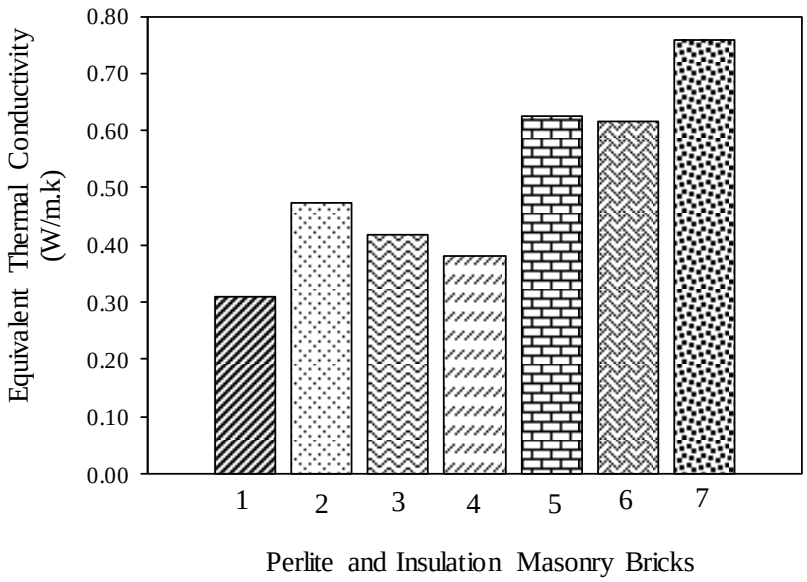

Figure 5.18: Equivalent thermal conductivity of perlite and insulation hollow bricks*

* Numbers in x-axis are referred to Table 5.10

As shown in Table 5.11, the data for thermal conductivity was summarized from the literature for many masonry bricks to compare them with the developed insulation hollow bricks in this investigation. The thermal performance of the developed hollow bricks (C, PL, PE and Ru) was highly efficient as compared with insulation bricks including many types of hollow clay bricks, polystyrene, vermiculite and mineral wool hollow bricks.

The control "optimum" hollow brick (C) was significantly reduced the thermal conductivity by 3 to 65% as compared with four types of clay hollow bricks, polystyrene, rubber and vermiculite hollow bricks. On the opposite side, four types of clay, mineral wool, rubber, polyethylene and perlite achieved lower thermal conductivity with amount of 9 to 33%.

For perlite hollow brick, the equivalent thermal conductivity was lower than seven types of normal clay hollow bricks in the range of 19 to 52%. Further, the reduction increased to 59% as compared with polystyrene, vermiculite and rubber hollow bricks.

Table 5.11: Equivalent thermal conductivity of developed and insulation hollow bricks

Brick ID	Author	k_{equ} (W/m.k)	Description	Improvement %			
				C	PL	PE	Ru
1	This work	0.460	Optimum design (without insulation material)	0	33	16	12
2		0.309	Perlite: 30% replacement with sand by weight	-33	0	-20	-24
3		0.387	PE: 20% replacement with coarse aggregate by weight	-16	20	0	-4
4		0.404	Rubber: 20% replacement with coarse aggregate by weight	-12	24	4	0
5	Al-Aqeeli et al. [52]	0.512	Hollow concrete brick with coarse rubber	11	40	24	21
6	Al-Hadhrami et al. [57]	0.65	Normal hollow clay brick	41	52	40	38
7		0.495	Normal hollow clay brick type 1	8	38	22	18
8		0.504	Normal hollow clay brick type 4	10	39	23	20
9		0.4	Normal hollow clay brick type 5	-13	23	3	-1
10		0.378	Normal hollow clay brick type 8	-18	18	-2	-7
11		0.402	Normal hollow clay brick type 9	-13	23	4	0
12	Aftab et al. [74]	0.382	Normal hollow clay brick type 10	-17	19	-1	-6
13		0.473	Hollow clay brick with body added polystyrene	3	35	18	15
14		0.419	Hollow clay brick with cavities filled with polystyrene	-9	26	8	4
15		0.382	Hollow clay brick with cavities filled with mineral wool	-17	19	-1	-6
16	Al-Jabri et al. [79]	0.626	Hollow concrete brick with body added polystyrene	36	51	38	35
17		0.616	Polystyrene sandwich concrete brick	34	50	37	34
18		0.76	Hollow concrete brick with body added vermiculite	65	59	49	47

On the other hand, the thermal efficiency of polyethylene hollow brick was considerably reduced as compared with perlite hollow brick with a reduction of 20%. The thermal conductivity of PE hollow brick was lower than the most types of clay hollow bricks, polystyrene, rubber and vermiculite hollow bricks with amounts 3 to 49% and with a slight increment with two types of clay hollow bricks and mineral wool brick by about 2%.

The developed rubber hollow brick was more thermally efficient by 21% compared with rubber hollow brick in the literature [52]. The inefficiency of rubber hollow brick was observed when compared with polyethylene, three types of clay and mineral wool hollow bricks by maximum amount of 7%, while this amount increased to 24% for perlite hollow brick. Contrary, the improvement of Ru hollow brick could reach up to 47% in a comparison with most types of clay, polystyrene and vermiculite hollow bricks.

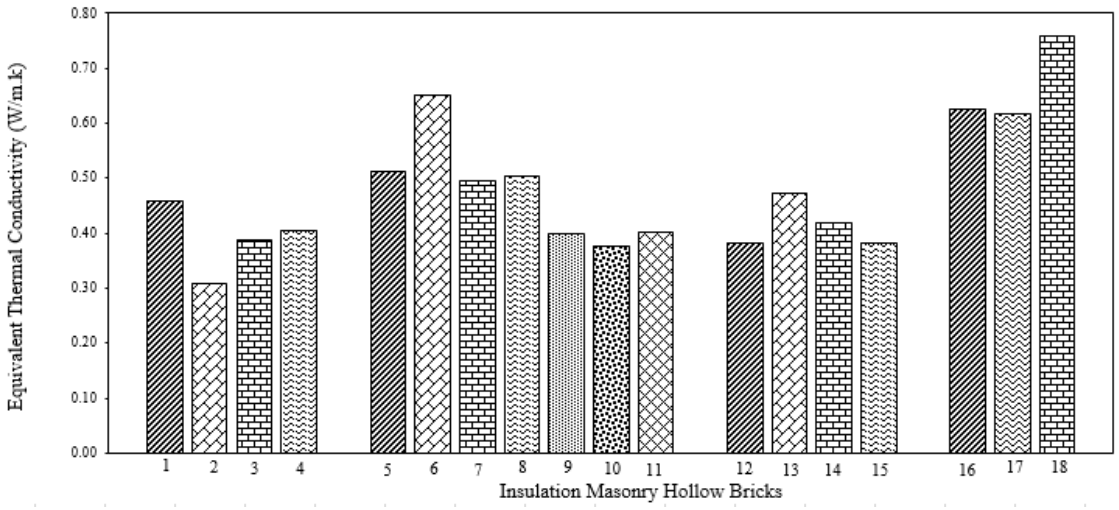

Figure 5.19: Equivalent thermal conductivity of developed and insulation hollow bricks*

* Numbers in x-axis are referred to Table 5.11

CHAPTER 6

CONCLUSIONS AND RECOMMENDATIONS

In this Chapter, the results of the simulation and experimental programs were summarized in the Conclusions section. Further, some relevant ideas and subjects, which could be executed in future studies, are presented in the Recommendations section.

6.1 Conclusions

This work reports the thermal and mechanical properties of concrete and masonry hollow bricks. The additive insulation materials (rubber, polyethylene and perlite) have a significant effect on increasing the thermal efficiency of concrete and bricks. The optimum design of cavities geometry layout increased the thermal resistance of concrete bricks. Based on the results reported in this investigation, the following conclusions could be drawn:

1. From the finite element model, the best "optimum" hollow brick was D-G1-HB5 (the optimum design developed in this thesis), while the worst was M-HB2 (the market type) with a difference in the average inner temperature of about 4.48°C for normal case (air cavities) in practice.

2. The factors that influence the heat transfer through the hollow bricks are many and interactive. However, the following factors have the main impact on the heat processes (conduction, convection and radiation):
    - Aspect ratio: Increasing this ratio tends to decrease the heat transfer through the cavities by convection and radiation.
    - Cavity width: Decreasing the width of the cavities (parallel to heat flux) decreases the heat transfer through the cavities by convection and radiation.
    - Hollow ratio: Increasing this ratio tends to decrease the heat transfer through solid parts of the brick by conduction.
    - Thermal Bridges: Decreasing the number of thermal bridges and increasing their length would decrease the heat transfer through solid parts of the brick by conduction.
    - Number of cavities: Decreasing the number of cavities tends to significantly reduce the heat transfer because the convection and radiation inside the cavities (and the number of thermal bridges) would be decreased.
3. For the normal concrete, its compressive and flexural strengths decreased significantly due to the addition of both materials (rubber and polyethylene), as compared to that of the control mix, which was ascribed to their much lower strength (as compared to concrete) and to the reduction of the adhesion between cement paste and the Ru and PE particles (due to their smooth surface). On the other hand, the thermal conductivity was improved with increasing the contents of rubber and polyethylene. The details of the compressive and flexural strengths as well as the thermal conductivity clarified as following:

- The maximum reduction in compressive strength was attained when the fine Ru and PE particles were used. Increasing the rubber and polyethylene content from 10 to 50% decreased the compressive strength by 31 to 90% for the coarse rubber particles and 22 to 82% for the polyethylene particles.
- The maximum reduction in flexural strength was attained when the both fine and coarse Ru and PE particles were used. The modulus of rupture was reduced with increasing rubber content from 10 to 50% with a reduction of 21 to 50% for fine rubber, which was similar to polyethylene.
- The maximum reduction in thermal conductivity was attained when the coarse Ru and PE particles were used. The k value decreased gradually as rubber content increased from 10 to 50% with the values of 13 to 37%, while the values decreased slightly from 10 to 32% for polyethylene.

4. Four hollow bricks were developed in this investigation including optimum "designed" without insulation materials, perlite, rubber and polyethylene hollow bricks. The results were summarized as following:
    - The four hollow bricks satisfied the strength requirements in the ASTM C 129 for non-load bearing masonry bricks, in which the minimum strength was 3.45 MPa.
    - The optimum hollow brick (without insulation material) was considered as medium weight masonry brick, while the other three hollow bricks (perlite, rubber and polyethylene) were considered as lightweight masonry bricks, according to ASTM C 129 standard.

- The four developed hollow bricks satisfied the limitations for water absorption stated in the ASTM C 129 standard, which are 272 and 320 kg/m^3 for medium and lightweight masonry bricks, respectively.
- The equivalent thermal conductivity (According to ASTM C 177) of the optimum "designed" brick developed in this investigation was the lowest as compared with the control hollow bricks (tested by many researchers) by about 20 to 70%.
- Perlite, rubber and polyethylene reduced the equivalent thermal conductivity by 33, 16 and 12%, respectively, as compared to the optimum brick.
- Perlite reduced the equivalent thermal conductivity by 52 and 31% as compared with the clay and sandwich polystyrene bricks, respectively.

6.2 Recommendations

From the analytical and experimental programs conducted in this research, the following recommendations could be stated for future studies:

1. Develop a finite element model to validate the experimental work to measure the equivalent thermal conductivity of hollow concrete bricks, in order to save the time to be spent for conducting the guarded hot plate test.
2. Develop a finite element model to predict the maximum sustainable load and failure behavior of the hollow brick.
3. Use another software, such as Ansys, to obtain more accurate and better simulation of the air circulation inside the cavities of the hollow brick.

4. Conduct a survey on the available bricks in the Saudi market to form a data bank to be used to assess their thermal efficiency using FEM without conducting experimental program.
5. For the experimental program, the cavities of the hollow bricks could be filled with other insulation materials, such as rubber pieces, plastic, graded perlite and polystyrene bubbles, which would increase the thermal resistance inside the cavities.
6. Use air-entrained agents in the concrete mix of the masonry bricks to increase the thermal resistance.
7. Apply plastering on one face or both faces of the hollow brick with different types of plasters such as gypsum, insulation mortars to study their influence on the thermal performance.
8. Use supplementary cementitious materials such as lime and powder perlite to increase the strength and reduce the cost of the masonry bricks.

References

[1] A. S. Al-Tamimi, M. A. Al-Osta, O. S. B. Al-Amoudi, and R. Ben-mansour, "Effect of Geometry of Holes on Heat Transfer of Concrete Masonry Bricks Using Numerical Analysis," *Arabian Journal for Science and Engineering*, pp.1–17, 2017.

[2] A. S. Al-Tamimi, M. A. Al-Osta, O. S. B. Al-Amoudi, and R. Ben-mansour, "Thermal Simulation for a Room with Solid and One-way Ribbed Slab Using FEM," *Proceedings, 2nd International Conference on Structural Engineering, New Technology and Methods (ICSENM'17)*, Spain, 2017.

[3] S. A. Al-Ghamdi, A. Al-Gargossh, and K. A. Al-Shaibani, "Energy Conservation by Retrofitting : An Overview of Office Buildings in Saudi Arabia," *Proceedings, International Conference on IT, Architecture and Mechanical Engineering- Dubai*-UAE, 2015.

[4] An Initiative of the: Regulation and Supervision Bureau - Powerwise - Air Conditioning". http://www.powerwise.gov.ae/en/section/how-can-i-save-electricity /residential /air-conditioning.

[5] A. Zhou, K. W. Wong, and D. Lau, "Thermal Insulating Concrete Wall Panel Design for Sustainable Built Environment," *The Scientific World Journal*, vol. 11, pp. 1–10, 2014.

[6] I. Al-Naimi, *The Potential for Energy Conservation in Residential Buildings in Dammam Region, Saudi Arabia*, PhD Dissertation in Architecture, University of Newcastle University, Australia, 1989.

[7] H. Duvier, J. Shamrock, and T. Brentwood, *Light Weight Insulating Building Blocks and Method of Making Same*, Patent No. US 4518431, 1985.

[8] O. Oluwole, J. Joshua, and H. Nwagwo, "Finite Element Modeling of Low Heat Conducting Building Bricks," *Journal of Minerals and Materials Characterization and Engineering*, vol. 11, pp. 800–806, 2012.

[9] J. J. Del Coz Díaz, F. P. Álvarez-Rabanal, O. Gencel, P. J. García Nieto, M. Alonso-Martínez, A. Navarro-Manso, and B. Prendes-Gero, "Hygrothermal Study of Lightweight Concrete Hollow Bricks: A New Proposed Experimental-Numerical Method," *Energy and Buildings*, vol. 70, pp. 194–206, 2014.

[10] I. Topc u and B. Iskdag, "Manufacture of High Heat Conductivity Resistant Clay Bricks Containing Perlite," *Buildings and Environment*, vol. 42, pp. 3540–3546, 2007.

[11] B. Yesilata, Y. Isiker, and P. Turgut, "Thermal Insulation Enhancement in Concretes by Adding Waste PET and Rubber Pieces," *Construction and Building Materials*, vol. 23, pp. 1878–1882, 2009.

[12] R. Demirboga and R. Gul, "The Effects of Expanded Perlite Aggregate, Silica Fume and Fly Ash on the Thermal Conductivity of Lightweight Concrete," *Cement and Concrete Research*, vol. 33, pp. 723–727, 2003.

[13] O. Sengul, S. Azizi, F. Karaosmanoglu, and M. Ali, "Effect of Expanded Perlite on the Mechanical Properties and Thermal Conductivity of Lightweight Concrete," *Energy and Buildings*, vol. 43, pp. 671–676, 2011.

[14] A. Gent, J. Walter, *The Pneumatic Tire*, U.S. Department of Transportation-National Highway Traffic Safety Adminstration, University of Akron, USA, 2006.

[15] W. M. Aljaaidi, H. M. Almohanna, A. Zaid, and B. Jumah, *Used Tires Recycling and Utilization in Saudi Arabia*, Design Project, King Saud University, KSA 2014.

[16] A. Fadiel, F. Al Rifaie, T. Abu-lebdeh, and E. Fini, "Use of Crumb Rubber to Improve Thermal Efficiency of Cement-Based Materials," *American Journal of Engineering and Applied Sciences*, vol. 7, pp. 1–11, 2014.

[17] C. A. Issa and G. Salem, "Utilization of Recycled Crumb Rubber as Fine Aggregates in Concrete Mix Design," *Construction and Building Materials*, vol. 42, pp. 48–52, 2013.

[18] N. Saikia and J. De Brito, "Use of Plastic Waste as Aggregate in Cement Mortar and Concrete Preparation: A Review," *Construction and Building Materials*, vol. 34, pp. 385–401, 2012.

[19] M. M. Rahman, A. Islam, M. Ahmed, and M. A. Salam, "Recycled Polymer Materials as Aggregates for Concrete and Blocks," *Journal of Chemical Engineering*, vol. 27, pp. 53–57, 2012.

[20] M. J. Islam, M. S. Meherier, and A. K. M. R. Islam, "Effects of Waste PET as Coarse Aggregate on the Fresh and Harden Properties of Concrete," *Construction and Building Materials*, vol. 125, pp. 946–951, 2016.

[21] N. Saikia and J. De Brito, "Mechanical Properties and Abrasion Behaviour of Concrete Containing Shredded PET Bottle Waste as A Partial Substitution of Natural Aggregate," *Construction and Building Materials*, vol. 52, pp. 236–244, 2014.

[22] M. Singh and M. Garg, "Perlite-Based Building Materials – A Review of Current Applications," *Construction and Building Materials*, vol. 5, pp. 75–81, 1991.

[23] M. Zukowski and G. Haese, "Experimental and Numerical Investigation of A Hollow Brick Filled with Perlite Insulation," *Energy and Buildings*, vol. 42, pp. 1402–1408, 2010.

[24] L. Gu and T. Ozbakkaloglu, "Use of Recycled Plastics in Concrete : A Critical Review," *Waste Management*, vol. 51, pp. 19–42, 2016.

[25] H. Toutanji, "The Use of Rubber Tire Particles in Concrete to Replace Mineral Aggregates," *Cement & Concrete Composites*, vol. 18, pp. 135–139, 1996.

[26] D. Fedroff, S. Ahmad, B. Savas "Mechanical Properties of Concrete with Ground Waste Tire Rubber," *Transportation Research Record*, vol. 1532, pp. 66–72, 2012.

[27] O. By, Z. K. Khatib, and F. M. Bayomy, "Rubberized Portland Cement Concrete," *Journal of Materials in Civil Engineering*, vol. 11, pp. 206–213, 1999.

[28] A. M. Ghaly and J. D. Cahill, "Correlation of Strength, Rubber Content and Water to Cement Ratio in Rubberized Concrete," *Canadian Journal of Civil Engineering*, vol. 32, pp. 1075–1081, 2005.

[29] A. Benazzouk, O. Douzane, K. Mezreb, B. Laidoudi, and M. Quéneudec, "Thermal Conductivity of Cement Composites Containing Rubber Waste Particles: Experimental Study and Modelling," *Construction and Building Materials*, vol. 22, pp. 573–579, 2008.

[30] A. R. Khaloo, M. Dehestani, and P. Rahmatabadi, "Mechanical Properties of Concrete Containing A High Volume of Tire-Rubber Particles," *Waste Management*, vol. 28, pp. 2472–2482, 2008.

[31] P. Sukontasukkul, "Use of Crumb Rubber to Improve Thermal and Sound Properties of Pre-cast Concrete Panel," *Construction and Building Materials*, vol. 23, pp. 1084–1092, 2009.

[32] T. R. Naik, S. S. Singh, C. O. Huber, and B. S. Brodersen, "Use of Post-consumer Waste Plastics in Cement-based Composites," *Cement and Concrete Research*, vol. 26, pp. 1489–1492, 1996.

[33] Z. Z. Ismail and E. A. AL-Hashmi, "Use of Waste Plastic in Concrete Mixture As Aggregate Replacement," *Waste Management*, vol. 28, pp. 2041–2047, 2008.

[34] I. Yadav, *Laboratory Investigations of the Properties of Concrete Containing Recycled Plastic Aggregates*, Master Thesis in Civil Engineering, Thapar University, India 2008.

[35] K. Swamy, M. Mohiuddin, and M. Haleem, "Laboratory Investigations of the Properties of Concrete Containing Recycled Plastic Aggregates," *International Journal of Research Sciences and Advanced Engineering*, vol. 2, pp. 133–139, 2016.

[36] Y. W. Choi, D. J. Moon, J. S. Chung, and S. K. Cho, "Effects of Waste PET Bottles Aggregate on the Properties of Concrete,", *Cement and Concrete Research*, vol. 35, pp. 776–781, 2005.

[37] Y. W. Choi, D. J. Moon, Y. J. Kim, and M. Lachemi, "Characteristics of Mortar and Concrete Containing Fine Aggregate Manufactured from Recycled Waste Polyethylene Terephthalate Bottles," *Construction and Building Materials*, vol. 23, pp. 2829–2835, 2009.

[38] M. Frigione, "Recycling of PET Bottles as Fine Aggregate in Concrete," *Waste Management*, vol. 30, pp. 1101–1106, 2010.

[39] J. L. Ruiz-Herrero, D. Velasco Nieto, A. Lpez-Gil, A. Arranz, A. Fernndez, A. Lorenzana, S. Merino, J. A. De Saja, and M. Ngel Rodrguez-Prez, "Mechanical and Thermal Performance of Concrete and Mortar Cellular Materials Containing Plastic Waste," *Construction and Building Materials*, vol. 104, pp. 298–310, 2016.

[40] B. P. Jelle, "Traditional State of the Art and Future Thermal Building Insulation Materials and Solutions - Properties, Requirements and Possibilities," *Energy and Buildings*, vol. 43, pp. 2549–2563, 2011.

[41] S. Akçaözoğlu, K. Akçaözoğlu, and C. D. Atiş, "Thermal Conductivity, Compressive Strength and Ultrasonic Wave Velocity of Cementitious Composite Containing Waste PET Lightweight Aggregate (WPLA)," *Composites Part B: Engineering*, vol. 45, pp. 721–726, 2013.

[42] A. M. Papadopoulos, "State of the Art in Thermal Insulation Materials and Aims for Future Developments," *Energy Buildings*, vol. 37, pp. 77–86, 2005.

[43] G. Hoff, "Porosity-Strength Considerations for Cellular Concrete," *Cement and Concrete Research*, vol. 6, pp. 183–192, 1976.

[44] H. S. Dweik, M. M. Ziara, and M. S. Hadidoun, "Enhancing Concrete Strength and Thermal Insulation Using Thermoset Plastic Waste," *International Journal of Polymeric Materials and Polymeric Biomaterials*, vol. 57, pp. 635–656, 2008.

[45] R. Baetens, B. Jelle, A. Gustavsen, "Aerogel Insulation for Building Applications: A State-of-the-Art Review," *Energy and Buildings*, vol. 3–3, pp. 1385–1412, 2015.

[46] O. Y. Marzouk, R. M. Dheilly, and M. Queneudec, "Valorization of Post-consumer Waste Plastic in Cementitious Concrete Composites," *Waste Management*, vol. 27, pp. 310–318, 2007.

[47] A. Pezzi, L., De Luca, P., Vuono, D., Chiappetta, F., Nastro, "Concrete Products with Waste's Plastic Material (bottle, glass, plate)," *Materials Science Forum*, vol. 1753–1760. pp. 514– 516, 2006.

[48] J. Isler, "*Assessment of Concrete Masonry Units Containing Aggregate Replacements of Waste Glass and Rubber Tire Particles*, Master Thesis in Civil Engineering, University of Colorado, USA, 2012.

[49] R. Frankowski, *Rubber-Crumb-Reinforced Cement Concrete*, Patent No. US 5391226, 1995.

[50] P. Sukontasukkul and C. Chaikaew, "Properties of Concrete Pedestrian Block Mixed with Crumb Rubber," *Construction and Building Materials*, vol. 20, pp. 450–457, 2006.

[51] T. C. Ling, "Prediction of Density and Compressive Strength for Rubberized Concrete Blocks," *Construction and Building Materials*, vol. 25, pp. 4303–4306, 2011.

[52] N. Al-Aqeeli, H. Assehdi, and M. Maslehuddin, *Crumb Rubber Augmented Masonry Blocks*, Patent No. US 20160185665 A1, 2016.

[53] E. Sodupe-Ortega, E. Fraile-Garcia, J. Ferreiro-Cabello, and A. Sanz-Garcia, "Evaluation of Crumb Rubber as Aggregate for Automated Manufacturing of Rubberized Long Hollow Blocks and Bricks," *Construction and Building Materials*, vol. 106, pp. 305–316, 2016.

[54] S. Safinia and A. Alkalbani, "Use of Recycled Plastic Water Bottles in Concrete Blocks," *Procedia Engineering*, vol. 164, pp. 214–221, 2016.

[55] S. Wonderlich, *Strength of Concrete Masonry Units with Plastic Bottle Cores*, Master in Architectural Engineering and Construction Science, Kansas State University, Manhattan, USA, 2014.

[56] P. Mathew, K. P. Ambika, P. Prakash, T. Barried, and P. Varsha, "Comparative Study on Waste Plastic Incorporated Concrete Blocks with Ordinary Concrete Blocks," *International Research Journal of Engineering and Technology*, vol. 03, pp. 1894–1896, 2016.

[57] L. M. Al-Hadhrami and A. Ahmad, "Assessment of Thermal Performance of Different Types of Masonry Bricks Used in Saudi Arabia," *Applied Thermal Engineering*, vol. 29, pp. 1123–1130, 2009.

[58] M. M. Al-Hazmy, "Analysis of Coupled Natural Convection-Conduction Effects on the Heat Transport through Hollow Building Blocks," *Energy and Buildings*, vol. 38, pp. 515–521, 2006.

[59] J. J. Del Coz Diaz, P. J. Garca Nieto, a. M. Rodriguez, a. L. Martinez-Luengas, and C. B. Biempica, "Non-Linear Thermal Analysis of Light Concrete Hollow Brick Walls by the Finite Element Method and Experimental Validation," *Applied Thermal Engineering*, vol. 26, pp. 777–786, 2006.

[60] J. Diaz, P. Nieto, C. Biempica, and M. Gero, "Analysis and Optimization of the Heat-Insulating Light Concrete Hollow Brick Walls Design by the Finite Element Method," *Applied Thermal Engineering*, vol. 27, pp. 1445–1456, 2007.

[61] J. Diaz, P. Nieto, J. Sierra, and C. Biempica, "Nonlinear Thermal Optimization of External Light Concrete Multi-holed Brick Walls by the Finite Element Method," *International Journal of Heat and Mass Transfer*, vol. 51, pp. 1530–1541, 2008.

[62] J. J. del Coz Díaz, P. J. García Nieto, J. L. Suárez Sierra, and I. Peñuelas Sánchez, "Non-linear Thermal Optimization and Design Improvement of A New Internal Light Concrete Multi-Holed Brick Walls by FEM,", *Applied Thermal Engineering* vol. 28, pp. 1090–1100, 2008.

[63] H. Baig and M. Antar, "Conduction/Natural Convection Analysis of Heat Transfer across Multi-Layer Building Blocks," *5th European Thermal-Sciences Conference, The Netherlands*, 2008.

[64] R. Fioretti and P. Principi, "Thermal Performance of Hollow Clay Brick with Low Emissivity Treatment in Surface Enclosures," *Coatings*, vol. 4, pp. 715–731, 2014.

[65] A. S. Al-Tamimi, M. A. Al-Osta, and O. S. B. Al-Amoudi, "Thermal Simulation for a Wall of Hollow Concrete Brick with Different Insulation Materials and Mortars," *International Conference on Water, Informatics, Sustainability, and Environment (IWISE), Carlton University, Ottawa, Canada*, 2017.

[66] S. Adekunle, *A Study on Developing Self-Cosolidation Concrete (SCC) Utilizing Indigenous Natural and Industrial Waste Materials*, Master Thesis in Civil Engineering, King Fahd University of Petroleum and Minerals, KSA, 2012.

[67] Thermtest Thermophysical Instruments, *Materials Thermal Properties Database*, 2017. https://www.thermtest.com/materials-database

[68] "Perlite Lightweight Insulating Concrete Insuperl- INSUPERL LWC," *Industrial Arabian Vermiculite*, 2017. httpwww.avi-sa.cominsuperl.html.

[69] ASTM Standard C-129, *Standard Specification for Nonloadbearing Concrete Masonry Units*, Annual Book of ASTM Standards, 2006.

[70] ASTM Standard C-140, *Standard Test Methods for Sampling and Testing Concrete Masonry Units and Related Units*, Annual Book of ASTM Standards, 2007.

[71] ASTM Standard C-1552, *Capping Concrete Masonry Units, Related Units and Masonry Prisms for Compression Testing*, Annual Book of ASTM Standards, 2002.

[72] *FOX50 Heat Flow Meter Instrument Manual*, LaserComp – TA Instruments, 2002-2016. www.lasercomp.com.

[73] L. M. Al-Hadhrami and A. Ahmad, "Assessment of Thermal Performance of Different Types of Masonry Bricks Used in Saudi Arabia," *Applied Thermal Engineering*, vol. 29, pp. 1123–1130, 2009.

[74] A. Ahmad and L. Al-Hadhrami, "Thermal Performance and Economic Assessment of Masonry Bricks," *Thermal Science*, vol. 13, pp. 221–232, 2009.

[75] M. Abdelrahman, S. Said, A. Ahmad, M. Inam, and H. Abul-Hamael, "Thermal Conductivity of Some Major Building Materials in Saudi Arabia," *Journal of Thermal Insulation*, vol. 13, pp. 294–300, 1990.

[76] N. N. Hilal, "Hardened Properties of Self-compacting Concrete with Different Crumb Rubber Size and Content," *International Journal of Sustainable Built Environment*, vol. 6, pp. 191–206, 2017.

[77] V. Malagavelli, R. S. Parmar, and P. N. Rao, “Thermal Conductivity and Impact Resistance of Concrete Using Partial Replacement of Coarse Aggregate with Rubber,” *Jordan Journal of Civil Engineering*, vol. 10, pp. 145–162, 2016.

[78] *Simulation of Energy and Cost Effectiveness Studies for Residential Buildings Built from Clay Brick Versus other Masonary Construction*, Final Report, the Research Insititute, King Fahd University of Petroulem and Minerals, KSA.

[79] K. S. Al-Jabri, A. W. Hago, A. S. Al-Nuaimi, and A. H. Al-Saidy, “Concrete Blocks for Thermal Insulation in Hot Climate,” *Cement and Concrete Research*, vol. 35, pp. 1472–1479, 2005.

Vitae

Eng. Ahmed S. Al-Tamimi

King Fahd University of Petroleum & Minerals
Dhahran 31261, Saudi Arabia
E-mails: ahmatt2013@gmail.com
Mobile: (+966) 533-124-226

PROFILE

I am a very organized person who enjoys making sure that jobs are done in a timely and efficient manner. I am self-motivated and spend a great deal of time working on projects on my own initiative, however, I also work as part of a bigger team. I can plan my time effectively and like to manage my list of tasks ensuring that each job gets completed on time.

EDUCATION

Master of Science in Civil Engineering (Structures and Materials) Dec. 2017
King Fahd University of Petroleum & Minerals, Dhahran, Saudi Arabia

Bachelor of Science in Civil Engineering Sept. 2008-June 2013
Hadhramout University, Mukalla, Yemen

English Diploma Certificate Awarded 2012
Hadhramout Est. for Human Development, Yemen

Executive Diploma in Project Management Awarded: June 2015
CAAD Center, Kuala Lumpur, Malaysia

WORK EXPERIENCE

Contractor Engineer, Dec. 2013-June 2014
Bin-Ladin Construction Group in Al-Haram Extension, Saudi Arabia

- Read the engineering drawings
- Supervise all structural elements and excavations
- Visit concrete factory and steel workshop to gather details
- Work closely with most of the departments of the project

Trainee Engineer, Aug. - Oct. 2013
Governorate Building, Yemen

- Read engineering drawings
- Supervise construction foundation
- Supervise the restoration of the building
- Make experiments for concrete cubes

Summer Training, Jan. 2012
Bin-Mahfoodh Towers, Yemen
- Read the engineering drawings
- Supervise the construction of flat slab and columns

TECHNICAL SKILLS

- **Microsoft Office**: Word – Excel – PowerPoint
- **Tools:** ABAQUS software – Primavera – AutoCAD – STAAd. Pro – Photoshop

PROFESSIONAL DEVELOPMENT (SHORT COURSES, WORKSHOPS, etc.)

- Assessment and Repair of Reinforced Concrete Structures: Principles and Applications, **2017**
- Protection of Reinforced Concrete Structures in Hot and Aggressive Exposures, **2016**
- Participating in the seventh and eighth volunteering day at KFUPM**, 2015-2016**
- PMP Preparatory Program, Malaysia, **2015**
- ACI (American Concrete Institute) membership, **2015**
- Leadership workshop, **2013**
- Quality Control of Concrete Structures, **2012**

HONORS & AWARDS

- 1st top student with honorable degree in BSc in Civil Engineering, **2013**
- Top student of the Engineering College, Hadhramout University, Yemen,**2013**
- Full-scholarship from Hadhramout Establishment for Human Development (HEHD) for completing Master Degree Program in Civil Engineering (Structure) at KFUPM **2015-2017**

Patents

[1] **"A New Design of Cavities Geometry for Masonry Hollow Bricks"**

[2] **"Insulation Lightweight Masonry Hollow bricks with New Designed Cavities"**

Publications

- **Journal Papers:**

  [1] Al-Tamimi, A.S., Al-Osta, M.A., Al-Amoudi, O.S.B. and Ben-Mansour, R., **"Effect of Geometry of Holes on Heat Transfer of Concrete Masonry Bricks Using Numerical Analysis",** *Arabian Journal for Science and Engineering*, pp.1-17, 2017.

  [2] **"Assessment of Heat Transfer through Masonry Bricks with Different Materials and Hole Arrangements Using Finite Element Method"**, Under reviewer.

  [3] **"Thermal and Mechanical Properties of Non-Load Bearing Hollow**

Concrete Bricks with Insulation Materials- Experimentally and Analytically", Under preparation.

[4] **"Thermal and Mechanical Properties of Normal Concrete with Tire Crumb Rubber- Experimentally",** Under preparation.

[5] **"Thermal and Mechanical Properties of Normal Concrete with Shredded High-Density Polyethylene (HDPE)- Experimentally",** Under preparation.

- **Conference Papers:**

[1] Al-Tamimi, A.S., Al-Osta, M.A., Al-Amoudi, O.S.B. and Ben-Mansour, R., **"Numerical Thermal Simulation for Plastered and Non-Plastered Room with Solid and One-way Ribbed Slab Using FEM"**, *The 2nd International conference on Structural Engineering*, *New Technology and Methods (ICSENM'17)*, Spain, 2017.

[2] Al-Tamimi, A.S., Al-Osta, M.A., Al-Awsh, W. A. and Al-Amoudi, O.S.B., **"Thermal Simulation for a Wall of Hollow Concrete Brick with Different Insulation Materials and Mortars"**, *International Conference on Water, Informatics, Sustainability & Environment (iWISE2017)*, Canada, 2017.

[3] Al-Tamimi, A.S., Al-Awsh, W. A., Al-Osta, M.A., Al-Amoudi, O.S.B. and Ben-Mansour, R., "**Mechanical and Thermal Properties of Perlite and Rubber Insulation Cement Mortar: Experimentally and Analytically**", *Ajman 5th International Environment Conference (AIEC2018)*, UAE, 2018. (Submitted)

REFERNCES

- Prof. Omar S. Baghabra Al-Amoudi
  Dean, Educational Services
  Department of Civil Engineering and Environment
  King Fahd University of Petroleum & Minerals
  E-mail: amoudi@kfupm.edu.sa
  Mobile: (+966) 505758489
- Dr. Mohammed A. Al-Osta
  Department of Civil Engineering and Environment
  King Fahd University of Petroleum & Minerals
  E-mail: malosta@kfupm.edu.sa
  Mobile: (+966) 507524950
- Dr. Tawfik Saleh
  Chemistry Department
  King Fahd University of Petroleum & Minerals
  E-mail: tawfik@kfupm.edu.sa
  Mobile: (+966) 13-860-1734
- Dr. Rached Ben Mansour
  Department of Mechanical Engineering
  King Fahd University of Petroleum & Minerals
  E-mail: rmansour@kfupm.edu.sa
  Mobile: (+966) 560872197